Control of Vein Network Formation by Auxin Signaling

by

Anmol Krishna

A thesis submitted in partial fulfillment of the requirements for the degree of

Master of Science

in

Plant Biology

Department of Biological Sciences

University of Alberta

Abstract

Multicellular organisms solve the problem of long-distance transport of signals and nutrients by means of tissue networks such as the vascular system of vertebrate embryos and the vein networks of plant leaves; therefore, how vascular networks form is a key question in biology. In vertebrates, the formation of the embryonic vascular system relies on direct cell-cell interaction and at least in part on cell migration. Both direct cell-cell interaction and cell migration are precluded in plants by a cell wall that keeps cells apart and in place; therefore, vascular networks form differently in plant leaves.

How vein networks form in plant leaves is unclear, but available evidence suggests that signal transduction of the plant hormone auxin is nonredundantly required for vein network formation. Nonredundant functions of auxin signaling in vein network formation in turn depend on nonredundant functions of the MONOPTEROS (MP) transcription factor. MP is expressed in all the cells of the leaf at early stages of tissue development, but over time, epidermal expression becomes restricted to the basalmost cells and inner-tissue expression becomes restricted to developing veins. However, it is currently unknown what the function of *MP* expression in the leaf epidermis and vascular tissue is in auxin-signaling-dependent vein-network formation.

Here we identify and characterize GAL4/GFP enhancer-trap lines for the targeted expression of genes of interest in specific cells and tissues of developing leaves. We combine GAL4-driven tissue-specific gene expression with cellular imaging and molecular genetic analysis to address the question what the function of *MP* expression in the leaf epidermis and vascular tissue is in auxin-signaling-dependent vein-network formation. We find that *MP* expression in the leaf epidermis is dispensable and that *MP* expression in the vascular tissue is sufficient for auxin-signaling-dependent vein-network formation. Moreover, we show that constitutively active auxin

signaling in the epidermis is insufficient for vascular differentiation anywhere in the leaf, whereas constitutively active auxin signaling in the vascular tissue is sufficient for supernumerary vein formation.

In the inner tissue of the developing leaf, broadly expressed MP activates expression of its target gene *ARABIDOPSIS THALIANA HOMEOBOX8* (*ATHB8*) in narrow domains that presage sites of vein formation. Activation of *ATHB8* expression in narrow domains depends on binding of MP to a low-affinity MP-binding site in the *ATHB8* promoter. However, the biological relevance of the activation of *ATHB8* expression by MP is unclear: whereas *MP* promotes vein formation, *ATHB8* seems to have only transient and conditional functions in vein network formation. Furthermore, whereas both *ATHB8* and MP are expressed in files of vascular cell precursors, MP is additionally expressed in surrounding nonvascular cells, which fail to activate *ATHB8* expression. However, it is unclear why *ATHB8* expression is only activated in a subset of MP-expressing cells.

Here we address this question by combining cellular imaging and molecular genetic analysis. We show that *ATHB8* promotes vein formation and that both levels of *ATHB8* expression and width of *ATHB8* expression domains are relevant to vein formation. Finally, we show that *ATHB8* expression is restricted to narrow preprocambial domains by a combination of (1) activation of *ATHB8* expression through binding of peak levels of MP to a low-affinity MP-binding site in the *ATHB8* promoter and (2) repression of *ATHB8* expression by MP target genes of the *INDOLE-3-ACETIC-ACID-INDUCIBLE* family. The very same regulatory logic that underlies activation of *ATHB8* expression in files of vascular cell precursors is most frequently used in animals to generate stripes of gene expression, suggesting unexpected conservation of

regulatory logic of striped gene expression in plants and animals in spite of the independent evolution of their multicellularity.

Preface

A part of this thesis has been published.

Chapter 3 of this thesis has been published as Amalraj, B., Govindaraju, P., Krishna, A., Lavania, D., Linh, N.M., Ravichandran, S. J. and Scarpella, E. (2020). GAL4/GFP enhancer-trap lines for identification and manipulation of cells and tissues in developing Arabidopsis leaves. *Developmental Dynamics*: 2020 Apr 21. doi: 10.1002/dvdy. 181. Online ahead of print. B. Amalraj, P. Govindaraju, A. Krishna, D. Lavania, and N.M. Linh contributed equally to this work.

All the authors and the publisher have given their permission for the inclusion of this publication in this thesis.

Acknowledgments

I would like to thank all those who came and played a part in my graduate school life, both directly and indirectly, and helped me complete this undertaking.

The first person who I thank for all his support and guidance is my supervisor, Dr. Enrico Scarpella. The training you have given me, both experimentally and conceptually, will always be an asset for me. You have taught me the importance of critical thinking and what it means to be dedicated to one's work and passion!

I would also like to thank Dr. Neil Harris for agreeing to be on my supervisory committee. Although we had a small class, I learned a whole lot of plant physiology from your botany course! I would also like to thank Dr. Gavin Chen for agreeing to be my arm's length examiner.

Completing my graduate work would not have been possible without hands-on material so I would like to extend my gratitude to the Arabidopsis Biological Resource Center (ABRC), Dolf Weijers, Gerd Jürgens, Hiroo Fukuda, Kyoko Ohashi-Ito, and Zachary Nimchuk for sharing seeds and plasmids.

It takes many good friends to make any learning experience enjoyable. I am fortunate to say that I had a welcoming lab and labmates who were always supportive: thank you Carla, Dhruv & Brindhi (a special thank you to you both for lending your ONEcard whenever I lost mine!), Linh, Priyanka, and Sree. I would also like to thank Arlene Oatway from the Microscopy Unit for all her assistance and cheerful attitude!

Finally, I would like to thank my mom, my dad, my sister and my spiritual guide. Your nurturing support, continued faith in me, and just being patient has made this journey doable. Thank you for taking care of me – love you always!

Table of Contents

List of Figures

Chapter 1

Chapter 2

Chapter 3

Chapter 4

List of Tables

Chapter 2

Chapter 3

Chapter 4

List of Abbreviations

Ab	Abaxial
Ad	Adaxial
Ap	Apical
Ar	Argon
ARF	AUXIN RESPONSE FACTOR
ATHB8	ARABIDOPSIS THALIANA HOMEOBOX8
AUX/IAA	AUXIN/INDOLE-3-ACETIC ACID
AuxRE	Auxin Responsive Element
Ba	Basal
BDL	BODENLOS
cDNA	Complementary DNA
CFP	CYAN FLUORESCENT PROTEIN
Col-0	Columbia-0
DAG	Days After Germination
Dex	Dexamethasone
DNA	Deoxyribonucleic Acid
EAR	ETHYLENE-RESPONSIVE-ELEMENT-BINDING FACTOR-Associated Amphiphilic Repression
e.g.	For example
erGFP	Endoplasmic-Reticulum-Localized GREEN FLUORESCENT PROTEIN
EP	End Point
Fig	Figure
GAL4	GALACTOSE-4

GFP	GREEN FLUORESCENT PROTEIN
GR	GLUCOCORTICOID RECEPTOR PROTEIN
HD-ZIP III	HOMEODOMAIN-LEUCINE ZIPPER Class III
He/Ne	Helium/Neon
Hv	Minor Vein
Hy	Hydathode
IAA	Indole-3-Acetic Acid
KP	Break Point
La	Lateral
Lm	Lamina
LUT	Look-up table
L1,L2,L3	Loop 1, Loop 2, Loop 3
mATHB8	Mutated ATHB8
Md	Median
Me	Marginal
MES	2-(N-morpholino)ethanesulfonic acid
miR	MicroRNA
mm	Millimeter
MP	MONOPTEROS
Mv	Midvein
nCFP	Nuclear CYAN FLUORESCENT PROTEIN
nm	Nanometer
NPA	1-N-Naphthylphtalamic Acid

nQFP	Nuclear TURQUOISE FLUORESCENT PROTEIN
nYFP	Nuclear YELLOW FLUORESCENT PROTEIN
ORF	Open Reading Frame
Pe	Petiole
pH	Power of Hydrogen
PIN	PIN-FORMED
PIN1	PIN-FORMED1
PB1	PHOX/BEM1
PEDs	PIN1 Expression Domains
RFP	RED FLUORESCENT PROTEIN
RNA	Ribonucleic Acid
rpm	Rotations per Minute
RPS5A	RIBOSOMAL PROTEIN S5A
R2D2	Ratiometric Version of 2 D's
$SCF^{TIR1/AFB}$	S-PHASE KINASE ASSOCIATED PROTEIN1 – CULLIN – F-BOX TRANSPORT INHIBITOR RESISTANT1/AUXIN SIGNALING F-BOX
SE	Standard Error
SHR	SHORT-ROOT
St	Stoma
TP	Touch Point
TPL	TOPLESS
TPR	TPL-RELATED
Tr	Trichome
WT	Wild type

YFP	YELLOW FLUORESCENT PROTEIN
U	Units
UAS	Upstream Activating Sequence
µm	Micrometer
VP16	VIRAL PROTEIN 16
XP	Exit Point

Notations

WT Gene	Uppercase, italics (e.g., *MP*)
Mutant Gene	Lowercase, italics (e.g., *mp*)
WT Protein	Uppercase (e.g., MP)
Fusions between promoter *A* and gene *A*	A::A (e.g., MP::MP)
Fusions between gene *A* and gene *B*	A:B (e.g., MP:YFP)

Gene Coordinates

All gene coordinates are relative to the adenine (position +1) of the start codon.

Chapter 1: General Introduction

1.1. Plant Vascular System

Plants transport minerals, signals, sugars, and water through their vascular system (Taiz & Zeiger, 2010). This transport system is a network of continuous vascular strands that connect the different parts of an organ and the different organs of a plant (Esau, 1965).

Vascular strands are cylinders of juxtaposed files of vascular cells and are named differently in different organs: veins in flat organs like cotyledons, leaves, petals, and sepals; vascular bundles in the stem; and vascular cylinder or stele in the root (Esau, 1965).

Mature vascular strands are composed of two separate vascular tissues: xylem, which transports minerals and water, and phloem, which transports the products of photosynthesis (Esau, 1965; Taiz & Zeiger, 2010). In flat organs, xylem is found at the upper side of the veins, and phloem is found at the lower side of the veins (Esau, 1965). In the stem, xylem is found at the inner side of the vascular bundles, and phloem is found at the outer side of the vascular bundles. In the root, xylem is found in the center of the vascular cylinder and from this xylem core, xylem “spokes” extend towards the periphery of the vascular cylinder; phloem is found between xylem spokes at the periphery of the vascular cylinder.

1.2. Formation of the First Vascular Cells

In Arabidopsis, the first vascular cells become anatomically recognizable in early globular-stage embryos (Scheres et al., 1994), but expression of vascular-specific markers suggests that the identity of those first vascular cells had been specified earlier, in dermatogen-stage embryos (Smit et al., 2020).

The Arabidopsis dermatogen-stage embryo is composed of sixteen cells: eight outer cells, which are the precursors of the epidermis, and eight inner cells, which are the precursors to all the other tissue types (Scheres et al., 1994). These eight inner cells divide longitudinally, and the resulting four innermost cells in the basal half of the early globular-stage embryo will become procambial cells: the narrow precursor cells that will give rise to all the mature vascular cells (Esau, 1965; Scheres et al., 1994).

1.3. Formation of the First Vascular Cells and Auxin Signaling

Formation of the first vascular cells requires signal transduction of the plant hormone auxin: dermatogen-stage embryos of mutants in components of auxin signaling express vascular-specific markers abnormally, and the eight inner cells of these embryos fail to divide longitudinally and to form procambial cells in early-globular-stage embryos (Berleth & Jurgens, 1993; Hamann et al., 1999; Hobbie et al., 2000; Dharmasiri et al., 2005; Yoshida et al., 2014; Smit et al., 2020).

At the core of auxin signal transduction is the interaction between two families of proteins: the AUXIN RESPONSE FACTOR (ARF) family of transcription factors and the AUXIN/INDOLE-3-ACETIC ACID INDUCIBILE (AUX/IAA) family of transcriptional repressors (recently reviewed in (Powers & Strader, 2020)) (Fig. 1.1).

The Arabidopsis genome codes for 29 AUX/IAA proteins, which contain three domains (Powers & Strader, 2020). Domain I contains an EAR (for ETHYLENE-RESPONSIVE ELEMENT-BINDING FACTOR-Associated Amphiphilic Repression) motif that binds members of the TOPLESS (TPL)/TPL-RELATED (TPR) family of transcriptional co-repressors. Domain II is the auxin-binding domain, and the PHOX/BEM1 (PB1) domain (previously referred to as domains III/IV) binds ARF proteins.

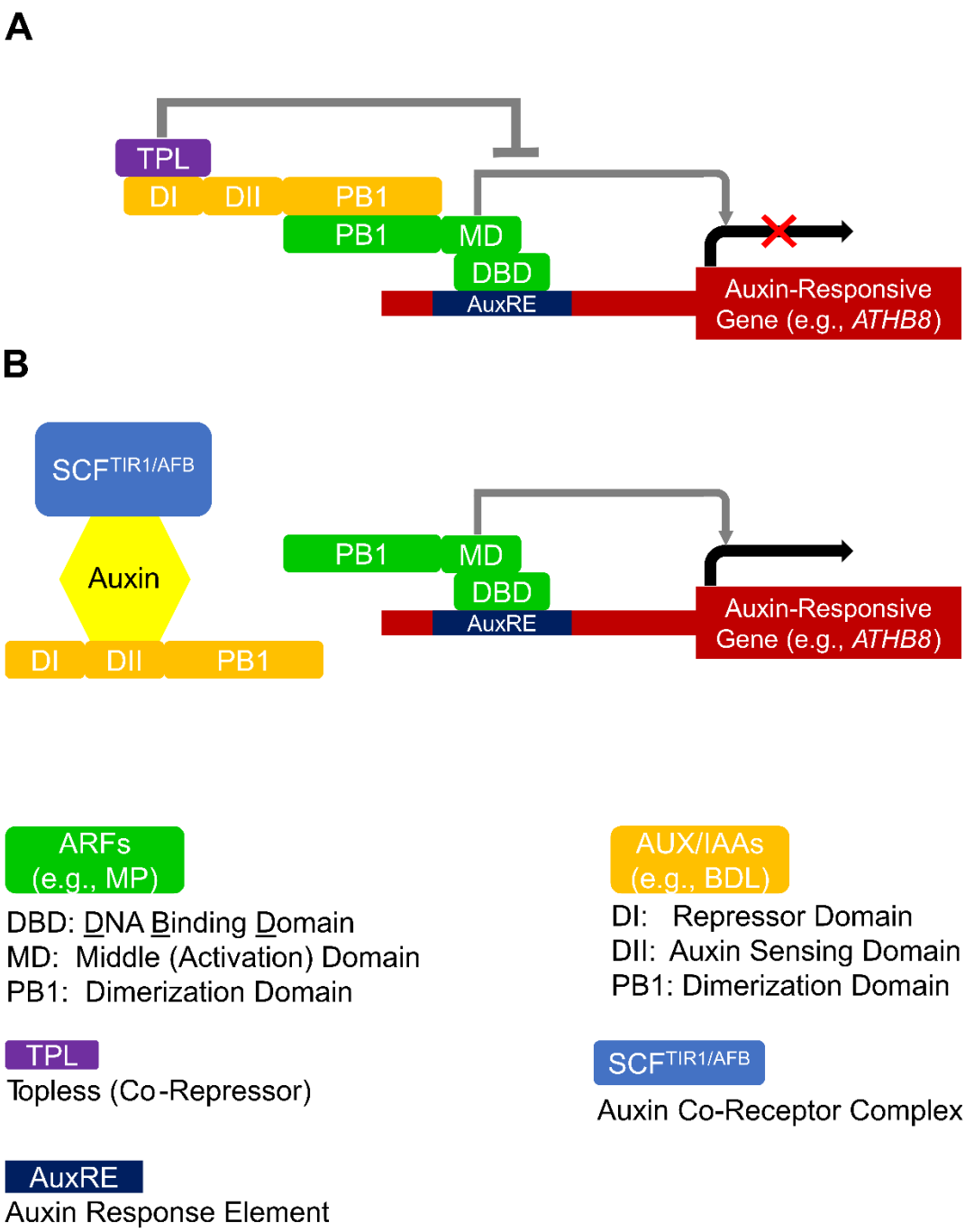

Figure 1.1. Auxin Signal Transduction Pathway.

(A) AUX/IAA-mediated repression of ARF transcription factors at low intracellular auxin concentrations. (B) ARF-mediated activation of target gene transcription at high intracellular auxin concentrations. See text for details.

In Arabidopsis, AUX/IAA proteins can be classified into six groups (Wu et al., 2017). The first group consists of 18 members that contain all three domains. The second group consists of four members that contain an incomplete domain I. The third group consists of three members that contain an incomplete PB1 domain. The fourth group consists of two members that contain incomplete domains I and II, and an incomplete PB1 domain. The fifth group consists of one member that lacks domains I and II. And the sixth group consists of one member that lacks domains I and II, and contains an incomplete PB1 domain.

The Arabidopsis genome encodes 23 ARF proteins, which are grouped into three classes: Class A contains five members that are transcriptional activators; Class B contains 15 members that are transcriptional repressors; and Class C contains three members that are also transcriptional repressors (Powers & Strader, 2020). Class-C ARF proteins diverged from the ancestral Class-A/-B ARF proteins in green algae — presumably before the dependence of plants on auxin — which could suggest that Class-C ARF proteins have functions outside of auxin response. Class-A/-B ARF proteins diverged into separate Class-A and Class-B ARF proteins in land plants (Mutte et al., 2018).

ARF proteins contain three domains (Powers & Strader, 2020). Domain I binds to Auxin Responsive Elements (AuxREs) — specific sequences of DNA found within the promoters of auxin inducible genes. Domain II confers transcriptional-activation- or transcriptional-repression-specificity, and the PB1 domain binds other ARF or AUX/IAA proteins.

At low levels of intracellular auxin, AUX/IAA proteins bind ARF proteins and prevent them from activating gene expression (Powers & Strader, 2020) (Fig. 1.1A). At high levels of intracellular auxin, auxin binds both the F-box subunit of the $SCF^{TIR1/AFB}$ (for S-PHASE KINASE ASSOCIATED PROTEIN1 – CULLIN – F-BOX TRANSPORT INHIBITOR

RESISTANT1/AUXIN SIGNALING F-BOX) E3 ubiquitin ligase complex and domain II of AUX/IAA proteins (Fig. 1.1B). Binding of auxin to the $SCF^{TIR1/AFB}$ complex and an AUX/IAA protein leads to the transfer of ubiquitin from the $SCF^{TIR1/AFB}$ complex to the AUX/IAA protein. The ubiquitinated AUX/IAA protein is targeted for degradation, thereby relieving ARF proteins from repression and allowing them to activate expression of their targets.

Though this model explains the mode of action of activating ARF proteins, it does not explain how repressor ARF proteins act. One possibility is that repressor ARF proteins repress transcription by directly binding to TPL/TPR proteins (Causier et al., 2012). One other possibility is that repressor ARF proteins bind to AuxRE sites and thus compete with activating ARF proteins (Causier et al., 2012; Chandler, 2016).

1.4. Formation of Vascular Strands and Auxin Transport

Though auxin signaling is essential for the formation of vascular cells, auxin transport seems to be required for the organization of those vascular cells into vascular strands (Berleth et al., 2000; Sachs, 1981). Auxin application to various plant tissues induces the differentiation of continuous files of vascular cells into vascular strands that connect the applied auxin to the pre-existing vascular strands basally to the site of auxin application. The auxin-induced vascular-strand formation is characterized by five properties: (1) the response is local, as vascular strands form from the site of auxin application; (2) the response is polar, as vascular strands form toward the pre-existing vasculature located basally to the site of auxin application; (3) the response is continuous, as it gives rise to uninterrupted files of vascular cells; (4) the response is constrained laterally, as vascular differentiation is restricted to files of cells; (5) the response is obstructed by polar auxin-transport inhibitors.

Auxin is indeed synthesized in apical, immature regions of the plant, and transported to the

root tip through vascular strands (Michniewicz et al., 2007; Normanly, 2010; Zhao, 2010). The apical-basal transport of auxin has been suggested to be the result of the polar localization of auxin efflux proteins to the basal plasma membrane of auxin-transporting cells (Raven, 1975; Rubery & Sheldrake, 1974). Indeed, the weak acid indole-3-acetic acid (IAA), which is the most abundant auxin in plants, is non-charged in the acidic extracellular space and can therefore freely diffuse into the cells through the plasma membrane. In the more alkaline intracellular space, IAA becomes negatively charged and therefore cannot leave the cell without the help of specialized efflux proteins of the PIN-FORMED (PIN) family (Petrasek et al., 2006; Wisniewska et al., 2006).

These observations form the basis of the "Auxin Canalization Hypothesis", which postulates that the more a cell transports auxin, the better it becomes at transporting auxin (Sachs, 1981, 1991, 2000). The hypothesis predicts that the pre-existing vascular strands, acting as an auxin sink, will gradually restrict dispersed auxin flow in the vicinity of the pre-existing vascular strands to preferential auxin-transport through narrow files of cells, which will eventually differentiate into vascular strands that connect to the pre-existing vascular strands.

Consistent with predictions of the Auxin Canalization Hypothesis, local application of auxin results in broad PIN1 expression domains (PEDs) between the site of auxin application and pre-existing vascular strands (Mazur et al., 2016; Sauer et al., 2006). Broad domains of PIN1 expression become restricted to sites of auxin-induced vascular-strand formation in which PIN1 is localized to the side of the plasma membrane opposite from the source of auxin application and toward the pre-existing vascular strands.

1.5. Leaf Vein Pattern

In the leaves of eudicots such as Arabidopsis, veins are arranged in a reticulate pattern with a central midvein that extends the length of the leaf (Telfer & Poethig, 1994; Nelson & Dengler, 1997; Kinsman & Pyke, 1998; Candela et al., 1999; Mattsson et al., 1999; Sieburth, 1999; Steynen & Schultz, 2003; Sawchuk et al., 2013; Verna et al., 2015). Lateral veins branch from the midvein and connect to distal veins to form loops. Minor veins branch from the midvein or loops and may connect to other veins or end freely in the leaf lamina. Minor veins and loops curve near the leaf margin to give rise to a scalloped vein-network outline.

1.6. Vein Patterning, Vein Formation, Auxin Transport, and Auxin Signaling

The reticulate vein-network pattern in Arabidopsis leaves seems to be the combined result of auxin transport and signaling (Verna et al., 2019). Expression and polar localization of PIN1 to the plasma membrane suggest that veins are formed by two different mechanisms: one by which the midvein and lateral veins form; the other by which minor veins form (Scarpella et al., 2006; Wenzel et al., 2007).

The midvein seems to form from sites of convergence of PIN1 polarity in the epidermis of the shoot apical meristem (Benkova et al., 2003; Reinhardt et al., 2003; Scarpella et al., 2006; Wenzel et al., 2007; Bayer et al., 2009). This epidermal convergence point of PIN1 polar localization is correlated with a broad PED in the inner tissue. Over time, PIN1 expression becomes restricted to the site of midvein formation, and PIN1 becomes localized to the basal side of the plasma membrane in the cells of the midvein. Likewise, positions of leaf lateral growth and broad inner PEDs associated with lateral vein formation seem to be connected to one another through epidermal convergence points of PIN1 polarity at the leaf margin (Hay et al., 2006;

Scarpella et al., 2006; Wenzel et al., 2007). However, recent evidence suggests that convergence points of epidermal PIN1 polarity and positioning of the midvein and lateral veins are correlations and not causally related to one another (Govindaraju et al., 2020).

In contrast to the midvein and lateral veins, minor veins form from PEDs that are not associated with epidermal convergence points of PIN1 polarity and instead branch from pre-existing veins (Scarpella et al., 2006; Wenzel et al., 2007; Marcos & Berleth, 2014). Over time, a few of those PEDs will weaken and disappear (Marcos & Berleth, 2014), but most of them will become restricted to narrow sites of minor vein formation (Scarpella et al., 2006; Wenzel et al., 2007; Marcos & Berleth, 2014). These PEDs can remain connected to pre-existing veins on one side only, in which case PIN1 is localized to the side of the plasma membrane facing the pre-existing veins the PEDs connect to (Scarpella et al., 2006; Wenzel et al., 2007; Marcos & Berleth, 2014). However, PEDs can, over time, connect to pre-existing veins on both sides, and at the ends of these PEDs, PIN1 is localized to the sides of the plasma membrane facing the pre-existing veins the PEDs connect to. The two resulting opposite polarities are connected by a "bipolar cell", a cell where PIN1 is localized to two opposite sides of the plasma membrane.

Vein loops have a composite origin: minor-vein-associated PEDs branch from lateral-vein-associated PEDs and connect to the midvein or other lateral veins to form continuous loops (Scarpella et al., 2006; Wenzel et al., 2007). At the ends of each loop-associated PED, PIN1 is localized to the sides of the plasma membrane facing the pre-existing veins the PED connects to, and the opposite PIN1 polarities are connected by a bipolar cell.

If vascular strand formation only depended on auxin transport, and auxin transport only depended on *PIN* gene function, the most severe *pin* mutants should form no vascular strands. Recent evidence suggests that it is not so: mutants in all the *PIN* genes with vascular function

form veins in a reproducible, albeit abnormal, pattern, implying that there is residual vein patterning activity in these mutants (Verna et al., 2019). Because these *pin* mutants still respond to auxin application by forming veins that connect the applied auxin to the pre-existing vasculature basal to the auxin application site, the residual vein patterning activity present in these mutants must depend on auxin signaling. Indeed, mutants in both auxin signaling and transport, or WT grown in the presence of inhibitors of both auxin signaling and transport, have completely new, more severe vein pattern defects; in the most severe cases, vascular elements are no longer aligned along the length of a vein, like in WT or auxin-transport-inhibited plants, but in random orientations (Verna et al., 2019). This suggests that it is indeed auxin signaling that provides the residual vein patterning activity in auxin transport mutants.

These results are unexpected as auxin signaling had never been associated with vein patterning: mutants in auxin signaling have fewer veins, but these veins form in a normal pattern (Przemeck et al., 1996; Hardtke & Berleth, 1998; Candela et al., 1999; Alonso-Peral et al., 2006; Strader et al., 2008; Esteve-Bruna et al., 2013; Verna et al., 2019). Therefore, it seems that the relationship between auxin signaling and auxin transport in vein patterning is asymmetrical: auxin transport mutants have an abnormal vein pattern, suggesting that auxin transport is required for vein patterning even in the presence of a normal auxin signaling pathway (Verna et al., 2019), but auxin signaling mutants have a normal vein pattern, suggesting that auxin signaling is not required for vein patterning in the presence of a normal auxin transport pathway (Przemeck et al., 1996; Hardtke & Berleth, 1998; Candela et al., 1999; Alonso-Peral et al., 2006; Strader et al., 2008; Esteve-Bruna et al., 2013; Verna et al., 2019). This suggests that auxin transport can compensate for the lack of auxin-signaling-dependent vein-patterning activity, but auxin signaling cannot compensate for the lack of auxin-transport-dependent vein-patterning

activity (Verna et al., 2019).

1.7. Scope and Outline of the Thesis

The evidence discussed above suggests that auxin signaling controls vascular strand formation; however, details of such control are scarce. The scope of my M.Sc. thesis is to address this limitation and advance our knowledge of how auxin signaling controls vascular strand formation. I focus my investigations on leaves because (1) like in embryos (Scheres et al., 1994; Yoshida et al., 2014; Smit et al., 2020), in leaves, vascular strands form de novo (Foster, 1952; Pray, 1955); (2) unlike embryos, leaves are readily accessible for imaging; (3) unlike in other accessible flat organs — such as sepals and petals — in leaves, stages of vein development have been extensively characterized (Mattsson et al., 1999; Sieburth, 1999; Steynen & Schultz, 2003; Kang & Dengler, 2004; Scarpella et al., 2004; Scarpella et al., 2006; Sawchuk et al., 2007; Wenzel et al., 2007; Marcos & Berleth, 2014).

Expression of the *ARABIDOPSIS THALIANA HOMEOBOX8* (*ATHB8*) gene is activated in files of isodiametric inner cells of the leaf (Kang and Dengler, 2004; Scarpella et al., 2004) (Fig. 1.2). *ATHB8*-expressing ground cells will elongate into procambial cells — the precursors to all vascular cells — and are therefore referred to as preprocambial cells (Kang and Dengler, 2004; Scarpella et al., 2004; Sawchuk et al., 2007; Marcos and Berleth, 2014). Activation of *ATHB8* expression in files of preprocambial cells depends on binding of the MONOPTEROS/AUXIN RESPONSE FACTOR5 (MP/ARF5; MP hereafter) transcription factor to a low-affinity MP-binding site in the *ATHB8* promoter (Donner et al., 2009). However, the biological relevance of activation of *ATHB8* expression by MP is unclear: whereas *MP* promotes vein formation (Przemeck et al., 1996), *ATHB8* seems to have only transient and conditional functions in vein network formation (Baima et al., 2001; Donner et al., 2009). Furthermore, whereas both *ATHB8*

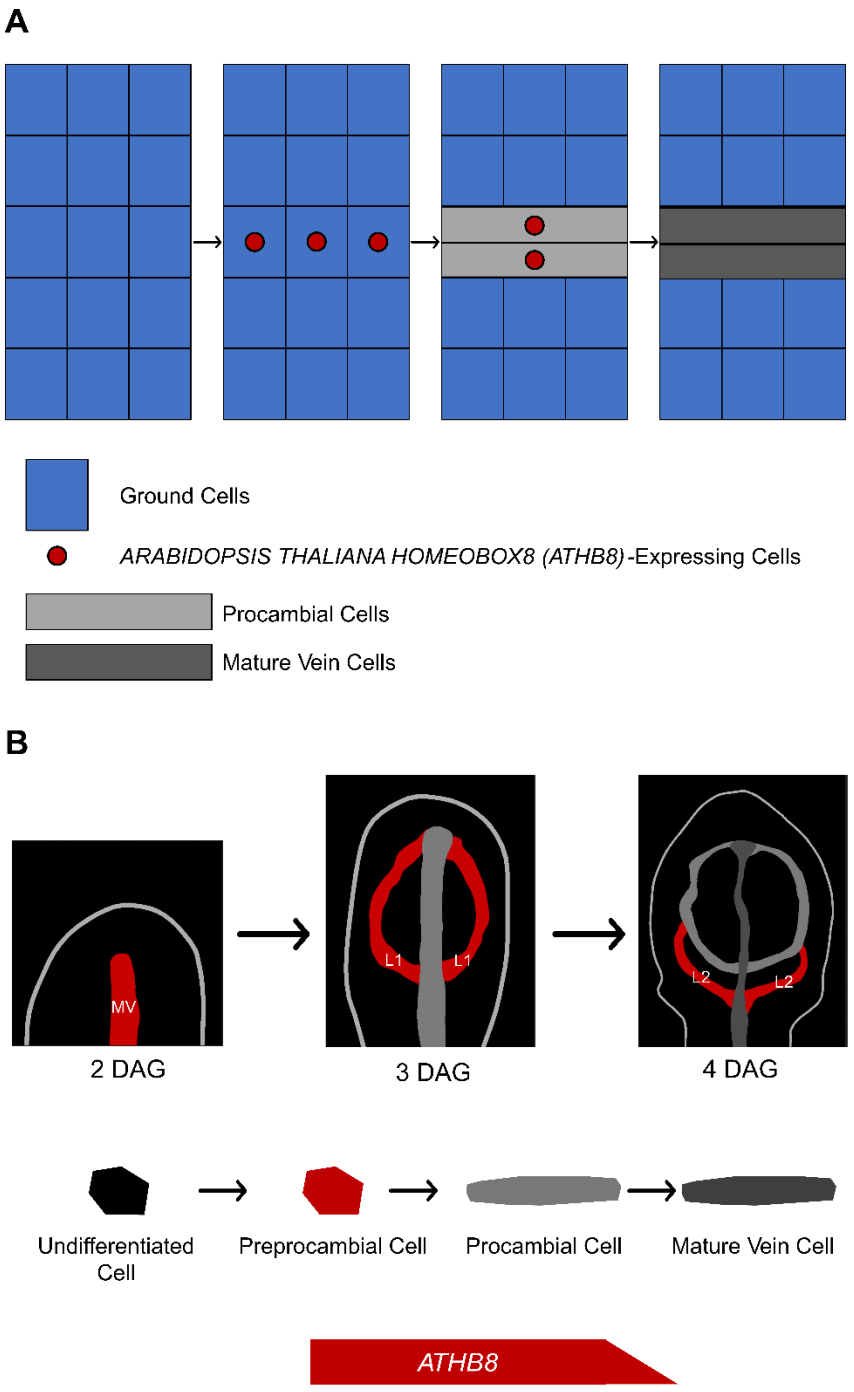

Figure 1.2. Formation of Vascular Cells and *ATHB8* Expression Dynamics.

(A) Vascular cell formation, from ground cells to mature vein cells. (B) Progression of *ATHB8* gene expression from 2 to 4 days after germination (DAG). See text for details.

and MP are expressed in files of preprocambial cells, MP is additionally expressed in surrounding nonvascular cells, which fail to activate *ATHB8* expression (Donner et al., 2009); why is *ATHB8* expression only activated in a subset of MP-expressing cells?

In Chapter 2, we show that *ATHB8* promotes vein formation and that both levels of *ATHB8* expression and width of *ATHB8* expression domains are relevant to vein formation. Furthermore, we show that *ATHB8* expression is restricted to files of preprocambial cells by a combination of (1) activation of *ATHB8* expression through binding of peak levels of MP to the low-affinity MP-binding site in the *ATHB8* promoter and (2) repression of *ATHB8* expression by MP target genes of the *AUX*/*IAA* family.

Testing *ATHB8* functions in vein formation (Chapter 2) requires expression of *ATHB8* by different promoters. This imposes the burden of generating different constructs for different promoter–*ATHB8* combinations. This approach could be simplified if GALACTOSE-4/GREEN FLUORESCENT PROTEIN (GAL4/GFP) enhancer-trap lines existed in Columbia-0 (Col-0), the genotype of reference in Arabidopsis (Koornneef & Meinke, 2010), with which to drive expression of genes of interest in desired cells and tissues of developing leaves. Unfortunately, such lines were not available when I started my M.Sc.. In Chapter 3 (Amalraj et al., 2020), we address this limitation and provide GAL4/GFP enhancer-trap lines in the Co-0 background of Arabidopsis for the identification and manipulation of cells and tissues in developing leaves.

Nonredundant functions of auxin signaling in vein formation depend on nonredundant MP functions (Przemeck et al., 1996; Ulmasov et al., 1997; Hardtke & Berleth, 1998; Ulmasov et al., 1999; Stamatiou, 2007). Like PIN1, MP is expressed in all the cells of the leaf at early stages of tissue development, and over time, epidermal expression becomes restricted to the basalmost cells, and inner-tissue expression becomes restricted to developing veins (Wenzel et al., 2007;

Donner et al., 2009; Krogan et al., 2012; Bhatia et al., 2016) (Chapter 2). Moreover, convergent points of epidermal PIN1 polarity are associated with peaks of auxin signaling (Benkova et al., 2003; Mattsson et al., 2003; Heisler et al., 2005; Hay et al., 2006; Scarpella et al., 2006; Smith et al., 2006; Wenzel et al., 2007; Kierzkowski et al., 2013; Marcos & Berleth, 2014). However, unlike for PIN1 in auxin-transport-dependent vein patterning (Govindaraju et al., 2020), it is unknown what the function is of *MP* expression in the leaf epidermis and vascular tissue in auxin-signaling-dependent vein formation.

In Chapter 4, we address this question by leveraging the resources we generated in Chapter 3 (Amalraj et al., 2020) and find that like PIN1 in auxin-transport-dependent vein patterning (Govindaraju et al., 2020), *MP* expression in the leaf epidermis is dispensable and *MP* expression in the vascular tissue is sufficient for auxin-signaling-dependent vein formation. Moreover, we show that constitutively active auxin signaling in the epidermis is insufficient for vascular differentiation anywhere in the leaf, whereas constitutively active auxin signaling in the vascular tissue is sufficient for supernumerary vein formation.

Finally, in Chapter 5, I propose and discuss a hypothesis of how constitutively active auxin signaling leads to supernumerary vein formation.

Chapter 2: Control of Vein-Formation-Inducing Gene Expression by Auxin Signaling

2.1. Introduction

Narrow domains of gene expression are fundamental units of biological patterning (e.g., (Papatsenko, 2009; Irion et al., 2016)). Therefore, how multicellular organisms activate gene expression in narrow domains is a central question in biology. In animals, where this question has been investigated extensively, broadly expressed transcription factors activate expression of their target genes in narrow domains by (1) differential affinity of such transcription factors for their binding sites in target genes and (2) combinatorial interactions between transcription-factor-encoding target genes (Ashe and Briscoe, 2006; Rogers and Schier, 2011; Hironaka and Morishita, 2012; Sagner and Briscoe, 2017). For example, the transcription factor Dorsal forms a ventral-to-dorsal gradient in Drosophila embryos (reviewed in (Reeves and Stathopoulos, 2009)). Expression of Dorsal target genes with high-affinity Dorsal-binding sites is activated already at low levels of Dorsal, whereas expression of Dorsal target genes with low-affinity Dorsal-binding sites is activated only at high levels of Dorsal. However, this mechanism alone is insufficient to account for the expression of Dorsal target genes in narrow domains: interaction between Dorsal target genes themselves is also required: Dorsal activates expression of *snail*, which encodes a transcription factor that represses the expression of the Dorsal target gene *ventral nervous system defective*. Thus, expression of some Dorsal target genes such as *ventral nervous system defective* is repressed at high levels of Dorsal, at which *snail* is expressed, but activated at lower levels of Dorsal, at which *snail* is not expressed.

In plants too, broadly expressed transcription factors activate expression of their target genes in narrow domains (e.g., (Brady et al., 2011)); however, how those broadly expressed

transcription factors do so is unclear. Here we addressed this question for the *MP – ATHB8* pair of Arabidopsis genes (Baima et al., 1995; Hardtke and Berleth, 1998). *ATHB8* expression is activated in single files of isodiametric ground cells of the leaf (Kang and Dengler, 2004; Scarpella et al., 2004). *ATHB8*-expressing ground cells will elongate into procambial cells — the precursors to all vascular cells — and are therefore referred to as preprocambial cells (Kang and Dengler, 2004; Scarpella et al., 2004; Sawchuk et al., 2007; Marcos and Berleth, 2014). Activation of *ATHB8* expression in narrow preprocambial domains depends on binding of the broadly expressed MP transcription factor to a low-affinity MP-binding site in the *ATHB8* promoter (Donner et al., 2009). However, the biological relevance of activation of *ATHB8* expression by MP is unclear: whereas *MP* promotes vein formation (Przemeck et al., 1996), *ATHB8* seems to have only transient and conditional functions in vein network formation (Baima et al., 2001; Donner et al., 2009).

Here we show that ATHB8 promotes vein formation and that both levels of *ATHB8* expression and width of *ATHB8* expression domains are relevant to vein formation. Finally, we show that *ATHB8* expression is restricted to narrow preprocambial domains by a combination of (1) activation of *ATHB8* expression through binding of peak levels of MP to a low-affinity MP-binding site in the *ATHB8* promoter and (2) repression of *ATHB8* expression by MP target genes of the *IAA* family.

2.2. Results & Discussion

2.2.1. Response of Vein Network Formation to Changes in ATHB8 Expression and Activity

To understand how in plants broadly expressed transcription factors activate expression of their target genes in narrow domains, we chose the *MP — ATHB8* pair of Arabidopsis genes. During leaf development, the broadly expressed MP transcription factor directly activates *ATHB8* expression in narrow preprocambial domains that mark the position where veins will form (Donner et al., 2009), but the biological relevance of the interaction between the two genes is unclear.

That *MP* promotes vein formation is known (Przemeck et al., 1996), but the function of *ATHB8* in this process is unresolved: *athb8* mutants seem to have only transient and conditional defects in vein network formation, and the mutants have normal vein patterns (Baima et al., 2001; Donner et al., 2009). Therefore, we first asked whether ATHB8 had any permanent functions in vein network formation. To address this question, we characterized the vein networks in mature first leaves of the *athb8-11* and -*27* loss-of-function mutants (Prigge et al., 2005) (Table 2.1), and of other genotypes in our study, by means of four descriptors: a cardinality index, a continuity index, and a connectivity index (Verna et al., 2015), and a cyclicity index.

The cardinality index is a proxy for the number of "veins" (i.e. stretches of vascular elements that contact other stretches of vascular elements at least at one of their two ends) in a network. The continuity index quantifies how close a vein network is to a network with the same pattern but in which at least one end of each "vein fragment" (i.e. a stretch of vascular elements that is free of contact with other stretches of vascular elements) contacts a vein. The connectivity index quantifies how close a vein network is to a network with the same pattern but in which both ends of each vein or vein fragment contact other veins. The cyclicity index is a proxy for the number of meshes in a vein network.

Table 2.1. Origin and Nature of Lines.

Line	Origin/Nature
athb8-11	ABRC (CS6969); (Prigge et al., 2005); WT at the *ER* (AT2G26330) locus
athb8-27	ABRC (CS111153)
SHR::miR165a	Transcriptional fusion of *SHR* (AT4G37650; -2505[1] to -10; primers: "SHR HindIII F" and "SHR SalI R") to *miR165a* (AT1G01183; - 138 to +323 relative to the transcriptional start-site; primers: "SalI FWD – MiRNA 165" and "KpnI REV – MiRNA 165")
SHR::mATHB8	(Ohashi-Ito et al., 2013)
SHR::mATHB8:EAR	Translational fusion of SHR::mATHB8 (Ohashi-Ito et al., 2013) (primers: "SalI SHR Promoter FP" and "XhoI mATHB8 RP") to the sequence encoding the EAR portable repressor domain (Hiratsu et al., 2003) (primers: "EAR XhoI + KpnI Forward" and "EAR Reverse")
MP::ATHB8	Transcriptional fusion of *MP* (AT1G19850; -3281 to -1; primers: "MP BamHI Fwd" and "MP KpnI Rev") to the *ATHB8* (AT4G32880) cDNA (GeneBank accession: BT008798; ABRC: U24724; +1 to +2502; primers: "ATHB8 cDNA KpnI FWD" and "ATHB8 cDNA SmaI Rev")
MP::mATHB8	Transcriptional fusion of *MP* (AT1G19850; -3281 to -1; primers: 63 "MP BamHI Fwd" and "MP KpnI Rev") to the *ATHB8* (AT4G32880) cDNA (GeneBank accession: BT008798; ABRC: U24724; +1 to +2502; primers: "ATHB8 cDNA KpnI FWD" and "ATHB8 cDNA SmaI Rev"; "ATHB8mut165FWD" and "ATHB8mut165REV")
ATHB8::nCFP	(Sawchuk et al., 2007)
MP::MP:YFP	Translational fusion of *MP* (AT1G19850; -3281 to +3815; primers: "MP Prom SalI Fwd" and "MP KpnI Rev-2"; "MP 3 kb SalI Fwd" and "MP 3 kb XhoI Rev") to the sequence encoding EYFP (primers: "ECFP AflII F" and "ECFP AflII R"); rescues the root (240/240 seedlings), vein (Fig. 2.2), and inflorescence (160/160 plants) defects of *mp-B4149*
mp-B4149	(Weijers et al., 2005)
RIBO::nCFP	ABRC (CS23898); (Gordon et al., 2007); WT at the *ER* (AT2G26330) locus
ATHB8::nYFP	(Sawchuk et al., 2007)

mp-U55	ABRC (CS8147); (Mayer et al., 1993; Donner et al., 2009)
mp-11	(Odat et al., 2014)
MP::MP	*MP* (AT1G19850; -3281 to +3830; primers: “MP Prom SalI Fwd” and “MP KpnI Rev-2”; “MP 3KB SalI Fwd” and “MP 3kb XhoI Rev”); rescues the root (169/176 seedlings), vein (Fig. 2.2), and inflorescence (6/6 plants) defects of *mp-B4149*
bdl	(Hamann et al., 1999); introgressed into Col-0
MP::VP16:bdlΔI	Transcriptional fusion of *MP* (AT1G19850; -3281 to -1; primers: “MP BamHI Fwd” and “MP KpnI Rev-1”) to a translational fusion of the sequence encoding the activation domain of the *Herpes simplex* virus protein 16 (VP16) (Sadowski et al., 1988) (primers: “VP16 NcoIF2” and “VP16 PstIR”) to a 5’- terminally deleted *bdl* (Hamann et al., 2002) (+94 to +1229; primers: “BDL PstIF” and “BDL BamHIR”; “BDL mut F1”, “BDL mut F2”, “BDL mut F3”, “BDL mut F4”, “BDL PstIF”, and “BDL MfeI mut R”; “BDLd1 PstI F” and “BDL BAMHI R”)
iaa12-1	ABRC (CS25213); (Overvoorde et al., 2005)
tpl-1	ABRC (CS65909); (Long et al., 2002)
MP::MPΔPB1:GR	Translational fusion of *MP* (AT1G19850; -3427 to +2388; primers: “MP SalI Forward – Primer # 2” and “MP EcoRI Reverse”) to the sequence encoding a fragment of the rat glucocorticoid receptor (GR) (Aoyama and Chua, 1997) (primers: “SpeI GR Forward” and “SacII + KpnI (Internal) GR Reverse”)
ATHB8::nQFP	Transcriptional fusion of *ATHB8* (AT4G32880; -2070 to -1; primers: “SalI 2KB ATHB8 Promoter Forward” and “ApaI 2KB ATHB8 Promoter Reverse”) to the sequence encoding 2xmTQ2-N7 (primers: “ApaI 2xmTurqoise Forward” and “KpnI 2xmTFP Reverse”)
R2D2	(Liao et al., 2015)
[TGTCTG]::nYFP	(Donner et al., 2009)
[TAGCTG]::nYFP	(Donner et al., 2009)
[TGTCAG]::nYFP	Transcriptional fusion of *ATHB8* (AT4G32880; -953 to -1; primers: “1NagARE” and “Athb8 R-5”) to the sequence encoding HTA6:EYFP (Zhang et al., 2005)

[TGTCTG]::nYFP	Transcriptional fusion of *ATHB8* (AT4G32880; -953 to -1; primers: “1NcARE” and “Athb8 R-5”) to the sequence encoding HTA6:EYFP (Zhang et al., 2005)

1. Unless otherwise indicated, all coordinates are relative to the translational start-site

The cardinality index of both *athb8-11* and *-27* was lower than that of wild type (WT) (Fig. 2.1A–C,K), suggesting that ATHB8 promotes vein formation.

ATHB8 encodes a transcription factor member of the HOMEODOMAIN-LEUCINE ZIPPER III (HD-ZIP III) family (Baima et al., 1995). To further test whether ATHB8 promoted vein formation and to test whether ATHB8 did so redundantly with other HD-ZIP III proteins, we expressed *microRNA165a* (*miR165a*) — which targets all the *HD-ZIP III* genes (Zhou et al., 2007) — by the *SHORT-ROOT* (*SHR*) promoter — which drives expression in the *ATHB8* expression domain (Gardiner et al., 2011) — in both the WT and *athb8-11* backgrounds.

The cardinality index of SHR::miR165a was lower than that of WT and the cardinality index of SHR::miR165a;*athb8-11* was lower than that of SHR::miR165a (Fig. 2.1D,E,K), supporting that ATHB8 promotes vein formation and suggesting that ATHB8 does so redundantly with other HD-ZIP III proteins.

HD-ZIP III proteins bind DNA as homo- or hetero-dimers (Sessa et al., 1998; Merelo et al., 2016). Therefore, to further test whether ATHB8 promoted vein formation and whether ATHB8 did so redundantly with other HD-ZIP III proteins, we generated a dominant-negative version of the ATHB8 transcriptional activator (Baima et al., 2014) by fusing the *ATHB8* ORF to the sequence encoding the EAR portable repressor domain (Hiratsu et al., 2003). We introduced in the resulting ATHB8:EAR silent mutations that abolish *miR165a*-mediated downregulation (Ohashi-Ito et al., 2013). We expressed the resulting mATHB8:EAR by the *SHR* promoter in both the WT and *athb8-27* backgrounds.

The cardinality index of SHR::mATHB8:EAR was lower than that of WT, and the cardinality index of SHR::mATHB8:EAR;*athb8-27* was lower than that of SHR::mATHB8:EAR

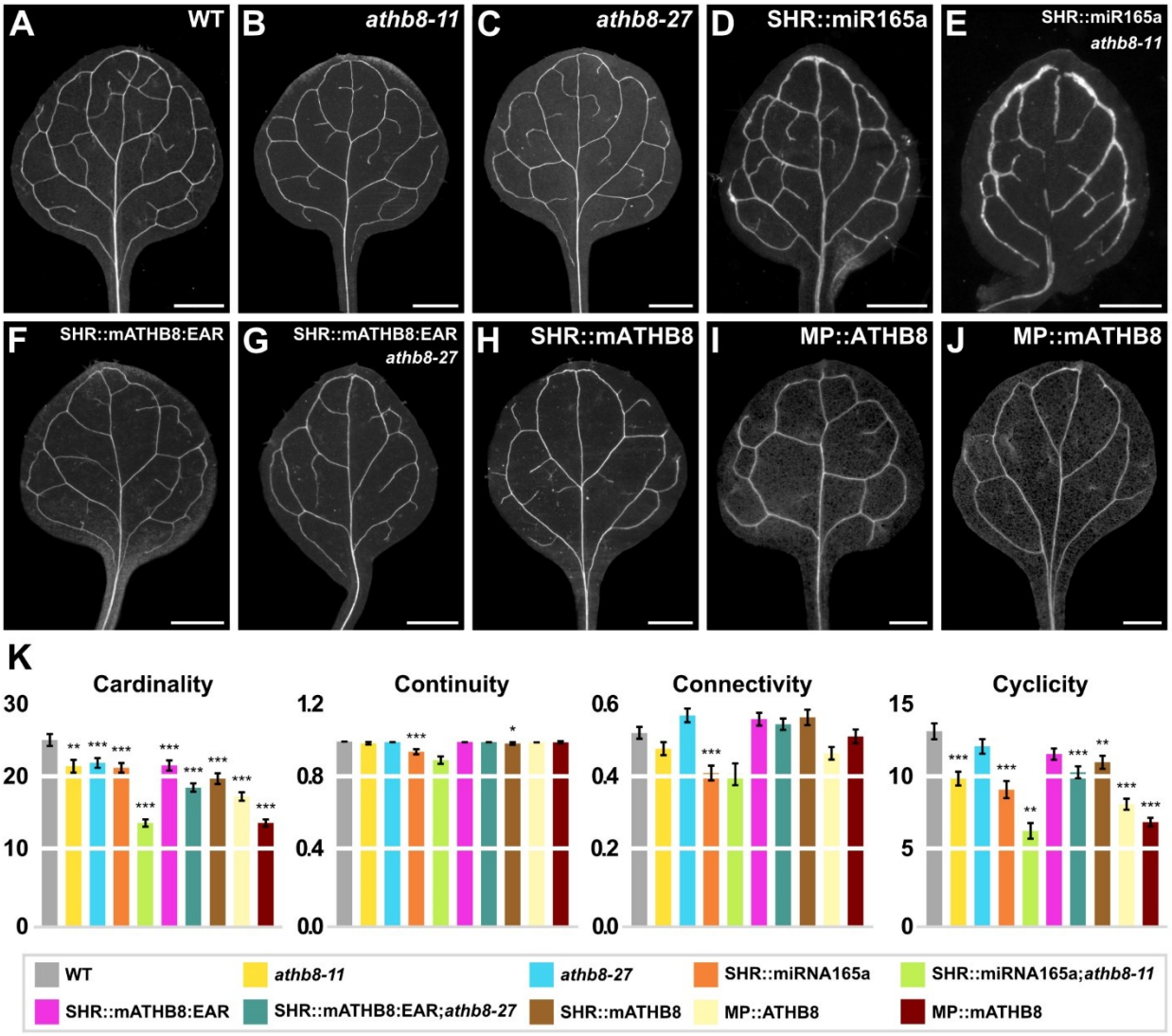

Figure 2.1. *ATHB8* Function in Vein Network Formation.

(A–J) Dark-field illumination of cleared first leaves 14 DAG; top right: genotype. (K) Cardinality, connectivity, and continuity index (mean ± SE) as defined in (Verna et al., 2019) and Materials & Methods; cyclicity index (mean ± SE) as defined in Materials & Methods. Difference between *athb8-11* and WT cardinality indices, between *athb8-27* and WT cardinality indices, between SHR::miR165a and WT cardinality indices, between SHR::miR165a;*athb8-11* and SHR::miR165a cardinality indices, between SHR::mATHB8:EAR and WT cardinality indices, between SHR::mATHB8:EAR;*athb8-27* and SHR::mATHB8:EAR cardinality indices,

between SHR::mATHB8 and WT cardinality indices, between MP::ATHB8 and WT cardinality indices, between MP::mATHB8 and WT cardinality indices, between SHR::miR165a and WT continuity indices, between SHR::mATHB8 and WT continuity indices, between SHR::miR165a and WT connectivity indices, between *athb8-11* and WT cyclicity indices, between SHR::miR165a and WT cyclicity indices, between SHR::miR165a;*athb8-11* and SHR::miR165a cyclicity indices, between SHR::mATHB8:EAR;*athb8-27* and SHR::mATHB8:EAR cyclicity indices, between SHR::mATHB8 and WT cyclicity indices, between MP::ATHB8 and WT cyclicity indices, and between MP::mATHB8 and WT cyclicity indices was significant at $P<0.05$ (*), $P<0.01$ (**), or $P<0.001$ (***) by *F*-test and *t*-test with Bonferroni correction. Sample population sizes: WT, 58; *athb8-11*, 39; *athb8-27*, 32; SHR::miR165a, 51; SHR::miRNA165a;*athb8-11*, 64; SHR::mATHB8:EAR, 38; SHR::mATHB8:EAR;*athb8-27*, 28; SHR::mATHB8, 33; MP::ATHB8, 37; MP::mATHB8, 47. Scale bars: (A,I,J) 0.5 mm; (B,C,F,G,H) 1 mm; (D,E) 0.2 mm.

(Fig. 2.1F,G,K), supporting that ATHB8 promotes vein formation and that ATHB8 does so redundantly with other HD-ZIP III proteins.

We next asked whether levels of *ATHB8* expression and width of *ATHB8* expression domains were relevant to vein formation. To address this question, we used SHR::mATHB8, which overexpresses *ATHB8* in its expression domain; MP::ATHB8, which expresses *ATHB8* in the broader *MP*-expression domain; and MP::mATHB8, which overexpresses *ATHB8* in the *MP* expression domain.

The cardinality index of SHR::mATHB8 was lower than that of WT; the cardinality index of MP::ATHB8 was lower than that of SHR::mATHB8; and the cardinality index of MP::mATHB8 was lower than that of MP::ATHB8 (Fig. 2.1H–K). These results suggest that both levels of *ATHB8* expression and width of *ATHB8* expression domains are relevant to vein formation.

2.2.2. Relation Between *ATHB8* Expression Domains and *MP* Expression Levels

Width of *ATHB8* expression domains is relevant to vein formation (Figure 2.1). Therefore, we asked how *ATHB8* expression is activated in narrow preprocambial domains by the broadly expressed MP. We hypothesized that *ATHB8* preprocambial expression is activated in narrow domains by binding of peak levels of the broadly expressed MP to a low affinity site in the *ATHB8* promoter. This hypothesis predicts that narrow domains of *ATHB8* preprocambial expression correspond to peak levels of MP expression. To test this prediction, we simultaneously imaged expression of ATHB8::nCFP (nuclear CYAN FLUORESCENT PROTEIN expressed by the *ATHB8* promoter) (Sawchuk et al., 2007) and MP::MP:YFP (MP:YFP fusion protein expressed by the *MP* promoter) in first leaves of the strong *mp-B4149* mutant (Weijers et al., 2005), whose defects were rescued by MP::MP:YFP expression (Fig. 2.2A–C) (Table 2.1).

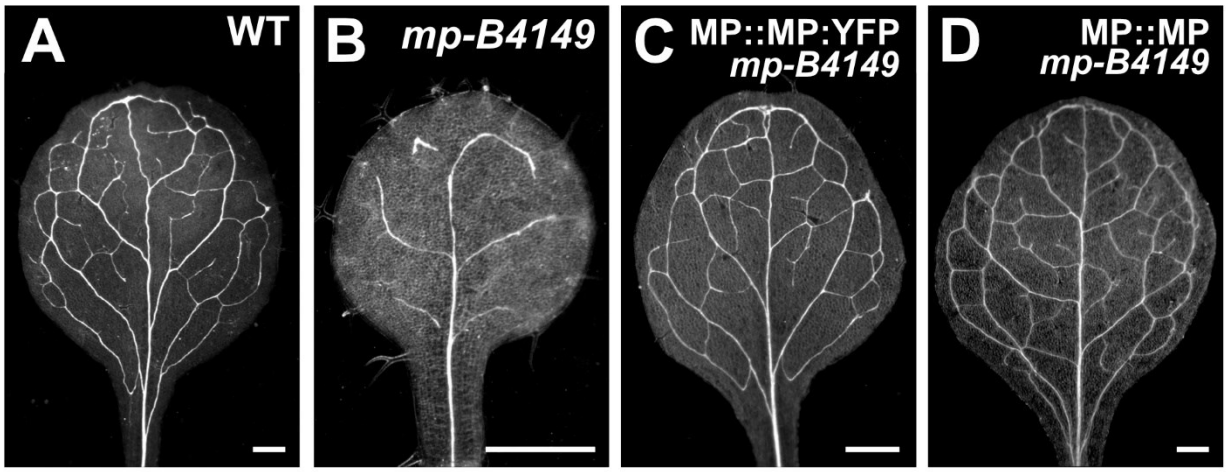

Figure 2.2. MP::MP:YFP and MP::MP Functionalities in Vein Network Formation.

Dark-field illumination of cleared first leaves 14 DAG. Top right: genotype. Scale bars: 0.5 mm.

ATHB8 preprocambial expression can be reproducibly observed in midvein, first loops of veins ("first loops"), and second loops of first leaves, respectively 2, 3, and 4 DAG (Donner et al., 2009; Gardiner et al., 2011; Donner & Scarpella, 2013). At these stages, MP::MP:YFP was expressed in ATHB8::nCFP-expressing cells at higher levels than in cells flanking ATHB8::nCFP-expressing cells (Figure 2.3; Fig. 2.4A,B).

To test whether the differential expression of MP::MP:YFP in ATHB8::nCFP-expressing cells and in cells flanking ATHB8::nCFP-expressing cells were an imaging artifact, we compared expression levels of nCFP driven by a ubiquitously active promoter (RIBO::nCFP) (Gordon et al., 2007) in cells expressing ATHB8::nYFP (Sawchuk et al., 2007) and in cells flanking ATHB8::nYFP-expressing cells. We focused our analysis on second loops of 4-DAG first leaves, in which *ATHB8* preprocambial expression can be reproducibly observed (Donner et al., 2009; Gardiner et al., 2011; Donner and Scarpella, 2013).

Because levels of RIBO::nCFP expression in ATHB8::nYFP-expressing cells were no higher than those in cells flanking ATHB8::nYFP-expressing cells (Fig. 2.4D,E; Figure 2.5), we conclude that the differential expression of MP::MP:YFP in ATHB8::nCFP-expressing cells and in cells flanking ATHB8::nCFP-expressing cells is not an imaging artifact, and therefore that narrow domains of *ATHB8* preprocambial expression correspond to peak levels of MP expression.

2.2.3. Response of *ATHB8* Expression and Vein Network Formation to Changes in *MP* Expression

The hypothesis — that *ATHB8* preprocambial expression is restricted to narrow domains by binding of peak levels of the broadly expressed MP transcription factor to a low affinity site in

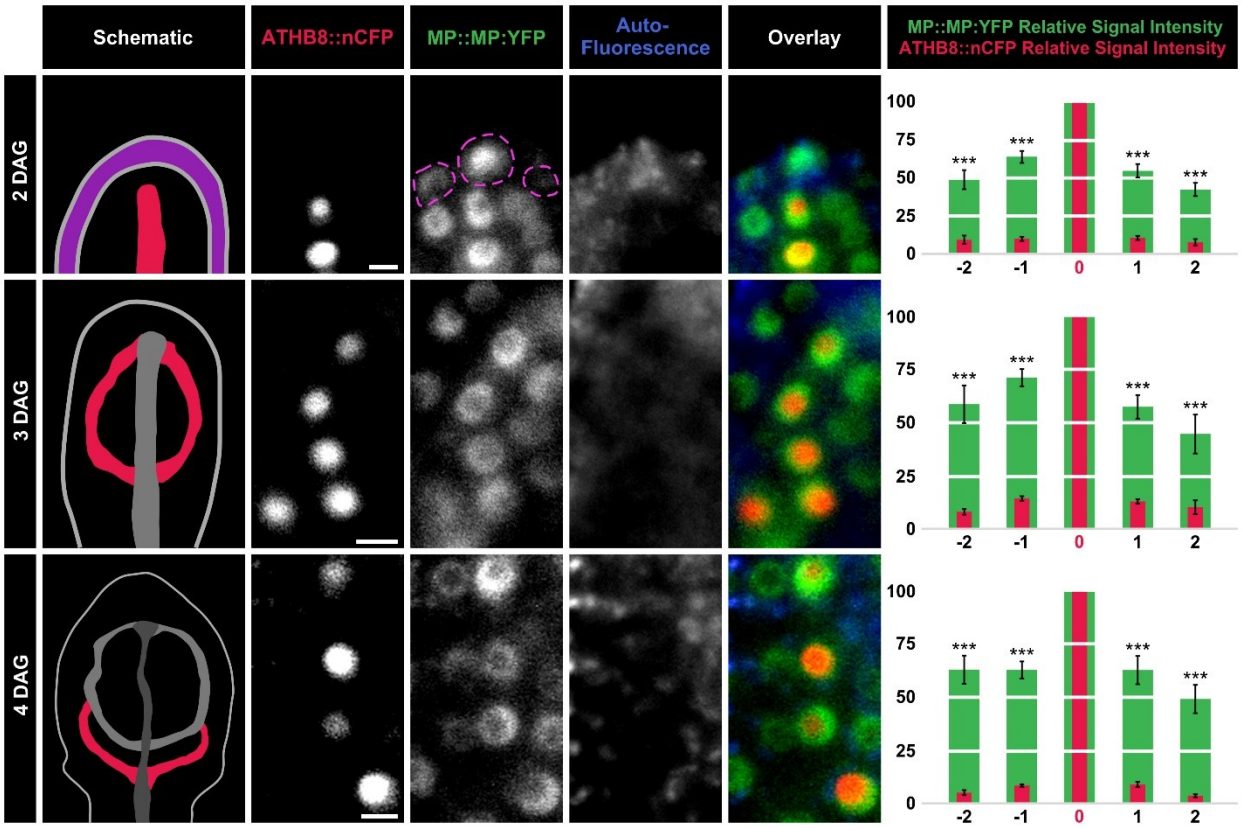

Figure 2.3. *ATHB8* and MP Expression Domains and Levels in Leaf Development.

First leaves 2, 3, and 4 DAG. Column 1: schematics of leaves — imaged in columns 2–5 — illustrating onset of *ATHB8* expression (red) — imaged in column 2 — associated with formation of midvein (2 DAG), first loop (3 DAG), or second loop (4 DAG) (Donner et al., 2009; Gardiner et al., 2011; Donner and Scarpella, 2013); magenta: epidermis; increasingly darker gray: progressively older *ATHB8* expression domains. Columns 2–5: confocal laser scanning microscopy. Column 2: ATHB8::nCFP expression. Column 3: MP::MP:YFP expression; dashed magenta outline: MP::MP:YFP-expressing epidermal nuclei. Column 4: autofluorescence. Column 5: overlays of images in columns 2–4; red: ATHB8::nCFP expression; green: MP::MP:YFP expression; blue: autofluorescence. Column 6: MP::MP:YFP and ATHB8::nCFP expression levels (mean ± SE) in nuclei flanking ATHB8::nCFP-expressing nuclei (positions "- 2", "-1", "1", and "2") relative to MP::MP:YFP and ATHB8::nCFP

expression levels in nuclei co-expressing ATHB8::nCFP (position “0”) during formation of midvein (top), first loop (middle), or second loop (bottom). Difference between MP::MP:YFP expression levels in nuclei at position -2, -1, 1, or 2 and MP::MP:YFP expression levels in nuclei at position 0, and between ATHB8::nCFP expression levels in nuclei at position -2, -1, 1, or 2 and ATHB8::nCFP expression levels in nuclei at position 0 was significant at $P<0.001$ (***) by one-sample *t*-test with Bonferroni correction. Sample population sizes: 35 (2 DAG), 29 (3 DAG), or 31 (4 DAG) leaves; position -2: 30 (2 DAG), 45 (3 DAG), or 50 (4 DAG) nuclei; position -1: 63 (2 DAG), 72 (3 DAG), or 67 (4 DAG) nuclei; position 0: 70 (2 DAG), 75 (3 DAG), or 70 (4 DAG) nuclei; position 1: 58 (2 DAG), 47 (3 DAG), or 59 (4 DAG) nuclei; position 2: 24 (2 DAG), 19 (3 DAG), or 38 (4 DAG) nuclei. Scale bars (shown, for simplicity, only in column 2): 5 μm.

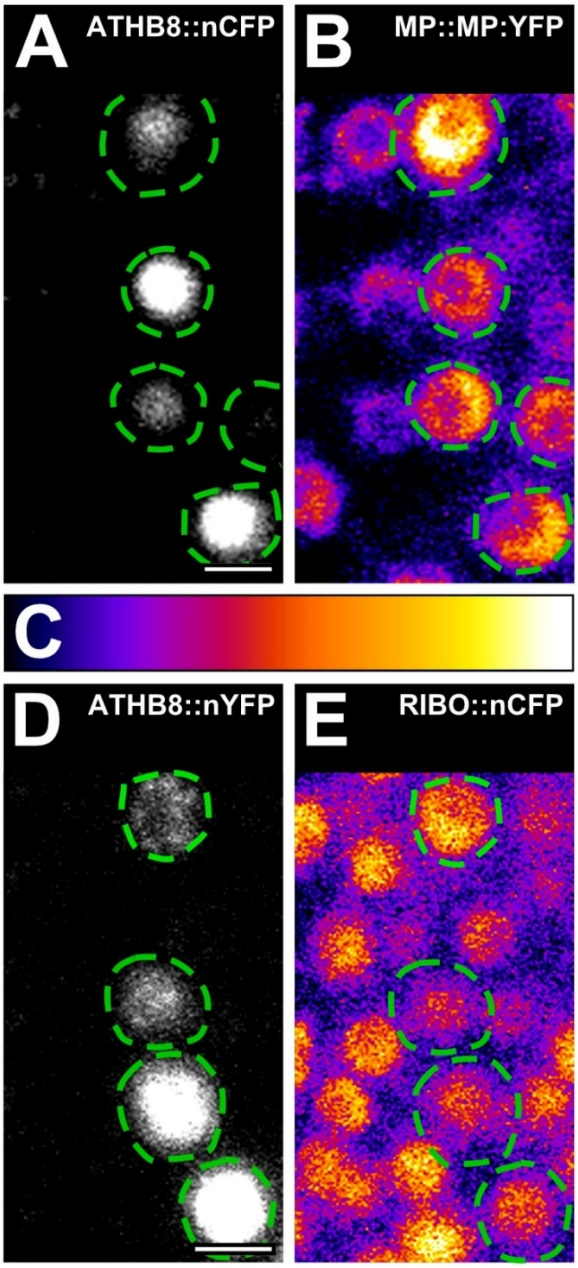

Figure 2.4. *ATHB8* Expression Domains and MP and *RIBO* Expression Levels.

First leaves 4 DAG. Confocal laser scanning microscopy. Top right: reporter. Dashed green outline: second loop nuclei expressing ATHB8::nCFP (A,B) or ATHB8::nYFP (D,E). (B,E) Look-up table — ramp in C — visualizes expression levels. Scale bars (shown, for simplicity, only in A and D): 5 µm.

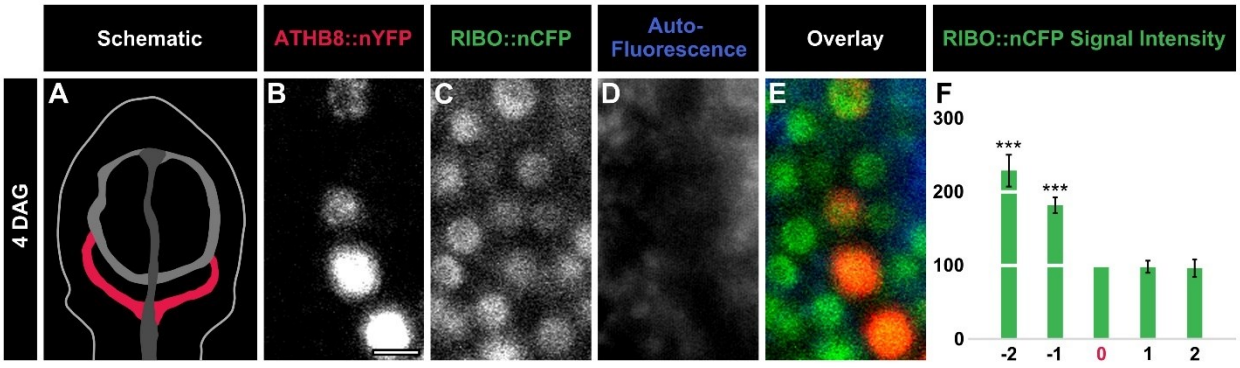

Figure 2.5. *ATHB8* Expression Domains and *RIBO* Expression Levels.

(A–F) First leaves 4 DAG. (A) Schematic of 4-DAG leaf — imaged in B–E — illustrating onset of *ATHB8* expression (red) — imaged in B — associated with second loop formation (Donner et al., 2009; Gardiner et al., 2011; Donner and Scarpella, 2013); increasingly darker gray: progressively older *ATHB8* expression domains. (B–E) Confocal laser scanning microscopy. (B) ATHB8::nYFP expression. (C) RIBO::nCFP expression. (D) Autofluorescence. (E) Overlay of images in B–D; red: ATHB8::nYFP expression; green: RIBO::nCFP expression; blue: autofluorescence. (F) RIBO::nCFP expression levels (mean ± SE) in nuclei at positions -2, -1, 1, and 2 — as defined in legend to Figure 2.3 — relative to RIBO::nCFP expression levels in nuclei at position 0 — as defined in legend to Figure 2.3 — during second loop formation. Difference between RIBO::nCFP expression levels in nuclei at position -2 or -1 and RIBO::nCFP expression levels in nuclei at position 0 was significant at $P<0.001$ (***) by one-sample *t*-test with Bonferroni correction. Sample population sizes: 26 leaves; position -2, 42 nuclei; position -1, 64 nuclei; position 0, 69 nuclei; position 1, 50 nuclei; position 2, 28 nuclei. Scale bars (shown, for simplicity, only in column 2): 5 μm.

the *ATHB8* promoter — predicts that loss of *MP* function will lead to extremely weak, or altogether absent, *ATHB8* preprocambial expression, otherwise normally visible in second loops of 4-DAG first leaves (Donner et al., 2009; Gardiner et al., 2011; Donner and Scarpella, 2013). To test this prediction, we quantified ATHB8::nYFP expression levels in second loops of 4-DAG first leaves of the strong *mp-U55* mutant (Mayer et al., 1993; Donner et al., 2009).

Consistent with previous observations (Donner et al., 2009), ATHB8::nYFP expression levels were greatly reduced in *mp-U55*, leading to near-complete loss of ATHB8::nYFP preprocambial expression (Fig. 2.6A,B,F). Moreover, consistent with previous observations (Przemeck et al., 1996; Donner et al., 2009), near-complete loss of *ATHB8* preprocambial expression in *mp-U55* developing leaves was associated with networks of fewer meshes and fewer, less frequently continuous, and less frequently connected veins in *mp-U55* mature leaves (Fig. 2.6G,H,K).

The hypothesis further predicts that lower levels of *MP* expression will lead to lower levels of *ATHB8* preprocambial expression. To test this prediction, we quantified ATHB8::nYFP expression levels in second loops of 4-DAG first leaves of the weak *mp-11* mutant, in which an insertion in the *MP* promoter (Odat et al., 2014) leads to ~85% reduction in levels of WT *MP* transcript (Figure 2.7).

In *mp-11*, ATHB8::nYFP expression levels were lower and expression along the domain was more heterogeneous than in WT, leading to seemingly fragmented domains of weak ATHB8::nYFP preprocambial expression (Fig. 2.6A,C,F). Moreover, like in *mp-U55*, defects in *ATHB8* expression in *mp-11* developing leaves were associated with networks of fewer meshes and fewer, less frequently continuous, and less frequently connected veins in *mp-11* mature leaves (Fig. 2.6G,I,K). However, the vein network and *ATHB8* expression defects of *mp-11* were weaker than those of *mp-U55* (Fig. 2.6A–C,G–I,K).

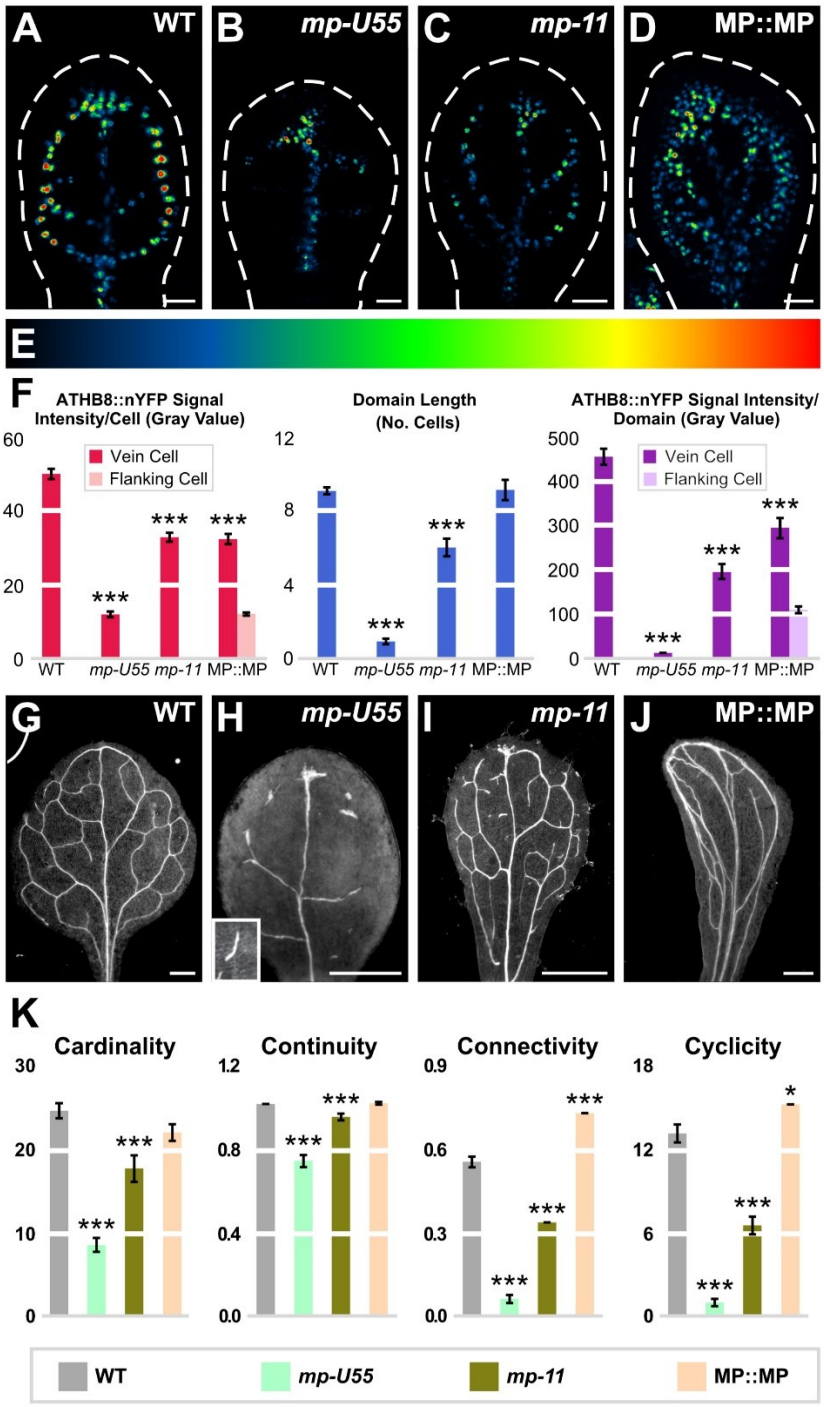

Figure 2.6. *MP* Expression, *ATHB8* Expression Domains and Levels, and Vein Network Formation.

(A–D,G–J) Top right: genotype. (A–D) First leaves 4 DAG; confocal laser scanning microscopy; dashed white line: leaf outline; ATHB8::nYFP expression (look-up table — ramp in E —

visualizes expression levels). (F) ATHB8::nYFP expression level per cell expressed as mean gray value ± SE, ATHB8::nYFP expression domain length expressed as mean number of cells ± SE, and ATHB8::nYFP expression levels per domain expressed as mean gray value ± SE. Difference between *mp-U55* and WT, between *mp-11* and WT, and between MP::MP and WT was significant at $P<0.001$ (***) by *F*-test and *t*-test with Bonferroni correction. Sample population sizes: 25 (WT), 72 (*mp-U55*), 27 (*mp-11*), or 24 (MP::MP) leaves; 345 (WT), 128 (*mp-U55*), 325 (*mp-11*), or 219 (MP::MP) vein cell nuclei, and 513 (MP::MP) flanking cell nuclei. (G–J) Dark-field illumination of cleared first leaves 14 DAG. (K) Cardinality index, connectivity index, and continuity index (mean ± SE) as defined in (Verna et al., 2019) and Materials & Methods; cyclicity index (mean ± SE) as defined in Materials & Methods. Difference between *mp-U55* and WT cardinality indices, between *mp-11* and WT cardinality indices, between *mp-U55* and WT continuity indices, between *mp-11* and WT continuity indices, between *mp-U55* and WT connectivity indices, between *mp-11* and WT connectivity indices, between MP::MP and WT connectivity indices, between *mp-U55* and WT cyclicity indices, between *mp-11* and WT cyclicity indices, and between MP::MP and WT cyclicity indices was significant at $P<0.05$ (*) or $P<0.001$ (***) by *F*-test and *t*-test with Bonferroni correction. Sample population sizes: WT, 39; *mp-U55*, 59; *mp-11*, 44; MP::MP, 41. Scale bars: (A–D) 25 μm; (G-J) 0.5 mm.

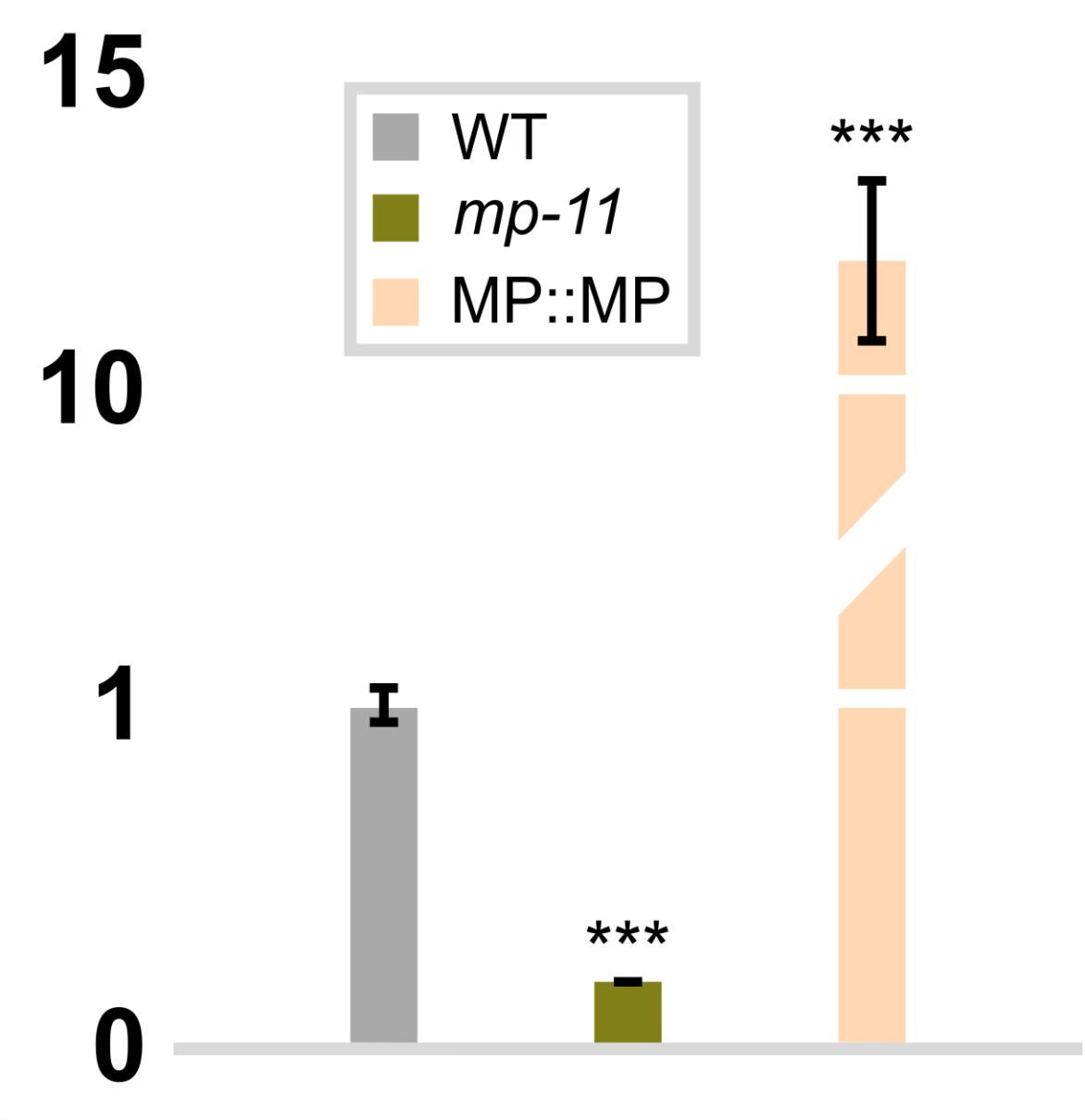

Figure 2.7. *mp-11* and MP::MP Effects on MP Expression.

MP transcript levels in *mp-11* and MP::MP seedlings relative to *MP* transcript levels in WT (mean ± SE of three technical replicates for each of three biological replicates); seedlings 4 DAG; RT-qPCR. Difference between *mp-11* and WT, and between MP::MP and WT was significant at $P<0.001$ (***) by *F*-test and *t*-test with Bonferroni correction

The hypothesis also predicts that higher levels of the broadly expressed MP will lead to higher levels of *ATHB8* preprocambial expression in both vein and flanking cells, leading to broader *ATHB8* expression domains. To test this prediction, we overexpressed *MP* by its own promoter (MP::MP) — which led to ~10-fold increase in *MP* expression levels (Figure 2.7) which rescued defects of the strong *mp-B4149* mutant (Fig. 2.2A,B,D) (Table 2.1) — and quantified ATHB8::nYFP expression levels in second loops of 4-DAG MP::MP first leaves.

In MP::MP, ATHB8::nYFP expression levels were higher in flanking cells, leading to broader ATHB8::nYFP expression domains; however, ATHB8::nYFP expression levels were lower in vein cells (Fig. 2.6A,D,F). Nevertheless, broader *ATHB8* expression domains in MP::MP developing leaves were associated with abnormal vein networks in MP::MP mature leaves: veins ran close to one another for varying stretches of the narrow leaf laminae, then diverged, and either ran close to other veins or converged back to give rise to elongated meshes (Fig. 2.6G,J,K).

In summary, lower levels of *MP* expression lead to fragmented domains of *ATHB8* preprocambial expression, and loss of *MP* function leads to near-complete loss of *ATHB8* preprocambial expression. These observations are consistent with the hypothesis and suggest that *MP* expression levels below a minimum threshold are unable to activate *ATHB8* preprocambial expression. However, that higher levels of *MP* expression fail to lead to higher levels of *ATHB8* preprocambial expression in vein cells is inconsistent with the hypothesis and suggests that *MP* expression levels above a maximum threshold both activate and repress *ATHB8* preprocambial expression. These observations are unaccounted for by the hypothesis; therefore, the hypothesis must be revised.

2.2.4. Response of *ATHB8* Expression and Vein Network Formation to Changes in MP Activity

MP expression levels above a maximum threshold both activate and repress *ATHB8* preprocambial expression (Figure 2.6). Activation of *ATHB8* preprocambial expression by MP is direct (Donner et al., 2009), but repression of *ATHB8* preprocambial expression by MP need not be: Repression of *ATHB8* preprocambial expression by MP could be mediated by BODENLOS (BDL)/ IAA12, whose expression is activated by MP and which binds to MP and inhibits its transcriptional activity (Hamann et al., 2002; Hardtke et al., 2004; Weijers et al., 2005; Lau et al., 2011). Were repression of *ATHB8* preprocambial expression by MP mediated by BDL, *ATHB8* preprocambial expression would be reduced in the *bdl* mutant, in which the unstable BDL/IAA12 protein is stabilized (Dharmasiri et al., 2005). To test this prediction, we quantified ATHB8::nYFP expression levels in second loops of 4-DAG first leaves of the *bdl* mutant.

Like in *mp*, in *bdl* ATHB8::nYFP expression levels were lower and expression along the domain was more heterogeneous than in WT, leading to seemingly fragmented domains of weak ATHB8::nYFP preprocambial expression (Fig. 2.6A–C,F; Fig. 2.8A,B,G). Moreover, like in *mp*, defects in *ATHB8* expression in *bdl* developing leaves were associated with networks of fewer meshes and fewer, less frequently continuous, and less frequently connected veins in *bdl* mature leaves (Fig. 2.6G–I,K; Fig. 2.8H,I,M).

Were repression of *ATHB8* preprocambial expression by MP mediated by BDL, reducing or eliminating inhibition of MP transcriptional activity by BDL would lead to higher levels of *ATHB8* preprocambial expression in both vein and flanking cells, leading to broader *ATHB8* expression domains. To test this prediction, we turned the unstable BDL/IAA12 transcriptional

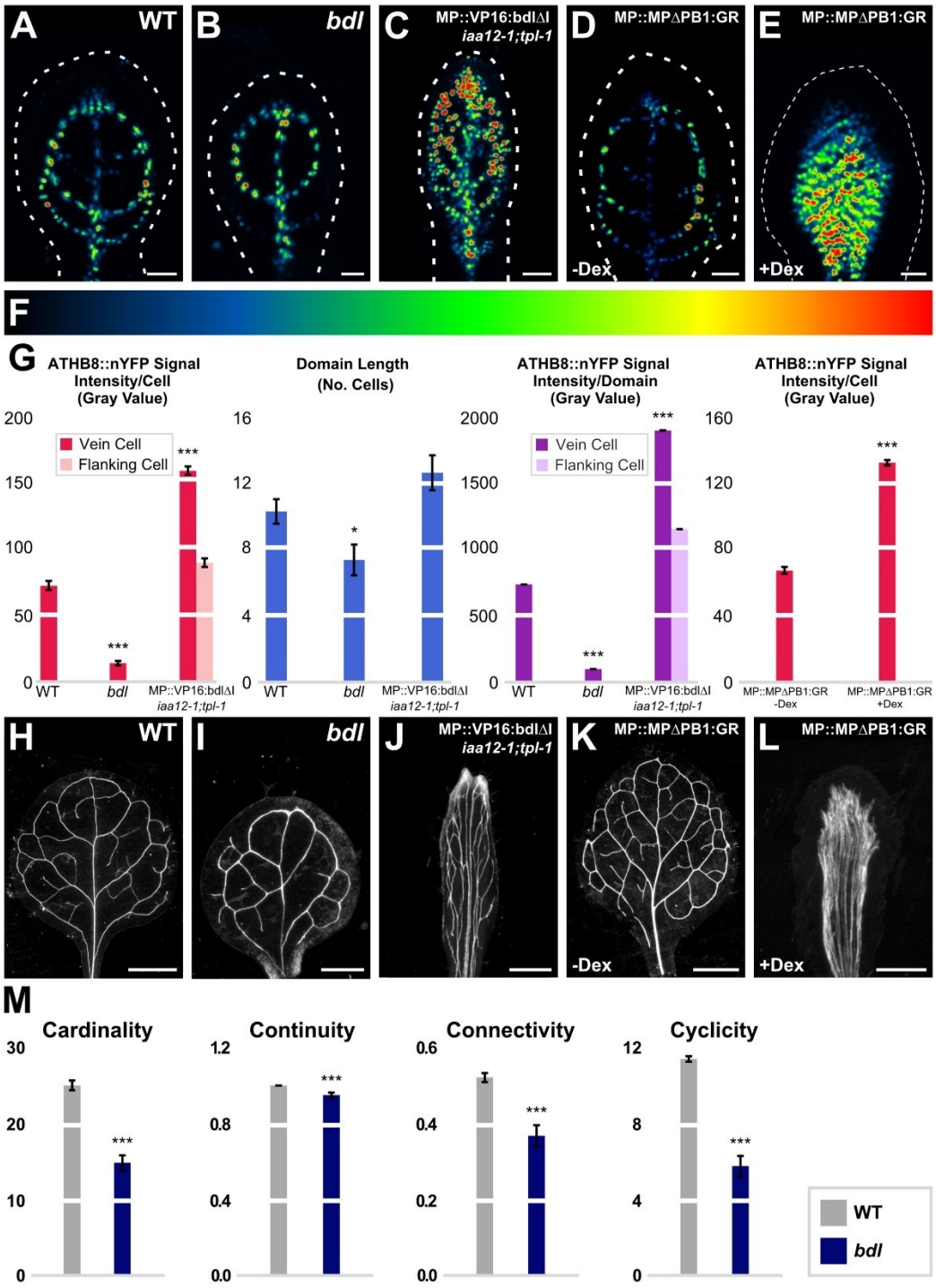

Figure 2.8. MP Activity, *ATHB8* Expression Domains and Levels, and Vein Network Formation.

(A–E,H–L) Top right: genotype. (A–E) First leaves 4 DAG; confocal laser scanning microscopy; dashed white line: leaf outline; ATHB8::nYFP expression (look-up table — ramp in F —

visualizes expression levels). (G) ATHB8::nYFP expression level per cell expressed as mean gray value ± SE, ATHB8::nYFP expression domain length expressed as mean number of cells ± SE, and ATHB8::nYFP expression levels per domain expressed as mean gray value ± SE. Difference between *bdl* and WT, between MP::VP16:bdlΔI;*iaa12-1*;*tpl-1* and WT, and between dex-grown MP::MPΔPB1:GR and MP::MPΔPB1:GR was significant at $P<0.05$ (*) or $P<0.001$ (***) by *F*-test and *t*-test with Bonferroni correction. Sample population sizes: 26 (WT), 27 (*bdl*), 27 (MP::VP16:bdlΔI;*iaa12-1*;*tpl-1*), 18 (MP::MPΔPB1:GR), or 19 (dex-grown MP::MPΔPB1:GR) leaves; 265 (WT), 199 (*bdl*), 338 (MP::VP16:bdlΔI;*iaa12-1*;*tpl-1*), 248 (MP::MPΔPB1:GR), or 269 (dex-grown MP::MPΔPB1:GR) vein cell nuclei, and 316 (MP::VP16:bdlΔI;*iaa12-1*;*tpl-1*) flanking cell nuclei. (H-L) Dark-field illumination of cleared first leaves 14 DAG. (M) Cardinality index, connectivity index, and continuity index (mean ± SE) as defined in (Verna et al., 2019a) and Materials & Methods; cyclicity index (mean ± SE) as defined in Materials & Methods. Difference between *bdl* and WT cardinality indices, between *bdl* and WT continuity indices, between *bdl* and WT connectivity indices, and between *bdl* and WT cyclicity indices, was significant at $P<0.001$ (***) by *F*-test and *t*-test with Bonferroni correction. Sample population sizes: WT, 30; *bdl*, 65; MP::VP16:bdlΔI;*iaa12-1*;*tpl-1*, 22; MP::MPΔPB1:GR, 42; dex-grown MP::MPΔPB1:GR, 38. Scale bars: (A-E) 25 μm; (I) 0.25 mm; (J) 0.5 mm; (H,K,L) 1 mm.

repressor into a stabilized transcriptional activator as previously done for other IAA proteins (Tiwari et al, 2001; Tiwari et al., 2003; Li et al, 2009): we replaced the repressor domain of BDL/IAA12 (Li et al., 2011) with the activator domain of the *Herpes simplex* Virus Protein 16 (VP16) (Sadowski et al., 1988) and introduced a mutation that lengthens the half-life of BDL/IAA12 (Hamann et al., 2002). We expressed the resulting VP16:bdlΔI by the *MP* promoter in the *iaa12-1*;*tpl-1* double mutant, which lacks *BDL*/*IAA12* function (Overvoorde et al., 2005) and partially lacks the co-repressor function that mediates the IAA-protein-dependent repression of MP (Szemenyei et al., 2008). We quantified ATHB8::nYFP expression levels in second loops of 4-DAG first leaves of the resulting MP::VP16:bdllΔI;*iaa12-1*;*tpl-1* background.

Like in MP::MP, in MP::VP16:bdlΔI;*iaa12-1*;*tpl-1* ATHB8::nYFP expression levels were higher in flanking cells (Fig. 2.6A,D,F; Fig. 2.8A,C,G). Unlike in MP::MP, however, in MP::VP16:bdlΔI;*iaa12-1*;*tpl-1* ATHB8::nYFP expression levels were also higher in vein cells (Fig. 2.6A,D,F; Fig. 2.8A,C,G). Accordingly, stronger *ATHB8* expression domains in MP::VP16:bdlΔI;*iaa12-1*;*tpl-1* developing leaves were associated with stronger — though qualitatively similar — vein network defects in MP::VP16:bdlΔI;*iaa12-1*;*tpl-1* mature leaves: in the middle of these leaves, veins ran parallel to one another for the entire length of the narrow leaf laminae to give rise to wide midveins; toward the margin, veins ran close to one another for varying stretches of the laminae, then diverged, and either ran close to other veins or converged back to give rise to elongated meshes (Fig. 2.6G,J,K; Fig. 2.8H,J).

Next, we further tested the prediction that reducing or eliminating inhibition of MP transcriptional activity by BDL would lead to higher levels of *ATHB8* preprocambial expression in both vein and flanking cells, leading to broader *ATHB8* expression domains. As previously done (Krogan et al., 2012; Smetana et al., 2019; Amalraj et al., 2020), we created an irrepressible

version of MP by deleting its PB1 domain, which is required for IAA-protein-mediated repression (Tiwari et al., 2003; Wang et al., 2005; Krogan et al., 2012; Korasick et al., 2014). We fused the resulting MPΔPB1 to a fragment of the rat glucocorticoid receptor (GR) (Picard et al., 1988) to confer dexamethsone (dex)-inducibility, expressed the resulting MPΔPB1:GR by the *MP* promoter, and quantified ATHB8::nYFP expression levels in 4-DAG first leaves of the dex-grown MP::MPΔPB1:GR background.

Consistent with previous observations (Garrett et al., 2012; Krogan et al., 2012), in dex-grown MP::MPΔPB1:GR ATHB8::nYFP expression was no longer restricted to narrow domains; instead, ATHB8::nYFP was expressed at higher levels in broad domains than spanned almost the entire width of the leaves (Fig. 2.8D,E,G). Accordingly, broader and stronger *ATHB8* expression domains in dex-grown MP::MPΔPB1:GR developing leaves were associated with veins running parallel to one another for the entire length of the narrow leaf laminae to give rise to midveins that spanned almost the entire width of dex-grown MP::MPΔPB1:GR mature leaves (Fig. 2.8H,K,L).

In conclusion, our results are consistent with the hypothesis that *MP* expression levels above a maximum threshold both activate and repress *ATHB8* preprocambial expression and that such repression of *ATHB8* preprocambial expression by MP is mediated by BDL/IAA12.

2.2.5. Relation Between *ATHB8* Expression Domains and Auxin Levels

IAA proteins, including BDL/IAA12, are degraded in response to auxin (Gray et al., 2001; Tiwari et al., 2001; Zenser et al., 2001; Dharmasiri et al., 2005). Auxin-dependent degradation of BDL/IAA12 and other IAA proteins releases MP from inhibition, thus allowing MP to activate expression of its targets, including *BDL*/*IAA12* and *ATHB8* (Hardtke et al., 2004; Weijers et al., 2005; Weijers et al., 2006; Donner et al., 2009; Ploense et al., 2009; Schlereth et al., 2010; Lau et

al., 2011; Garrett et al., 2012; Krogan et al., 2012; Krogan et al., 2014; Wu et al., 2015). Therefore, domains of *ATHB8* preprocambial expression should correspond to peak levels of auxin. To test this prediction, we simultaneously imaged in midvein, first loops, and second loops of developing first leaves expression of ATHB8::nQFP (nuclear TURQUOISE FLUORESCENT PROTEIN expressed by the *ATHB8* promoter) and of the auxin ratiometric reporter R2D2 (Liao et al., 2015), which expresses an auxin-degradable nYFP and a non-auxin-degradable nRFP by the *RIBOSOMAL PROTEIN S5A* promoter, which is highly active in developing leaves (Weijers et al., 2001). In the R2D2 reporter, a high RFP/YFP ratio thus indicates high levels of auxin, whereas a low RFP/YFP ratio indicates low levels of auxin (Liao et al., 2015).

At all tested stages, the RFP/YFP ratio was higher in ATHB8::nQFP-expressing cells than in cells flanking ATHB8::nQFP-expressing cells (Figure 2.9), suggesting that — consistent with previous observations (Scarpella et al., 2004) — domains of *ATHB8* preprocambial expression correspond to peak levels of auxin.

2.2.6. Response of *ATHB8* Expression to Manipulation of MP-Binding Site Affinity

The hypothesis that *MP* expression levels below a minimum threshold are unable to activate *ATHB8* preprocambial expression predicts that reducing the affinity of MP for its binding site in the *ATHB8* promoter will lead to extremely weak, or altogether absent, *ATHB8* preprocambial expression.

To test this prediction, we mutated the MP-binding site in the *ATHB8* promoter (TGTCTG) to lower (TGTCAG) or negligible (TAGCTG) affinity for MP-binding (Ulmasov et al., 1997; Ulmasov et al., 1999; Donner et al., 2009), and imaged nYFP expressed by the native or mutant promoters in second loops of 4-DAG first leaves.

Mutation of the MP-binding site in the *ATHB8* promoter to negligible affinity for MP-

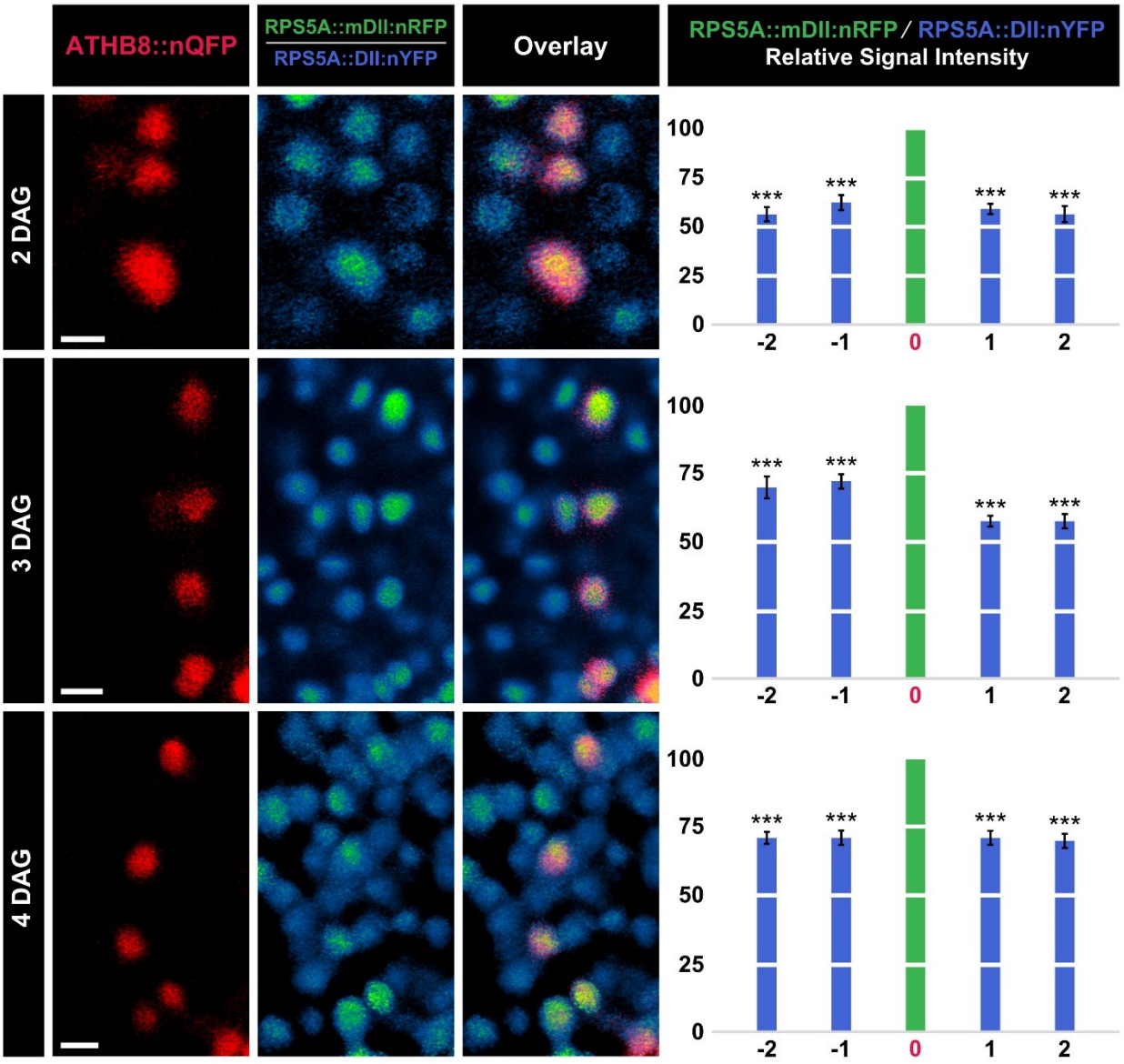

Figure 2.9. *ATHB8* Expression Domains and Auxin Levels.

First leaves 2, 3, and 4 DAG. Columns 1–3: confocal laser scanning microscopy. Column 1: ATHB8::nQFP expression (red) associated with formation of midvein (2 DAG), first loop (3 DAG), or second loop (4 DAG) (Donner et al., 2009; Gardiner et al., 2011; Donner and Scarpella, 2013). Column 2: Ratio of RPS5A::mDII:nRFP expression to RPS5A::DII:nYFP expression. Look-up table visualizes expression ratio levels: high

RPS5A::mDII:nRFP/RPS5A::DII:nYFP ratio (green) indicates high auxin levels; low RPS5A::mDII:nRFP/RPS5A::DII:nYFP ratio (blue) indicates low auxin levels. Column 3: overlays of images in columns 1 and 2; blue: low RPS5A::mDII:nRFP/RPS5A::DII:nYFP ratio, i.e. low auxin levels; yellow: co-expression of ATHB8::nQFP (red) and high RPS5A::mDII:nRFP/RPS5A::DII:nYFP ratio (green), i.e. high auxin levels. Column 4: Ratio of RPS5A::mDII:nRFP expression levels to RPS5A::DII:nYFP expression levels (mean ± SE) in nuclei flanking ATHB8::nQFP-expressing nuclei (positions "- 2", "-1", "1", and "2") relative to ratio of RPS5A::mDII:nRFP expression levels to RPS5A::DII:nYFP expression levels in nuclei co-expressing ATHB8::nQFP (position "0") during formation of midvein (top), first loop (middle), or second loop (bottom). Difference between ratio of RPS5A::mDII:nRFP expression levels to RPS5A::DII:nYFP expression levels in nuclei at position -2, -1, 1, or 2 and ratio of RPS5A::mDII:nRFP expression levels to RPS5A::DII:nYFP expression levels in nuclei at position 0 was significant at $P<0.001$ (***) by one-sample *t*-test with Bonferroni correction. Sample population sizes: 26 (2 DAG), 27 (3 DAG), or 29 (4 DAG) leaves; position -2: 56 (2 DAG), 42 (3 DAG), or 60 (4 DAG) nuclei; position -1: 52 (2 DAG), 37 (3 DAG), or 58 (4 DAG) nuclei; position 0: 74 (2 DAG), 85 (3 DAG), or 102 (4 DAG) nuclei; position 1: 44 (2 DAG), 44 (3 DAG), or 62 (4 DAG) nuclei; position 2: 42 (2 DAG), 25 (3 DAG), or 44 (4 DAG) nuclei. Scale bars (shown, for simplicity, only in column 2): 5 μm.

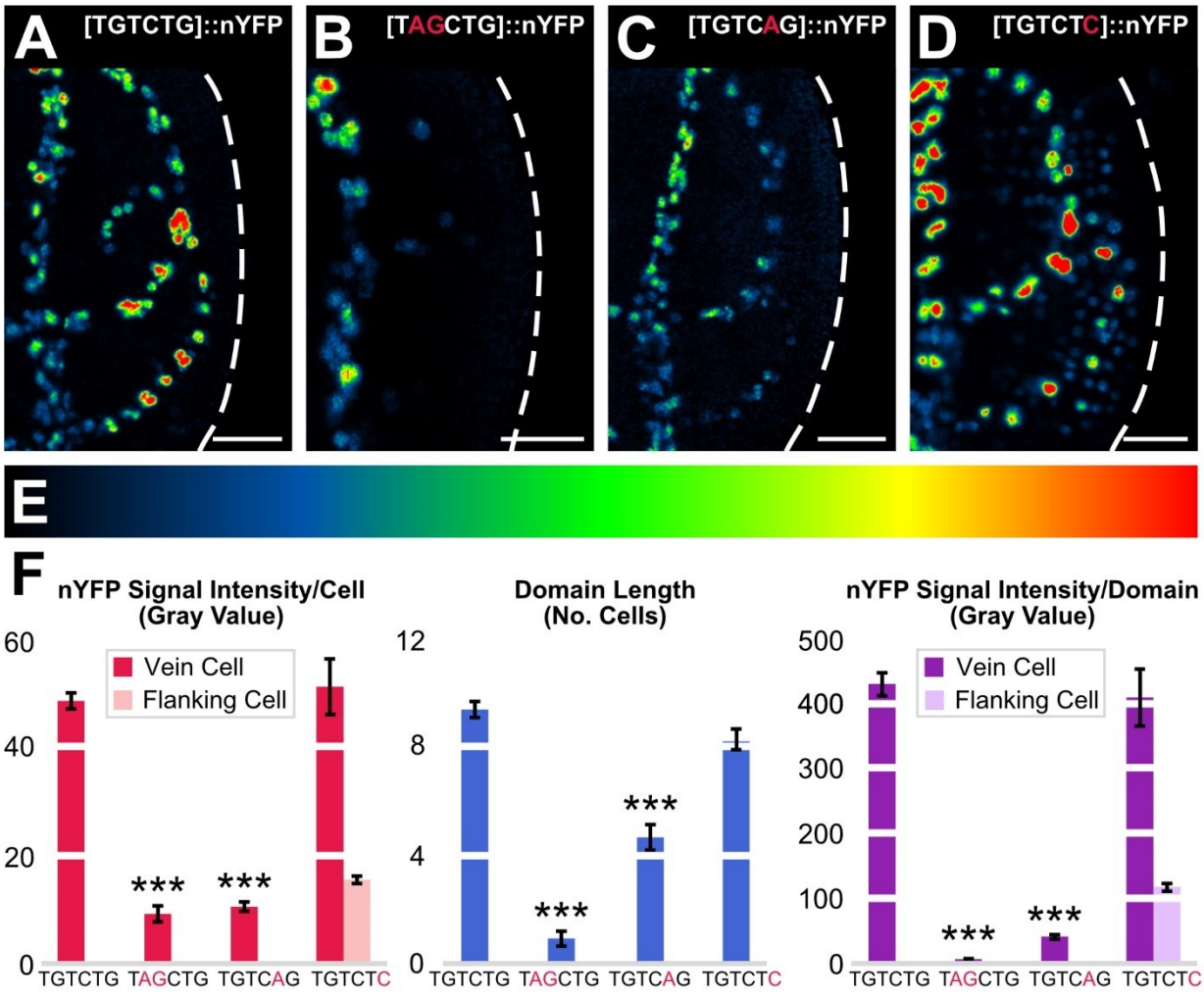

Figure 2.10. Activity of *ATHB8* Promoter Variants.

(A–D) First leaves 4 DAG; confocal laser scanning microscopy; nYFP expression (look-up table — ramp in E — visualizes expression levels) driven by promoter variants (top right) with native ([TGTCTG]::nYFP≡ATHB8::nYFP) (A), negligible ([TAGCTG]::nYFP) (B), lower ([TGTCAG]::nYFP) (C), or higher ([TGTCTC]::nYFP) (D) affinity for MP-binding. Dashed white line: leaf outline. (F) nYFP expression level per cell expressed as mean gray value ± SE, nYFP expression domain length expressed as mean number of cells ± SE, and nYFP expression level per domain expressed as mean gray value ± SE. Difference between [TAGCTG]::nYFP and ([TGTCTG]::nYFP, and between [TGTCAG]::nYFP and ([TGTCTG]::nYFP was significant at

P<0.001 (***) by *F*-test and *t*-test with Bonferroni correction. Sample population sizes: 21 ([TGTCTG]::nYFP), 22 ([TAGCTG]::nYFP), 21 ([TGTCAG]::nYFP), or 16 ([TGTCTC]::nYFP) leaves; 391 ([TGTCTG]::nYFP), 41 ([TAGCTG]::nYFP), 194 ([TGTCAG]::nYFP), or 261 ([TGTCTC]::nYFP) vein cell nuclei, and 611 ([TGTCTC]::nYFP) flanking cell nuclei. Scale bars: 25 μm.

binding led to greatly reduced levels of nYFP expression (Fig. 2.10A,B,F), resembling near-complete loss of ATHB8::nYFP preprocambial expression in *mp-U55* (Donner et al., 2009) (Fig. 2.6A,B,F). Mutation of the MP-binding site in the *ATHB8* promoter to lower affinity for MP-binding led to lower levels of nYFP expression (Fig. 2.10A,C,F). Furthermore, expression along the domains was more heterogeneous than when nYFP was expressed by the native promoter (Fig. 2.10A,C,F), leading to seemingly fragmented domains of weak nYFP expression similar to those in *mp-11* (Fig. 2.6A,C,F) and *bdl* (Fig. 2.8A,B,G).

The hypothesis that *MP* expression levels above a maximum threshold both activate and repress *ATHB8* preprocambial expression predicts that increasing the affinity of MP for its binding site in the *ATHB8* promoter will lead to higher levels of *ATHB8* preprocambial expression in flanking cells, leading to broader *ATHB8* expression domains, and to levels of *ATHB8* preprocambial expression in vein cells that are no lower — though not necessarily any higher — than those in WT.

To test this prediction, we mutated the MP-binding site in the *ATHB8* promoter (TGTCTG) to higher (TGTCTC) affinity for MP-binding (Ulmasov et al., 1997; Ulmasov et al., 1999; Donner et al., 2009), and imaged nYFP expressed by the native or mutant promoter in second loops of 4-DAG first leaves.

Mutation of the MP-binding site in the *ATHB8* promoter to higher affinity for MP-binding led to higher levels of nYFP expression in flanking cells (Fig. 2.10A,D,F), resulting in broader domains of nYFP expression similar to those in MP::MP (Fig. 2.6A,D,F) and, to a lesser extent, MP::VP16:bdlΔI;*iaa12-1*;*tpl-1* (Fig. 2.8A,C,G) and dex-grown MP::MPΔPB1:GR (Fig. 8D,E,G). However, unlike in MP::MP — in which ATHB8::nYFP expression levels in vein cells were lower than in WT (Fig. 2.6A,D,F) — and MP::VP16:bdlΔI;*iaa12-1*;*tpl-1* and dex-grown

MP::MPΔPB1:GR — in which those levels were higher (Fig. 2.8A,C–E,G) — nYFP expression levels in vein cells were unchanged by mutation of the MP-binding site in the *ATHB8* promoter to higher affinity for MP-binding (Fig. 2.10A,D,F).

In conclusion, our results are consistent with the hypothesis that *MP* expression levels below a minimum threshold are unable to activate *ATHB8* preprocambial expression and that *MP* expression levels above a maximum threshold both activate and repress *ATHB8* preprocambial expression.

2.2.7. An Incoherent Feedforward Loop Activating Gene Expression in Narrow Domains

Consistent with interpretation of similar findings in animals (e.g., (Bellusci et al., 1997; Latinkić et al., 1997; Sato and Saigo, 2000)), our results suggest that an incoherent type-I feedforward loop (Mangan and Alon, 2003) restricts activation of expression of the plant gene *ATHB8* in narrow preprocambial domains and leads to vein network formation (Figure 2.11). Auxin activates *MP*, which in turn activates expression of intermediate-loop *AUX*/*IAA* genes like *BDL*/*IAA12*. Both *MP* and *AUX*/*IAA* genes jointly regulate expression of *ATHB8*, which converts the auxin signal input into vein-network formation output.

In the future, it would be interesting to understand what generates peaks of auxin and MP levels. However, already now, our results suggest a mechanism by which in plants a broadly expressed transcription factor activates target gene expression in narrow domains. The very same regulatory mechanism that controls activation of *ATHB8* expression in single files of preprocambial cells is most frequently used in animals to generate stripes of gene expression (Cotterell and Sharpe, 2010), suggesting unexpected conservation of regulatory logic of striped gene expression in multicellular organisms.

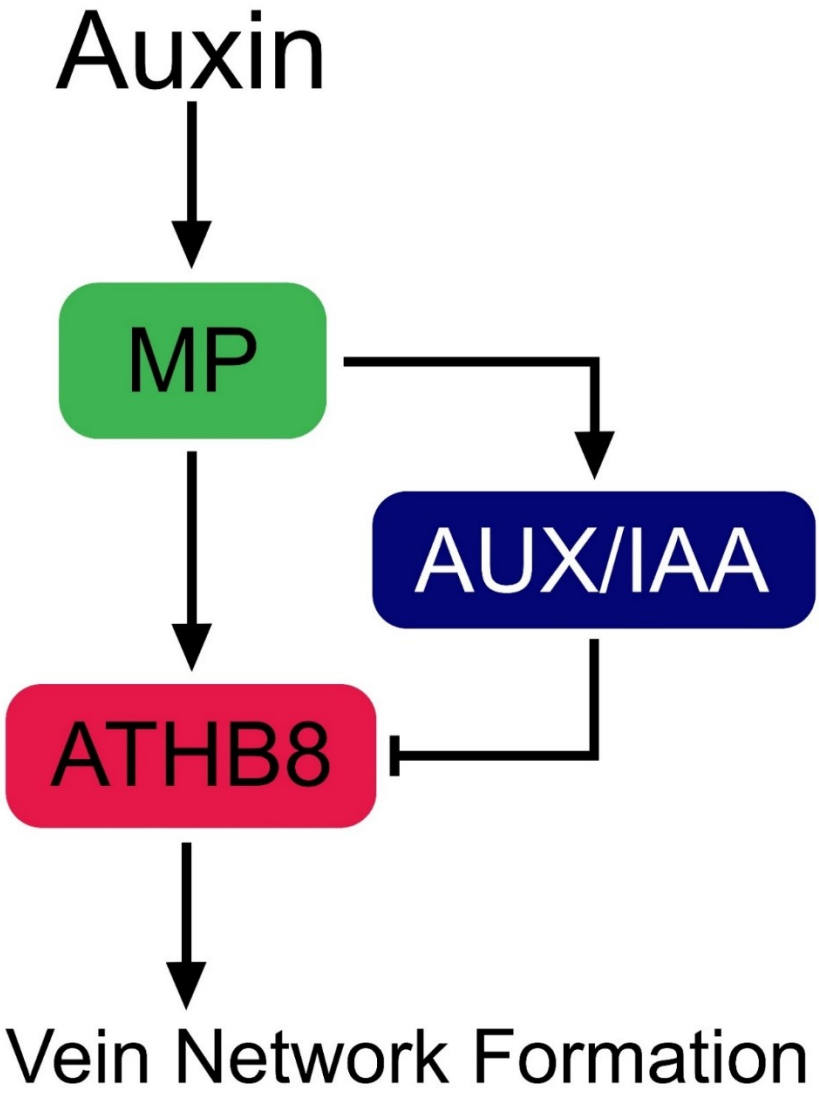

Figure 2.11. Summary and Interpretation.

A three-gene incoherent type-I feedforward loop (Mangan and Alon, 2003) activates *ATHB8* expression in narrow preprocambial domains ("stripes") and leads to vein network formation. *MP* receives the auxin input and activates expression of intermediate-loop *AUX*/*IAA* genes like *BDL*/*IAA12*. Both *MP* and *AUX*/*IAA* genes jointly regulate expression of the stripe gene *ATHB8*, which converts the auxin input into vein-network formation output. Arrows indicate positive effects; blunt-ended lines indicate negative effects.

2.3. Materials & Methods

2.3.1. Plants

Origin and nature of lines, genotyping strategies, and oligonucleotide sequences are in Tables 2.1, 2.2, and 3.3, respectively. Seeds were sterilized and sowed as in (Sawchuk et al., 2008). Stratified seeds were germinated and seedlings were grown at 22°C under continuous light (~90 μmol m^{-2} s^{-1}). Plants were grown at 25°C under fluorescent light (~100 μmol m^{-2} s^{-1}) in a 16-h-light/8-h-dark cycle and transformed as in (Sawchuk et al., 2008).

2.3.2. RT-qPCR

Total RNA was extracted with Qiagen's RNeasy Plant Mini Kit from 4-day-old seedlings grown in half-strength Murashige and Skoog salts, 15 g l^{-1} sucrose, 0.5 g l^{-1} MES, pH 5.7, at 23°C under continuous light (~80 μmol m^{-2} s^{-1}) on a rotary shaker at 50 rpm. DNA was removed with Invitrogen's TURBO DNA-free kit, and RNA was stabilized by the addition of 20 U of Thermo Fisher Scientific's Superase-In RNase Inhibitor. First-strand complementary DNA (cDNA) was synthesized from ~100 ng of DNase-treated RNA with Thermo Fisher Scientific's RevertAid Reverse Transcriptase according to manufacturer's instructions, except that 50 pmol of Thermo Fisher Scientific's Oligo$(dT)_{18}$ Primer, 50 pmol of Thermo Fisher Scientific's Random Hexamer Primer, and 20 U of Superase-In RNase Inhibitor were used. qPCR was performed with Applied Biosystems' 7500 Fast Real-Time PCR System on 2 μl of 1:3-diluted cDNA with 5 pmol of each gene-specific primers (Table 2.3), 2.5 pmol of gene-specific probe (Table 2.3), and Applied Biosystems' TaqMan 2× Universal PCR Master Mix in a 10-μl reaction volume. Probe and primers were designed with Applied Biosystems' Primer Express. Relative *MP* transcript levels were

Table 2.2. Genotyping Strategies.

Line	Strategy
athb8-11	*ATHB8*: “Athb8 0.5” and “athb8attB2R”; *athb8*: “athb8 - 5944” and “PD991- RB”
athb8-27	*ATHB8*: “athb8-27 RP” and “athb8-27 LP”; *athb8-27*: “athb8-27 RP” and “Spm32”
mp-B4149	“MP 1498-s” and “MP2082-AS”; *Mse*I
mp-U55	“MP Seq 2061” and “U55 Geno Rev”; *Sml*I
mp-11	*MP*: “Sail_1265_F06LP” and “Sail_1265_F06RP”; *mp*: “LB3” and “Sail_1265_F06RP”
bdl	“bdl geno F” and “bdl geno R”; *Hae*III
iaa12-1	*IAA12*: “SALK_138684 LP” and “SALK_138684 RP”; *iaa12*: “LBb1.3” and “SALK_138684 RP”
tpl-1	“tpl Caps Genotyping Forward” and “tpl Caps Genotyping Reverse”; *Nco*I

Table 2.3. Oligonucleotide Sequences.

Name	Sequence (5' to 3')
SHR HindIII F	GAGAAGCTTGACAAAGAAGCAGAGCGTGG
SHR SalI R	TGGGTCGACTTAATGAATAAGAAAATGAATAGAAGA AAGGG
SalI FWD – MiRNA 165	ATTGTCGACCCACTCATCATTCCCTCATC
KpnI REV – MiRNA 165	AGCGGTACCCTTATAGAAAATACTTCGTTAGCTTG
SalI SHR Promoter FP	GGGGTCGACACATAAACCAGTAGACAT
XhoI mATHB8 RP	GGGCTCGAGTATAAAAGACCAGTTGAGG
EAR XhoI + KpnI Forward	TCGAGCTAGATCTGGATCTAGAACTCCGTTTGGGTTTCGCTT AAGGTAC
EAR Reverse	CTTAAGCGAAACCCAAACGGAGTTCTAGATCCAGATCATGC
MP BamHI Fwd	AAGGGATCCTCCGGGTTAATCAGTATTATTAC
MP KpnI Rev	ACAGGTACCACAGAGAGATTTTTCAATGTTCTG
ATHB8 cDNA KpnI FWD	GTCGGTACCATGGGAGGAGGAAGCAATAATAG
ATHB8 cDNA SmaI Rev	ATGCCCGGGATCATATAAAAGACCAGTTGAGG
ATHB8mut165FWD	ATAGGAATCGTTGCTATTTCTC
ATHB8mut165REV	GGAATCTGGTCCAGGCTTCATC
MP Prom SalI Fwd	CCCGTCGACGTATATATAAACAATACCACCTTATAAC
MP KpnI Rev-2	CATGGTACCTGCAGAATTAGCATACCACAC
MP 3 kb SalI Fwd	TCTGTCGACTCCGGGTTAATCAGTATTATTAC
MP 3 kb XhoI Rev	ATTCTCGAGTTAAGAGTTAAGACCACCTCC
ECFP AflII F	TTACTTAAGGTGAGCAAGGGCGACGAGC

ECFP AflII R	AGACTTAAGATTGTACAGCTCGTCCATGCC
VP16 NcoIF2	TTACCATGGCCCCCCCGACCGATGTC
VP16 PstIR	TTTCTGCAGCCCCACCGTACTCGTCAATTC
BDL PstIF	ATACTGCAGCTCGTGGTGTGTCAGAATTGGAC
BDL BamHIR	TACGGATCCACTAAACTGGGTTGTTTCTTTGTC
BDL mut F1	AATCTTCCGGCGGAGAGTGTTAGAGAATTGGG
BDL mut F2	GTGGGTAAAAGTAATCTTCCGGCGGAGAGTG
BDL mut F3	GTGTCAGAATTGGAGGTGGGTAAAAGTAATCTTCCG
BDL mut F4	CGTGGTGTGTCAGAATTGGAGGTGGGGAAGAGTAATC
BDL MfeI mut R	TAACAATTGGTGACCATCCTACCACTTGAC
BDLd1 PstI F	AAACTGCAGCGTGGAAAGAGCGTGGG
MP SalI Forward – Primer # 2	GGGGTCGACCGGATTCGTGATCTTCGTATCCCAT
MP EcoRI Reverse	ATTGAATTCGGTTCGGACGCGGGGTGTCGCAATT
SpeI GR Forward	GGGACTAGTGGAGAAGCTCGAAAAACAAAG
SacII + KpnI (Internal) GR Reverse	AATCCGCGGGGTACCTCATTTTTGATGAAACAGAAG
SalI 2KB ATHB8 Promoter Forward	CGCGTCGACCATTATAAATATCACGACTGTA
ApaI 2KB ATHB8 Promoter Reverse	ATTGGGCCCCTTTGATCCTCTCCGATCTCT
ApaI 2xmTurqoise Forward	ATTGGGCCCATGGTGAGCAAGGGCGAGGA
KpnI 2xmTFP Reverse	CGAGGTACCTCACTCTTCTTCTTGATCAGCTTCTG
1NagARE	GGGGACAAGTTTGTACAAAAAAGCAGGCTTGGTTGTC TCGTATTAAGGG

Athb8 R-5	GGGGACCACTTTGTACAAGAAAGCTGGGTCTTTGATC CTCTCCGATCTCTC
1NcARE	GGGGACAAGTTTGTACAAAAAAGCAGGCTTGGTTACC TGGTATTAAGGG
athb8-27 FP	TGTGAAGAATGGATCCACCTC
athb8-27 RP	AGTGGTCAACACCACTTGACC
Spm32	TACGAATAAGAGCGTCCATTTTAGAGTG
Athb8 0.5	GGGGACAAGTTTGTACAAAAAAGCAGGCTTCCTTTGC TTCCAGAGACCAGCG
athb8attB2R	GGGGACCACTTTGTACAAGAAAGCTGGGTCTTTGATC CTCTCCGATCTCTC
athb8 -5944	GGTTTGGCATAAAAGTGCGG
PD991- RB	AAAACCTGGCGTTACCCAACT
MP 1498-s	CTCTCAGCGGATAGTATGCACATCGG
MP2082-AS	ATGGATGGAGCTGACGTTTGAGTTC
MP Seq 2061	CATAATGTTACTCTTCATGTACGCC
U55 Geno Rev	GTGCTGTTTGTTGGCGATTGG
Sail_1265_F06LP	GCTTCATCTCTTCAAGCAAGG
Sail_1265_F06RP	TCCCAAAGTCTCACCACTCAC
LB3	TAGCATCTGAATTTCATAACCAATCTCGATACAC
bdl geno F	GCTCAAATCTTGTGATGTGAGTG
bdl geno R	AGTCCACTAGCTTCTGAGGTTCCC
SALK_138684 LP	GTGGGGAAGAGTAATCTTCCG
SALK_138684 RP	CTTCTGCTCTTGACGTCTTGG

LBb1.3	ATTTTGCCGATTTCGGAAC
tpl Caps Genotyping Forward	GCCCTGAAAATGACATCGGT
MP PrimeTime Probe	/56-FAM/CAGACTCAC/ZEN/AGGCCTTCTCTCGCCA/3IABkFQ/
MP PrimeTime Primer 2	TGTACCAGTGCCTCCAGAATTATC
MP PrimeTime Primer 1	TCCAGTCGCAGATCACATCAG
ACT2 PrimeTime Probe	/56-FAM/ACAGCACTT/ZEN/GC CCAAG AGCATGA/3IABkFQ/
ACT2 PrimeTime Primer 2	TACTTCCTTTCAGGTGGTGC A
ACT2 PrimeTime Primer 1	GCTGACCGTATGAGCAAAGAAAT

calculated with the $2^{-\Delta\Delta Ct}$ method (Livak and Schmittgen, 2001) using *ACTIN2* transcript levels for normalization.

2.3.3. Imaging

Developing leaves were mounted and imaged as in (Sawchuk et al., 2013), except that emission was collected from ~1.5–5.0-µm-thick optical slices. In single-fluorophore marker lines, YFP was excited with the 514-nm line of a 30-mW Argon (Ar) laser, and emission was collected with a BP 520–555 filter. In multiple-fluorophore marker lines, CFP, QFP, and autofluorescent compounds were excited with the 458-nm line of a 30-mW Ar laser; YFP was excited with the 514-nm line of a 30-mW Ar laser; and RFP was excited with the 543-nm line of a HeNe laser; CFP/QFP emission was collected with a BP 475–525 filter; YFP emission was collected with a BP 520–555 filter; RFP emission was collected between 581 and 657 nm; and autofluorescence was collected between 604 and 700 nm. Signal intensity levels of 8-bit grayscale images acquired at identical settings were quantified in the Fiji distribution of ImageJ (Schindelin et al., 2012; Schneider et al., 2012; Schindelin et al., 2015; Rueden et al., 2017). To visualize RFP/YFP ratios, the histogram of the YFP images was linearly stretched in the Fiji distribution of imageJ such that the maximum gray value of the YFP images matched that of the corresponding RFP images, and the RFP images were divided by the corresponding YFP images. Mature leaves were fixed, cleared, and mounted as in (Verna et al., 2019b; Amalraj et al., 2020) (Chapter 3), and mounted leaves were imaged as in (Odat et al., 2014). Image brightness and contrast were adjusted by linear stretching of the histogram in in the Fiji distribution of ImageJ.

2.3.4. Vein Network Analysis

The cardinality, continuity, and connectivity indices were calculated as in (Verna et al., 2015). Briefly, number of "touch points" (TPs, where a TP is the point where a vein end contacts another vein or a vein fragment), "end points" (EPs, where an EP is the point where an "open" vein — a vein that contacts another vein only at one end — terminates free of contact with another vein or a vein fragment), "break points" (KPs, where a KP is each of the two points where a vein fragment terminates free of contact with veins or other vein fragments), and "exit points" (XPs, where an XP is the point where a vein exits leaf blade and enters leaf petiole) in dark-field images of cleared mature leaves was calculated with the Cell Counter plugin in the Fiji distribution of ImageJ.

Because a vein network can be understood as an undirected graph in which TPs, EPs, KPs, and XPs are vertices, and veins and vein fragments are edges, and because each vein is incident to two TPs, a TP and an XP, a TP and an EP, or an XP and an EP, the cardinality index — a measure of the size (i.e. the number of edges) of a graph — is a proxy for the number of veins and is calculated as: $[(TPs+XPs-EPs)/2]+EPs$, or: $(TPs+XPs+EPs)/2$.

The continuity index quantifies how close a vein network is to a network with the same number of veins, but in which at least one end of each vein fragment contacts a vein, and is therefore calculated as the ratio of the cardinality index of the first network to the cardinality index of the second network: $[(TP + XP + EP)/2]/[(TP + XP + EP + KP)/2]$, or: $(TP + XP + EP)/(TP + XP + EP + KP)$.

The connectivity index quantifies how close a vein network is to a network with the same number of veins, but in which both ends of each vein or vein fragment contact other veins, and is therefore calculated as the ratio of the number of "closed" veins — those veins which contact vein fragments or other veins at both ends — in the first network to the number of closed veins

in the second network (i.e. the cardinality index of the second network): [(TP + XP − EP)/2]/[(TP + XP + EP + KP)/2], or: (TP + XP − EP)/(TP + XP + EP + KP).

Finally, because the number of meshes in a vein network equals the number of closed veins, the cyclicity index — a proxy for the number of meshes in a vein network — is calculated as: (TP+XP-EP)/2.

Chapter 3: GAL4/GFP Enhancer-Trap Lines for Identification and Manipulation of Cells and Tissues in Developing Arabidopsis Leaves[1]

3.1. Introduction

The unambiguous identification of cell and tissue types and the selective manipulation of their properties is key to our understanding of developmental processes. Both the unambiguous identification and the selective manipulation can most efficiently be achieved by the GAL4 system (Brand and Perrimon, 1993). In such a system, a minimal promoter in a construct randomly inserted in a genome responds to neighboring regulatory elements and activates the expression of a gene, included in the same construct, encoding a variant of the GAL4 transcription factor of yeast; the same construct also includes a GAL4-responsive, UAS-driven lacZ, GUS, or GFP, which reports GAL4 expression. Independent, phenotypically normal lines, in which the construct is inserted in different genomic locations, are selected because they reproducibly express the GAL4-responsive reporter in cell- or tissue-specific patterns. Lines with cell- or tissue-specific GAL4-driven reporter expression can then be used to characterize the behavior of the labeled cells or tissues (Yang et al., 1995), to identify mutations that interfere with that behavior (Guitton et al., 2004), or to identify genes expressed in the labeled cells or tissues by cloning the DNA flanking the insertion site of the enhancer-trap construct (Calleja et al., 1996). Furthermore, lines with cell- or tissue-specific GAL4 expression can be crossed with lines with UAS-driven RNAi constructs to trigger cell or tissue-specific gene silencing (Nagel et

[1] Adapted from Amalraj, B., Govindaraju, P., Krishna, A., Lavania, D., Linh, N. M., Ravichandran, S. J. and Scarpella, E. (2020). GAL4/GFP enhancer-trap lines for identification and manipulation of cells and tissues in developing Arabidopsis leaves. *Developmental Dynamics*: 2020 Apr 21. doi: 10.1002/dvdy.181. Online ahead of print.

al., 2002), dominant-negative alleles to interfere with the WT gene function in specific cells or tissues (Elefant and Palter, 1999), toxic genes to induce cell- or tissue-specific ablation (Reddy 1997), or genes of interest to investigate necessary or sufficient functions in specific cells or tissues (Gunthorpe et al., 1999). Though the GAL4 system does not allow to restrict the expression of UAS-driven transgenes to a temporal window that is narrower than that in which GAL4 is expressed, the system allows exquisite spatial control of transgene expression (McGuire et al., 2004).

One of the first implementations of the GAL4 system in Arabidopsis was the Haseloff collection of GAL4/GFP enhancer-trap lines, in which an endoplasmic-reticulum-localized GFP (erGFP) responds to the activity of a fusion between the GAL4 DNA-binding domain and the activating domain of VP16 of *Herpes simplex* (Berger et al., 1998; Haseloff, 1999). The Haseloff collection is the most extensively used GAL4 system in Arabidopsis (e.g., (Sabatini et al., 1999; Weijers et al., 2003; Laplaze et al., 2005; Sawchuk et al., 2007; Gardner et al., 2009; Wenzel et al., 2012)), even though it is in the C24 background. This is problematic because the phenotype of hybrids between C24 and Col-0, generally considered the reference genotype in Arabidopsis (Koornneef and Meinke, 2010), is different from that of either parent (e.g., (Groszmann et al., 2014; Kawanabe et al., 2016; Radoeva et al., 2016; Zhang et al., 2016)). The use of GAL4/GFP enhancer-trap lines in the C24 background to investigate processes in the Col-0 background thus imposes the burden of laborious generation of ad-hoc control backgrounds. Therefore, most desirable is the generation and characterization of GAL4/GFP enhancer-trap collections in the Col-0 background. Two such collections have been reported: the Berleth collection, which has been used to identify lines that express GAL4/GFP in vascular tissues (Ckurshumova et al., 2009); and the Poethig collection, which has been used to identify lines that express GAL4/GFP

in stomata (Garnder et al., 2009).

Here we screened the Poethig collection; we provide a set of lines for the specific labeling of cells and tissues during early leaf development, and we show that these lines can be used to address key questions in plant developmental biology.

3.2. Results & Discussion

To identify enhancer-trap lines in the Col-0 background of Arabidopsis with reproducible GAL4-driven GFP expression during early leaf development, we screened the collection that Scott Poethig had generated with Jim Haseloff's GAL4/GFP enhancer-trap construct (Fig. 3.1A) and had donated to the Arabidopsis Biological Resource Center. We screened 312 lines for GFP expression in first leaves 4 and 5 DAG by fluorescence stereomicroscopy (see Materials & Methods); 29 lines satisfied this criterion (Table 3.1). In 10 of these 29 lines, we detected GFP in specific cells or tissues in first leaves 4 and 5 DAG by epifluorescence microscopy (see Materials & Methods); nine of these 10 lines were phenotypically normal (Table 3.1). We imaged GFP expression in first leaves of these nine lines from 2 to 5 DAG by confocal laser scanning microscopy.

The development of Arabidopsis leaves has been described previously (Pyke et al., 1991; Larkin et al., 1994; Telfer and Poethig, 1994; Kinsman and Pyke, 1998; Candela et al., 1999; Donnelly et al., 1999; Mattsson et al., 1999; Kang and Dengler., 2002; Kang and Dengler., 2004; Mattsson et al., 2003; Scarpella et al., 2004). Briefly, at 2 DAG the first leaf is recognizable as a cylindrical primordium with a midvein at its center (Fig. 3.1B). By 2.5 DAG, the primordium has elongated and expanded (Fig. 3.1C). By 3 DAG, the primordium has continued to expand, and

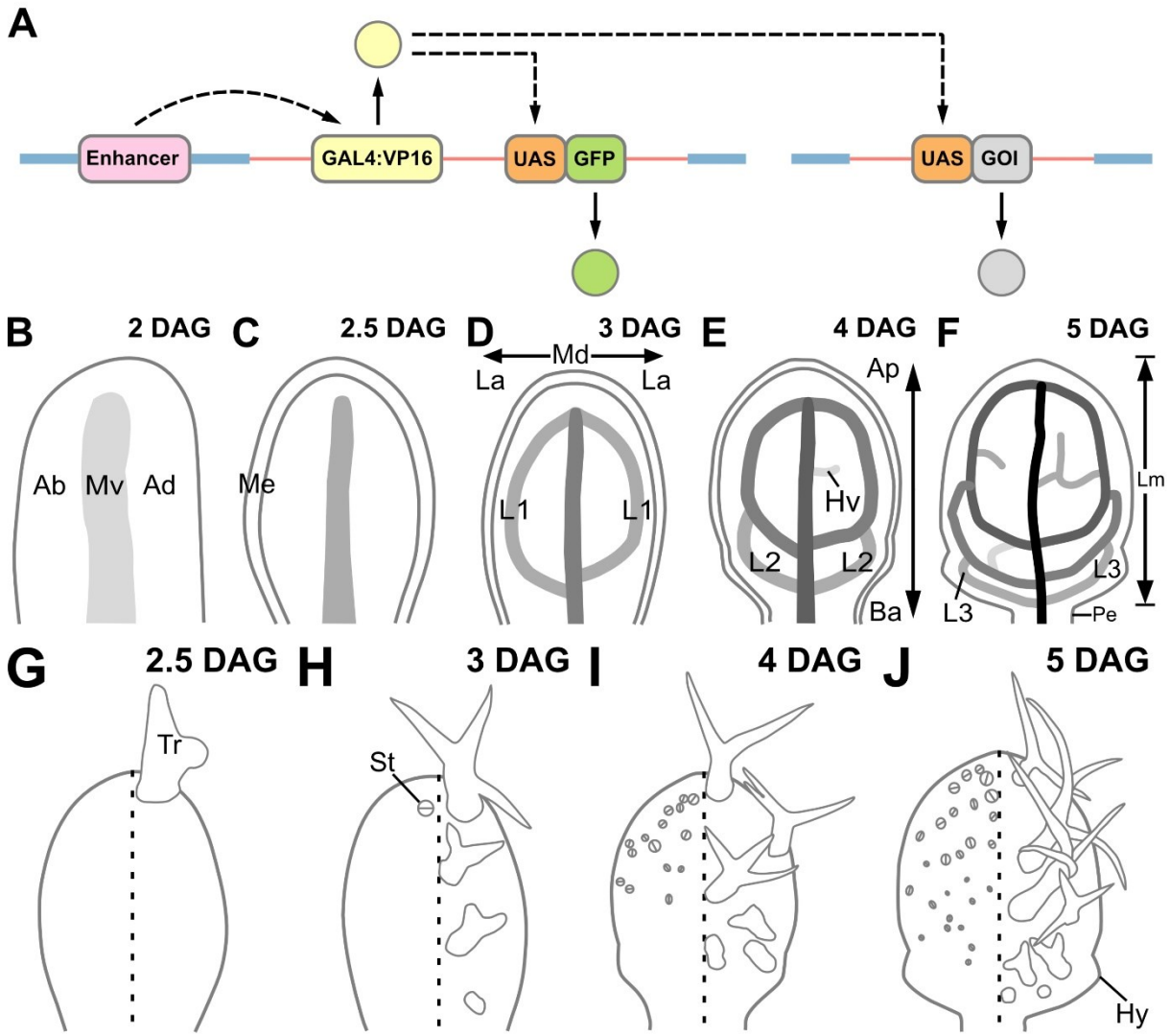

Figure 3.1. Poethig GAL4/GFP Enhancer-Trap Lines and Arabidopsis Leaf Development.

(A) Cell- or tissue-specific enhancers in the Arabidopsis genome (blue line) activate transcription (dashed arrow) of a codon-usage-optimized translational fusion between the sequence encoding the GAL4 DNA-binding domain and the sequence encoding the activating domain of the Viral Protein 16 of *Herpes simplex* (GAL4:VP16) in a T-DNA construct (red line) that is randomly inserted in the Arabidopsis genome. Translation of the GAL4:VP16 fusion gene (solid arrow) leads to cell- or tissue-specific activation of transcription of a UAS-driven, endoplasmic-reticulum-localized, improved GFP gene (mGFP5) (Siemering et al., 1996; Haseloff et al., 1997).

Crosses between lines with cell- or tissue-specific expression of GAL4:VP16 and lines with UAS-driven genes of interest (GOIs) lead to activation of GOI transcription in specific cells or tissues. See text and (Berger et al., 1998; Haseloff, 1999) for details. (B–J) First leaves. Top right: leaf age in DAG; see Materials & Methods for definition. (B–F) Development of leaf and veins; increasingly darker grays depict progressively later stages of vein development. (B) Side view, median plane. Abaxial (ventral) side to the left; adaxial (dorsal) side to the right. (C–F) Front view, median plane. See text for details. (G–J) Development of stomata and trichomes in abaxial (left) or adaxial (right) epidermis. Front ventral (left) or dorsal (right) view, epidermal plane. See text for details. Ab: abaxial; Ad: adaxial; Ap: apical; Ba: basal; Hv: minor vein; Hy: hydathode; L1, L2 and L3: first, second and third loop; La: lateral; Lm: lamina; Md: median; Me: marginal epidermis; Mv: midvein; Pe: petiole; St: stoma; Tr: trichome.

Table 3.1. Origin and Nature of Lines.

ABRC Stock No.	Donor Stock No.	Expression in Developing Leaves	Tissue- and/or Stage-Specific Expression	Phenotypically Normal
CS24240	E53	N[a]	…	…
CS24241	E306	N	…	…
CS24242	E337	N	…	…
CS24243	E362	N	…	…
CS24244	E456	N	…	…
CS24245	E513	N	…	…
CS24246	E652	N	…	…
CS24247	E751	N	…	…
CS24248	E788	N	…	…
CS24249	E829	N	…	…
CS24250	E1012	N	…	…
CS24251	E1075	N	…	…
CS24252	E1195	N	…	…
CS24253	E1247	N	…	…
CS24254	E1287	N	…	…
CS24255	E1324	N	…	…
CS24256	E1332	Y[b]	N	…
CS24257	E2042	N	…	…
CS24258	E2065	N	…	…
CS24259	E2072	N	…	…
CS24260	E2119	N	…	…
CS24262	E2168	N	…	…
CS24264	E2242	N	…	…
CS24265	E2263	N	…	…
CS24266	E2271	N	…	…
CS70072	E1092	N	…	…

CS70073	E1100	N	…	…
CS70074	E1127	N	…	…
CS70075	E1128	N	…	…
CS70076	E1130	N	…	…
CS70077	E1155	N	…	…
CS70078	E1161	N	…	…
CS70079	E1176	N	…	…
CS70080	E1222	N	…	…
CS70081	E1223	N	…	…
CS70082	E1237	N	…	…
CS70083	E1238	N	…	…
CS70084	E1250	N	…	…
CS70085	E1252	N	…	…
CS70086	E1271	N	…	…
CS70087	E1289	Y	N	…
CS70088	E1304	N	…	…
CS70089	E1322	N	…	…
CS70090	E1325	N	…	…
CS70091	E1331	N	…	…
CS70092	E1341	N	…	…
CS70093	E1344	N	…	…
CS70094	E1356	N	…	…
CS70095	E1361	N	…	…
CS70096	E1362	N	…	…
CS70097	E1370	N	…	…
CS70098	E1387	N	…	…
CS70099	E1388	N	…	…
CS70100	E1395	N	…	…
CS70101	E1396	N	…	…

CS70102	E1405	N	…	…
CS70103	E1416	N	…	…
CS70104	E1439	N	…	…
CS70105	E1439m	N	…	…
CS70106	E1457	N	…	…
CS70107	E1567	N	…	…
CS70108	E1570	N	…	…
CS70109	E1607	N	…	…
CS70110	E1626	N	…	…
CS70111	E1627	N	…	…
CS70112	E1628	N	…	…
CS70113	E1638	N	…	…
CS70114	E1644	N	…	…
CS70115	E1662	N	…	…
CS70116	E1663	Y	N	…
CS70117	E1665	N	…	…
CS70118	E1678	N	…	…
CS70119	E1684	N	…	…
CS70120	E1689	N	…	…
CS70121	E1691	N	…	…
CS70122	E1701	N	…	…
CS70123	E1728	N	…	…
CS70125	E1751	N	…	…
CS70126	E1765	N	…	…
CS70127	E1767	N	…	…
CS70128	E1785	N	…	…
CS70129	E1786	N	…	…
CS70130	E1797	N	…	…
CS70131	E1801	N	…	…

CS70132	E1809	N	…	…
CS70133	E1815	N	…	…
CS70134	E1817	N	…	…
CS70135	E1818	N	…	…
CS70136	E1819	N	…	…
CS70137	E1825	N	…	…
CS70138	E1828	N	…	…
CS70139	E1832	N	…	…
CS70140	E1833	N	…	…
CS70141	E1853	N	…	…
CS70142	E1868	N	…	…
CS70143	E1950	N	…	…
CS70144	E1998	N	…	…
CS70145	E2034	N	…	…
CS70146	E217	N	…	…
CS70147	E562	N	…	…
CS70148	E1001	N	…	…
CS70149	E1368	N	…	…
CS70150	E1690	N	…	…
CS70151	E1704-1	N	…	…
CS70152	E1704-3	N	…	…
CS70153	E1715	N	…	…
CS70154	E1723	N	…	…
CS70155	E1735	N	…	…
CS70156	E1935	N	…	…
CS70157	E1967	N	…	…
CS70158	E2014	N	…	…
CS70159	E2057	N	…	…
CS70160	E2207	N	…	…

CS70161	E2406	N	…	…
CS70162	E2408	Y	Y	Y
CS70163	E2410	N	…	…
CS70164	E2415	N	…	…
CS70165	E2425	N	…	…
CS70166	E2425	N	…	…
CS70167	E2441	N	…	…
CS70168	E2443	N	…	…
CS70169	E2448	N	…	…
CS70170	E2491	N	…	…
CS70171	E2502	N	…	…
CS70172	E2513	N	…	…
CS70173	E2563	N	…	…
CS70174	E2609	N	…	…
CS70175	E2633	N	…	…
CS70176	E2676	N	…	…
CS70177	E2692	Y	N	…
CS70178	E2724	N	…	…
CS70179	E2763	N	…	…
CS70180	E2764	N	…	…
CS70181	E2779	N	…	…
CS70182	E2861	N	…	…
CS70183	E2862	N	…	…
CS70184	E2897	N	…	…
CS70185	E2904	N	…	…
CS70186	E2905	N	…	…
CS70187	E2947	N	…	…
CS70188	E2993	N	…	…
CS70189	E3004	N	…	…

CS70190	E3006	N	…	…
CS70191	E3017	N	…	…
CS70192	E3065	N	…	…
CS70193	E3134	N	…	…
CS70194	E3190	N	…	…
CS70195	E3198	N	…	…
CS70196	E3258	N	…	…
CS70197	E3267	N	…	…
CS70198	E3298	N	…	…
CS70199	E3313	N	…	…
CS70200	E3317	Y	Y	N
CS70201	E3430	N	…	…
CS70202	E3459	N	…	…
CS70203	E3462	N	…	…
CS70204	E3474	N	…	…
CS70205	E3478	N	…	…
CS70206	E3501	N	…	…
CS70207	E3505	N	…	…
CS70208	E3530	N	…	…
CS70209	E3531	N	…	…
CS70210	E3598-1	N	…	…
CS70211	E3598-2	N	…	…
CS70212	E3637	N	…	…
CS70213	E3642	N	…	…
CS70214	E3655	Y	N	…
CS70215	E3683	N	…	…
CS70216	E3700	N	…	…
CS70217	E3754	N	…	…
CS70218	E3756	N	…	…

CS70219	E3783	Y	N	…
CS70220	E3806	N	…	…
CS70221	E3816	N	…	…
CS70222	E3826	N	…	…
CS70223	E3876	N	…	…
CS70224	E3879	N	…	…
CS70225	E3880	N	…	…
CS70226	E3885	Y	N	…
CS70227	E3912	Y	Y	Y
CS70228	E3927	N	…	…
CS70229	E3930	Y	N	…
CS70230	E3963	N	…	…
CS70231	E3980	N	…	…
CS70232	E4009	N	…	…
CS70233	E4028	Y	N	…
CS70234	E4058	N	…	…
CS70235	E4096	N	…	…
CS70236	E4104	N	…	…
CS70237	E4105	N	…	…
CS70238	E4110	N	…	…
CS70239	E4118	Y	N	…
CS70240	E4129	N	…	…
CS70241	E4148	N	…	…
CS70242	E4150	N	…	…
CS70243	E4151	N	…	…
CS70244	E4162	N	…	…
CS70245	E4223	N	…	…
CS70246	E4247	N	…	…
CS70247	E4256	N	…	…

CS70248	E4272	N	…	…
CS70249	E4285	N	…	…
CS70250	E4295	Y	Y	Y
CS70251	E4350	N	…	…
CS70252	E4396	N	…	…
CS70253	E4411	N	…	…
CS70254	E4423	N	…	…
CS70255	E4491	N	…	…
CS70256	E4506	Y	N	…
CS70257	E4522	Y	N	…
CS70258	E4583	N	…	…
CS70259	E4589	N	…	…
CS70260	E4633	N	…	…
CS70261	E4680	N	…	…
CS70262	E4695	N	…	…
CS70263	E4715	N	…	…
CS70264	E4716	Y	Y	Y
CS70265	E4722	Y	Y	Y
CS70266	E4751	N	…	…
CS70267	E4791	N	…	…
CS70268	E4801	N	…	…
CS70269	E4811	N	…	…
CS70270	E4812	N	…	…
CS70271	E4820	N	…	…
CS70272	E4856	Y	N	…
CS70273	E4907	N	…	…
CS70274	E4930	N	…	…
CS70275	E4940	N	…	…
CS70276	E4970	N	…	…

CS70277	E5008	N	…	…
CS70278	E5025	N	…	…
CS70279	E5026	N	…	…
CS70280	E5085	N	…	…
CS70281	E5096	Y	N	…

N, No; Y, Yes

the first loops of veins ("first loops") have formed (Fig. 3.1D). By 4 DAG, a lamina and a petiole have become recognizable, second loops have formed, and minor veins have started to form the top half of the lamina (Fig. 3.1E). By 5 DAG, lateral outgrowths (hydathodes) have become recognizable in the lower quarter of the lamina, third loops have formed, and minor vein formation has spread toward the base of the lamina (Fig. 3.1F). Leaf hairs (trichomes) and pores (stomata) can be first recognized at the tip of 2.5- and 3-DAG primordia, respectively, and their formation spreads toward the base of the lamina during leaf development (Fig. 3.1G–J).

Consistent with previous observations (Huang et al., 2014), E100>>erGFP was expressed at varying levels in all the cells of 2-, 2.5-, 3-, and 4-DAG leaf primordia (Fig. 3.2B–E).

Consistent with previous observations (Krogan and Berleth, 2012), E861>>erGFP was expressed in all the inner cells of the 2-DAG primordium, though more strongly in its innermost cells (Fig. 3.2F). At 2.5 DAG, expression had been activated in the lowermost epidermal cells of the primordium margin and persisted in all the inner cells of the bottom half of the primordium; in the top half of the primordium, weaker expression persisted in inner cells, except near the midvein, where by then it had been terminated (Fig. 3.2G). At 3 DAG, expression continued to persist in all the inner cells of the bottom half of the primordium, though expression was stronger in the areas where second loops were forming; in the top half of the primordium, weaker expression had become restricted to the midvein, first loops, and minor veins (Fig. 3.2H). At 4 DAG, expression in the top half of the leaf remained restricted to the midvein, first loops, and minor veins, and in the bottom half of the leaf it had declined in inner cells between the first loops and the developing second loops (Fig. 3.2I). In summary, E861>>erGFP was expressed ubiquitously at early stages of inner-cell development; over time, however, expression became restricted to developing veins. As such, expression of E861>>erGFP resembles that of

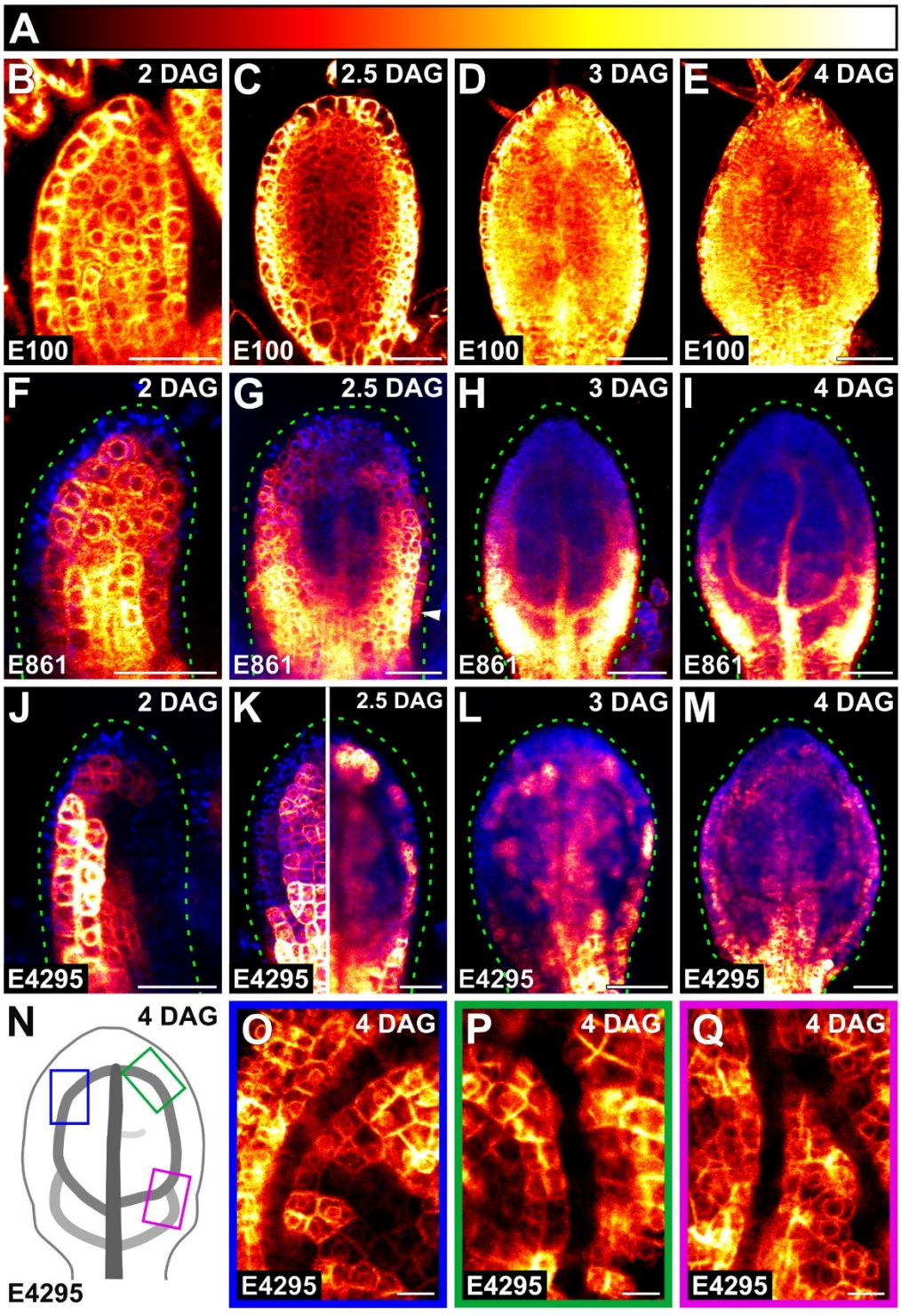

Figure 3.2. Expression of E100>>, E861>> and E4295>>erGFP in Leaf Development.

(A) Look-up table visualizes global background (black) and erGFP expression levels (red to white through yellow). (B–Q) First leaves. Top right: leaf age in DAG; see Materials & Methods

for definition. (B–M,O–Q) Confocal laser scanning microscopy. Bottom left: genotype. Look-up table (ramp in A) visualizes erGFP expression levels (red to white through yellow). Blue: autofluorescence. Black: global background. Dashed green line delineates leaf outline. White arrowhead points to epidermal expression. (B,F,J) Side view, median plane. Abaxial (ventral) side to the left; adaxial (dorsal) side to the right. (C–E,G–I,L,M,O–Q) Front view, median plane. (K) Front ventral view, subepidermal plane (left); front view, median plane (right). (N) Increasingly darker grays depict progressively later stages of vein development. Boxes illustrate positions of closeups in O, P, and Q. See Table 3.2 for reproducibility of expression features. Bars: (B,C,F,G,J,K) 30 µm; (D,E,H,I,L,M) 60 µm; (O–Q) 10 µm.

Table 3.2. Reproducibility of Expression and Pattern Features.

Figure	Panel	No. Leaves With Displayed Features / No. Analyzed Leaves	Assessed Expression or Pattern Features
3.2	B	15/18	Ubiquitous
3.2	C	15/17	Ubiquitous
3.2	D	19/19	Ubiquitous
3.2	E	33/33	Ubiquitous
3.2	F	26/29	Inner cells
3.2	G	29/29	Vascular cells in top half of primordium, inner cells in basal half of primordium
3.2	H	31/31	Vascular cells in top half of primordium, inner cells in basal half of primordium
3.2	I	19/19	Vascular cells in top half of leaf, inner cells in basal half of leaf
3.2	J	16/19	Abaxial inner cells
3.2	K	34/36	Abaxial inner cells & middle tissue layer
3.2	L	24/25	Abaxial inner cells & middle tissue layer
3.2	M	34/34	Abaxial inner cells & middle tissue layer
3.2	O	14/14	Inner, nonvascular cells
3.2	P	14/14	Inner, nonvascular cells
3.2	Q	14/14	Inner, nonvascular cells
3.3	A	26/28 (abaxial) 15/28 (adaxial)	Upper third of adaxial epidermis & whole abaxial epidermis

3.3	B (left)	30/30	Whole epidermis
3.3	B (right)	22/23	Top three-quarters of epidermis & trichomes
3.3	C (left)	15/15	Whole epidermis
3.3	C (right)	14/14	Top three-quarters of epidermis & trichomes
3.3	D (left)	18/18	Whole epidermis
3.3	D (right)	16/16	Epidermis of whole lamina and petiole midline & trichomes
3.3	E	16/16	Trichomes
3.3	F	17/18	Top three-quarters of marginal epidermis
3.3	G	14/14	Whole marginal epidermis
3.3	H	16/16	Whole marginal epidermis
3.3	I	59/59	Whole epidermis
3.3	J (left)	45/45	Whole epidermis
3.3	J (right)	42/42	All cells of marginal epidermis, except few cells in top half of primordium
3.3	K (left)	21/21	Whole epidermis, including stomata
3.3	K (right)	33/38	Bottom quarter and few cells in top three-quarters of marginal epidermis
3.3	L (left)	21/21	Whole epidermis, including stomata
3.3	L (right)	31/31	Bottom quarter and few cells in top three-quarters of marginal epidermis
3.3	M	29/30	Absent
3.3	N	26/26	Top quarter of primordium
3.3	O	18/18	Top three-quarters of primordium
3.3	P	18/18	Whole leaf

3.3	Q	31/33	Absent
3.3	R	19/21	Top quarter of primordium
3.3	S	23/28	Top half of lamina
3.3	T	16/18	Top three-quarters of lamina
3.4	A	22/22	Midvein
3.4	B	30/30	Midvein
3.4	C	16/17	Midvein & first loop
3.4	D	34/48	Midvein & first and second loop
3.4	E	25/25	Absent
3.4	F	20/20	Midvein
3.4	G	27/37	Midvein & first loop
3.4	H	24/28	Midvein & first and second loop
3.6	A	NDa	Narrow midvein & scalloped vein-network outline
3.6	B	19/20	Shapeless vascular cluster
3.6	C	32/46	Midvein & first and second loop
3.6	D	21/21	Shapeless vascular domain
3.6	E	16/23	Midvein & first and second loop
3.6	F	18/18	Broad vascular domain
3.6	G	21/21	Narrow midvein & scalloped vein-network outline
3.6	H	19/19	Broad vascular zone

[a]Not Determined

MONOPTEROS and *PIN-FORMED1*, which marks the gradual selection of vascular cells from within the leaf inner tissue (Scarpella et al., 2006; Wenzel et al., 2007).

E4295>>erGFP expression was restricted to inner cells in 2-, 2.5-, 3-, and 4-DAG leaf primordia (Fig. 3.2J–M,O–Q). At 2 DAG, E4295>>erGFP was expressed almost exclusively in the inner cells of the abaxial side of the primordium (Fig. 3.2J), but by 2.5 DAG E4295>>erGFP was additionally expressed in the middle tissue layer (Fig. 3.2K), from which veins form (Stewart 1978; Tilney-Bassett 1986). Expression persisted in the inner cells of the abaxial side and of the middle tissue layer in 3- and 4-DAG primordia (Fig. 3.2L,M). High-resolution images of the middle tissue layer showed that expression was excluded from developing veins (Fig. 3.2O–Q), suggesting that it marks inner, non-vascular cells. Therefore, expression of E4295>>erGFP resembles that of *LIGHT HARVESTING COMPLEX A6* and *SCARECROW-LIKE32* (Sawchuk et al., 2008; Gardiner et al., 2011), and that of J0571>>erGFP in the C24 background (Wenzel et al., 2012).

As described below, expression of E4259>>erGFP and E4722>>erGFP was restricted to the epidermis at all analyzed stages (Fig. 3.3A–L).

At 2 DAG, E4259>>erGFP was expressed in the upper third of the adaxial epidermis and in the whole abaxial epidermis, though expression was stronger in the top half of the primordium (Fig. 3.3A). By 2.5 DAG, E4259>>erGFP was strongly expressed in the whole abaxial epidermis and the top three-quarters of the marginal epidermis; E4259>>erGFP was also expressed in the top three-quarters of the adaxial epidermis, but expression was stronger in the top half of the primordium (Fig. 3.3B,F). At 3 DAG, E4259>>erGFP was strongly expressed in the top three-quarters of the adaxial epidermis and in the whole marginal epidermis, and strong expression persisted in the whole abaxial epidermis (Fig. 3.3C,G). At 4 DAG, strong expression persisted in

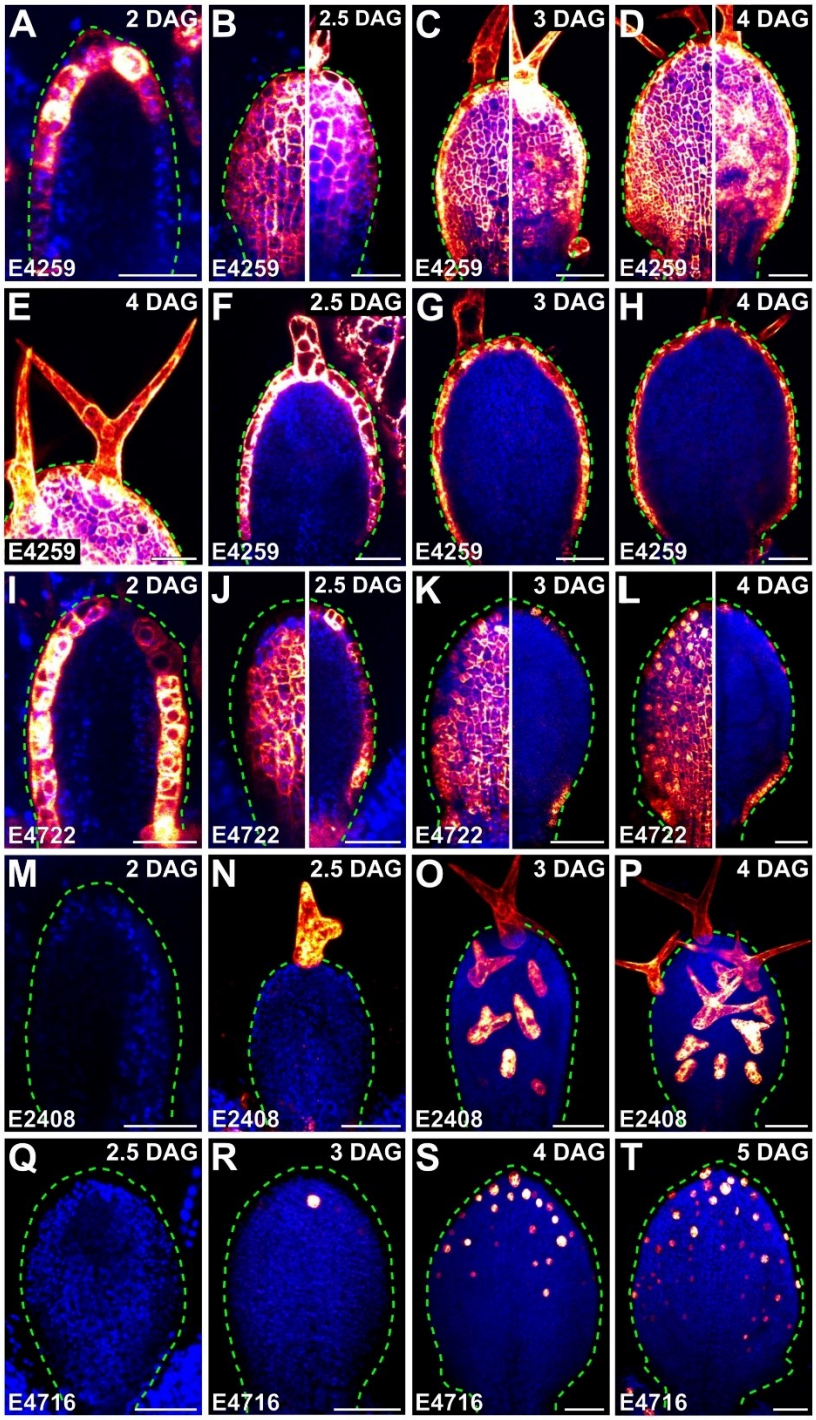

Figure 3.3. Expression of E4259>>, E4722>>, E2408>> and E4716>>erGFP in Leaf Development.

(A–T) Confocal laser scanning microscopy. First leaves. Top right: leaf age in DAG; see Materials & Methods for definition. Bottom left: genotype. Look-up table (ramp in Fig. 3.2A)

visualizes erGFP expression levels (red to white through yellow). Blue: autofluorescence. Black: global background. Dashed green line delineates leaf outline. (A,I,M) Side view, median plane. Abaxial (ventral) side to the left; adaxial (dorsal) side to the right. (B–D) Front ventral (left) or dorsal (right) view, epidermal plane. (E) Closeup of trichome in D, right. (F–H) Front view, median plane. (J–L) Front ventral view, epidermal plane (left); front view, median plane (right). (N–P) Front dorsal view, epidermal plane. (Q–T) Front ventral view, epidermal plane. See Table 3.2 for reproducibility of expression features. Bars: (A,B,F,I,J,M,N,Q) 30 μm; (C,D,E,G,H,K,L,O,P,R,S,T) 60 μm.

the whole marginal epidermis, continued to persist in the whole abaxial epidermis, and E4259>>erGFP was now strongly expressed also in the adaxial epidermis of the whole lamina and the petiole midline (Fig. 3.3D,H). At all analyzed stages, E4259>>erGFP was expressed in trichomes but was not expressed in mature stomata (Fig. 3.3B–H). In conclusion, expression of E4259>>erGFP resembles that of *ARABIDOPSIS THALIANA MERISTEM LAYER1* (Lu et al., 1996; Sessions et al., 1999), which marks epidermal cells and whose promoter is used to drive epidermis-specific expression (e.g., (Takada and Jürgens, 2007; Bilsborough et al., 2011; Kierzkowski et al., 2013; Govindaraju et al., 2020)).

E4722>>erGFP was expressed in all the epidermal cells of the 2-DAG primordium, though more weakly at its tip (Fig. 3.3I). E4722>>erGFP was expressed in all the epidermal cells of the 2.5-DAG primordium too, except at its margin, where expression had been terminated in a few cells of its top half (Fig. 3.3J). At 3 DAG, expression persisted in all the epidermal cells, except at the primordium margin, where expression had been terminated in most of the cells of its top three-quarters (Fig. 3.3K). At 4 DAG, expression continued to persist in all the epidermal cells, except at the leaf margin, where expression had been terminated in nearly all the cells of its top three-quarters (Fig. 3.3L). Unlike E4259>>erGFP, E4722>>erGFP was expressed in stomata but was not expressed in trichomes (Fig. 3.3J–L).

At all analyzed stages, expression of E2408>>erGFP and E4716>>erGFP was restricted to trichomes and stomata, respectively (Fig. 3.3M–T). E2408>>erGFP was first expressed in developing trichomes at the tip of the 2.5-DAG primordium (Fig. 3.3M,N). By 3 DAG, E2408>>erGFP was expressed in the developing and mature trichomes of the top three-quarters of the primordium (Fig. 3.3O), and by 4 DAG in those of the whole lamina (Fig. 3.3P). E4716>>erGFP was first expressed in stomata at the tip of the 3-DAG primordium (Fig.

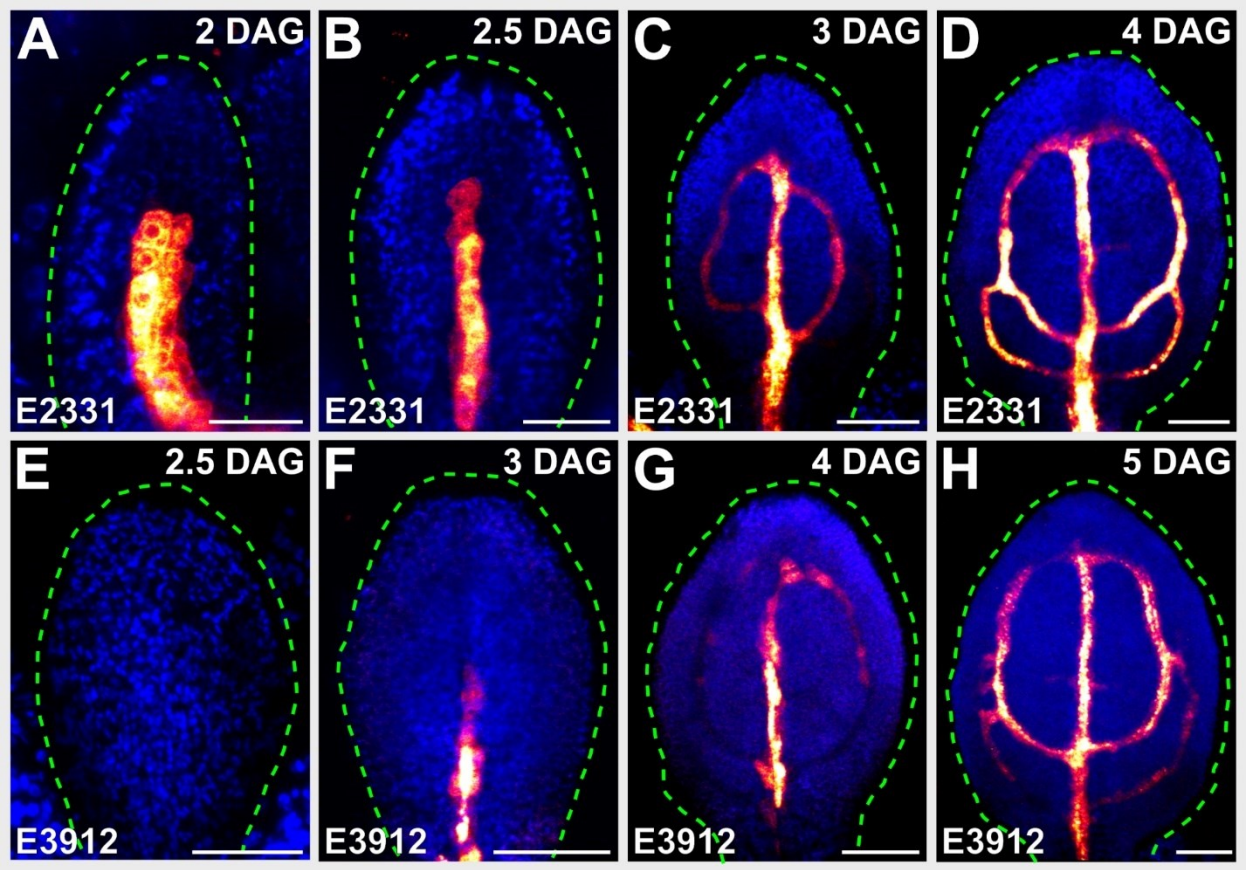

Figure 3.4. Expression of E2331>> and E3912>>erGFP in Leaf Development.

(A–H) Confocal laser scanning microscopy. First leaves. Top right: leaf age in DAG; see Materials & Methods for definition. Bottom left: genotype. Look-up table (ramp in Fig. 3.2A) visualizes erGFP expression levels (red to white through yellow). Blue: autofluorescence. Black: global background. Dashed green line delineates leaf outline. (A) Side view, median plane. Abaxial (ventral) side to the left; adaxial (dorsal) side to the right. (B–H) Front view, median plane. See Table 3.2 for reproducibility of expression features. Bars: (A,B,E) 30 µm; (C,D,F–H) 60 µm.

3.3Q,R). By 4 DAG, E4716>>erGFP was expressed in the stomata of the top half of the lamina (Fig. 3.3S), and by 5 DAG in those of its top three-quarters (Fig. 3.3T).

At all analyzed stages, expression of E2331>>erGFP and E3912>>erGFP was restricted to developing veins (Figure 3.4). E2331>>erGFP was expressed in both isodiametric and elongated cells of the midvein in 2- and 2.5-DAG primordia (Fig. 4A,B). By 3 DAG, E2331>>erGFP was expressed in first loops, and by 4 DAG in second loops and minor veins (Fig. 3.4C,D). E3912>>erGFP was first expressed in the midvein of the 3-DAG primordium (Fig. 3.4E,F). By 4 DAG, E3912>>erGFP was expressed in first loops, and by 5 DAG in second loops and minor veins (Fig. 3.4G,H). These observations suggest that expression of E3912>>erGFP is initiated later than that of E2331>>erGFP in vein development. Furthermore, because the expression of E2331>>erGFP resembles that of the preprocambial markers ATHB8::nYFP, J1721>>erGFP, and SHR::nYFP (Sawchuk et al., 2007; Donner et al., 2009; Gardiner et al., 2011), we suggest that E2331>>erGFP expression marks preprocambial stages of vein development, a conclusion that is consistent with E2331>>erGFP expression during embryogenesis (Gillmor et al., 2010). Finally, because E3912>>erGFP expression resembles that of the procambial marker Q0990>>erGFP in the C24 background (Sawchuk et al., 2007), we suggest that E3912>>erGFP expression marks procambial stages of vein development.

In the lines characterized above, GFP was expressed in specific cells and tissues during early leaf development; however, as it is most frequently the case for other enhancer-trap lines (e.g., (Ckurshumova et al., 2009; Gardner et al., 2009; Gardiner et al., 2011; Wenzel et al., 2012; Radoeva et al., 2016)), in the lines reported here GFP was additionally expressed in other organs (Figure 3.5).

To show the informative power for plant developmental biology of the lines characterized

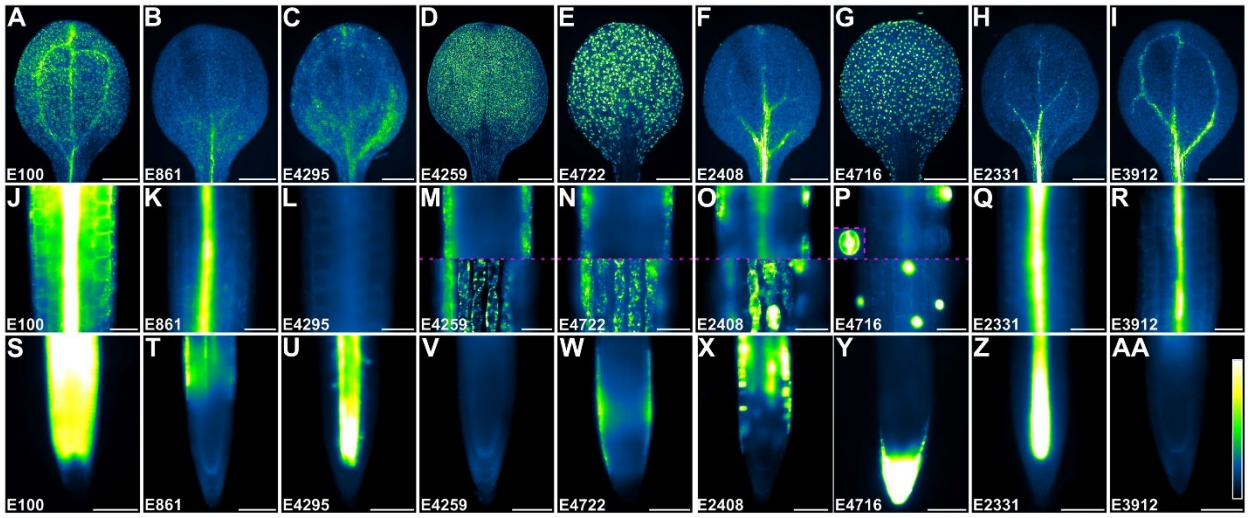

Figure 3.5. Expression of E100>>, E861>>, E4295>>, E4259>>, E4722>>, E2408>>, E4716>>, E2331>> and E3912>>erGFP in Seedling Organs.

(A–AA) Epifluorescence microscopy. Seedlings 5 DAG (see Materials & Methods for definition). Bottom left: genotype. Look-up table (ramp in AA) visualizes global background (black), and levels of autofluorescence (blue to cyan) and erGFP expression (green to white through yellow). (A–I) Cotyledon. (J–R) Hypocotyl. (P) Inset: stoma. (S-AA) Root. (A–I) Front view, median plane. (J–L,Q–AA) Median plane. (M–P) Median (top) or tangential (bottom) plane. Bars: (A–I) 500 µm.; (J–AA) 100 µm.

above, we selected the E2331 line, which marks early stages of vein development (Fig. 3.4A–D).

In WT leaves, the elongated vascular cells are connected to one another into continuous veins (Esau 1965) (Fig. 3.6A). By contrast, in mature leaves of the *gnom* (*gn*) mutant, putative vascular cells fail to elongate and to connect to one another into continuous veins; instead, they accumulate into shapeless clusters of seemingly disconnected and randomly oriented cells (Shevell et al., 2000; Verna et al., 2019) (Fig. 3.6B). Though the cells in these clusters have some features of vascular cells (e.g., distinctive patterns of secondary cell-wall thickenings), they lack others (e.g., elongated shape and end-to-end connection to form continuous veins). Therefore, it is unclear whether the clustered cells in *gn* mature leaves are abnormal vascular cells or nonvascular cells that have recruited a cellular differentiation pathway that is normally, but not always (e.g., (Solereder 1908; Kubo et al., 2005; Yamaguchi et al., 2010)), associated with vascular development. To address this question, we imaged E2331>>erGFP expression in developing leaves of WT and *gn*.

As shown above (Fig. 3.4D), E2331>>erGFP was expressed in midvein, first, and second loops, and minor veins in WT (Fig. 3.6C). In *gn*, the pattern of E2331>>erGFP expression in developing leaves recapitulated that of vascular differentiation in mature leaves (Fig. 3.6B,D), suggesting that the putative vascular cells in the shapeless clusters are indeed vascular cells, albeit abnormal ones.

Auxin signals are transduced by multiple pathways (reviewed in (Leyser 2018) and (Gallei et al., 2020)); best characterized is the auxin signaling pathway that releases from repression activating transcription factors of the ARF family, thereby allowing them to induce transcription of auxin-responsive genes (reviewed in (Powers and Strader, 2019)). Auxin signaling is thought to be required for vein formation because mutations

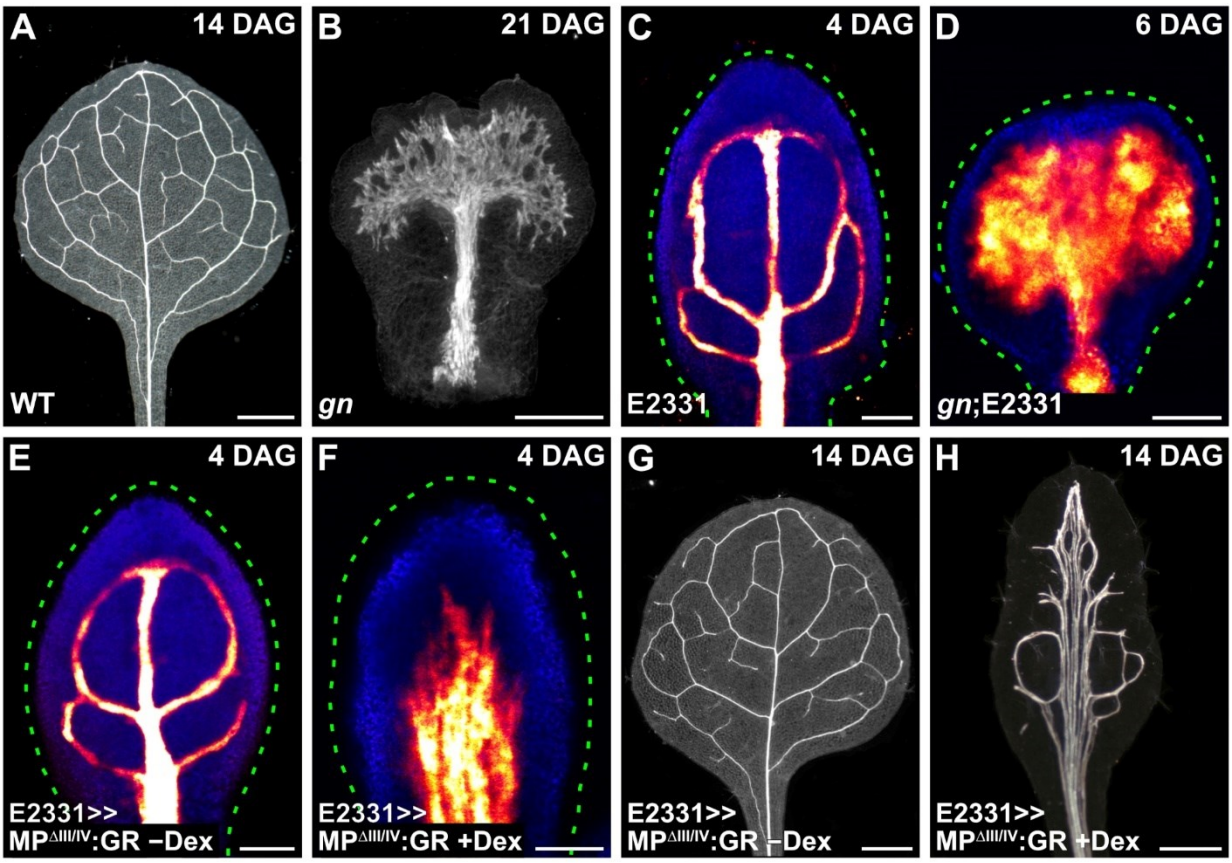

Figure 3.6. E2331-Mediated Visualization and Manipulation of Developing Veins.

(A–H) First leaves. Top right: leaf age in DAG; see Materials & Methods for definition. Bottom left: genotype and treatment. (A,B,G,H) Dark-field microscopy of cleared leaves. (C–F) Confocal laser scanning microscopy. Look-up table (ramp in Fig. 3.2A) visualizes erGFP expression levels (red to white through yellow). Blue: autofluorescence. Black: global background. Dashed green line delineates leaf outline. Front view, median plane. See Table 3.2 for reproducibility of expression and pattern features. Bars: (A,B,G,H) 500 µm; (C–F) 60 µm.

in genes involved in auxin signaling or treatment with inhibitors of auxin signaling leads to the formation of fewer, incompletely differentiated veins (Przemeck et al., 1996; Hardtke and Berleth, 1998; Mattsson et al., 2003; Verna et al., 2019). Increasing auxin signaling by means of broadly expressed mutations or transgenes leads to the formation of supernumerary veins, suggesting that auxin signaling is also sufficient for vein formation (Krogan et al., 2012; Garett et al., 2012). This interpretation assumes that it is the increased auxin signaling in the cells that normally would not differentiate into vein elements that leads those cells to differentiate in fact into such elements. However, it is also possible that it is the increased auxin signaling in the cells that normally differentiate into vein elements that leads the flanking cells, which normally would not differentiate into such elements, to do in fact so. To discriminate between these possibilities, we increased auxin signaling in developing veins by expressing by the E2331 driver a dexamethasone (dex)-inducible, constitutively active variant of the MP protein — the only activating ARF with non-redundant functions in vein formation (Stamatiou, 2007). As previously reported (Schena et al., 1991; Krogan et al., 2012; Smetana et al., 2019), we constitutively activated MP by deleting domains III and IV, which are required for ARF repression (Tiwari et al., 2003; Wang et al., 2005; Krogan et al., 2012), and fused the resulting MPΔIII/IV to a fragment of the rat glucocorticoid receptor (GR) (Picard 1998) to confer dex-inducibility. We imaged E2331>>erGFP expression in developing leaves and vein patterns in mature leaves of E2331>>MPΔIII/IV:GR grown with or without dex.

Consistent with previous observations (Fig. 3.4D; Fig. 3.6C), in developing leaves of E2331>>MPΔIII/IV:GR grown without dex, E2331>>erGFP was expressed in narrow domains (Fig. 3.6E). By contrast, E2331>>erGFP was expressed in broad domains in developing leaves of dex-grown E2331>>MPΔIII/IV:GR (Fig. 3.6F). Whether with or without dex, the patterns of

E2331>>erGFP expression in developing leaves of E2331>>MPΔIII/IV:GR presaged those of vein formation in mature leaves: narrow zones of vein formation in the absence of dex; broad areas of vascular differentiation in the presence of dex, often with multiple veins running parallel next to one another (Fig. 3.6G,H). Though the areas of vascular differentiation in dex-grown E2331>>MPΔIII/IV:GR are not as broad as those of leaves in which MPΔIII/IV is expressed in all the inner cells (Krogan et al., 2012), they are broader than those of E2331>>MPΔIII/IV:GR grown without dex. These observations suggest that, at least in part, it is the increased auxin signaling in the cells that normally differentiate into vein elements that leads the flanking cells, which normally would not differentiate into such elements, to do in fact so. Our conclusion is consistent with interpretations of similar findings in other plant organs (e.g., (Simon et al., 1996; Pautot et al., 2001; Hay et al., 2003; Fukaki et al., 2005; Nakata et al., 2018)) and, more in general, with organ-specific interpretations of genetic mosaics that span multiple organs in other organisms (e.g., (Morgan et al., 1919; Sturtevant 1920; Sturtevant 1932)). Nevertheless, we cannot rule out an effect on leaf vein patterning of increased auxin signaling in the vascular tissue of non-leaf organs, where E2331>>erGFP is also expressed (Fig. 3.5H,Q,Z); in the future, that possibility will have to be addressed by complementary approaches such as clonal analysis (e.g., (Posakony et al., 1991; Burke and Basler., 1996)).

In conclusion, we provide a set of GAL4/GFP enhancer-trap lines in the Col-0 background of Arabidopsis for the specific labeling of cells and tissues during early leaf development (Figure 3.7), and we show that these lines can be used to address key questions in plant developmental biology.

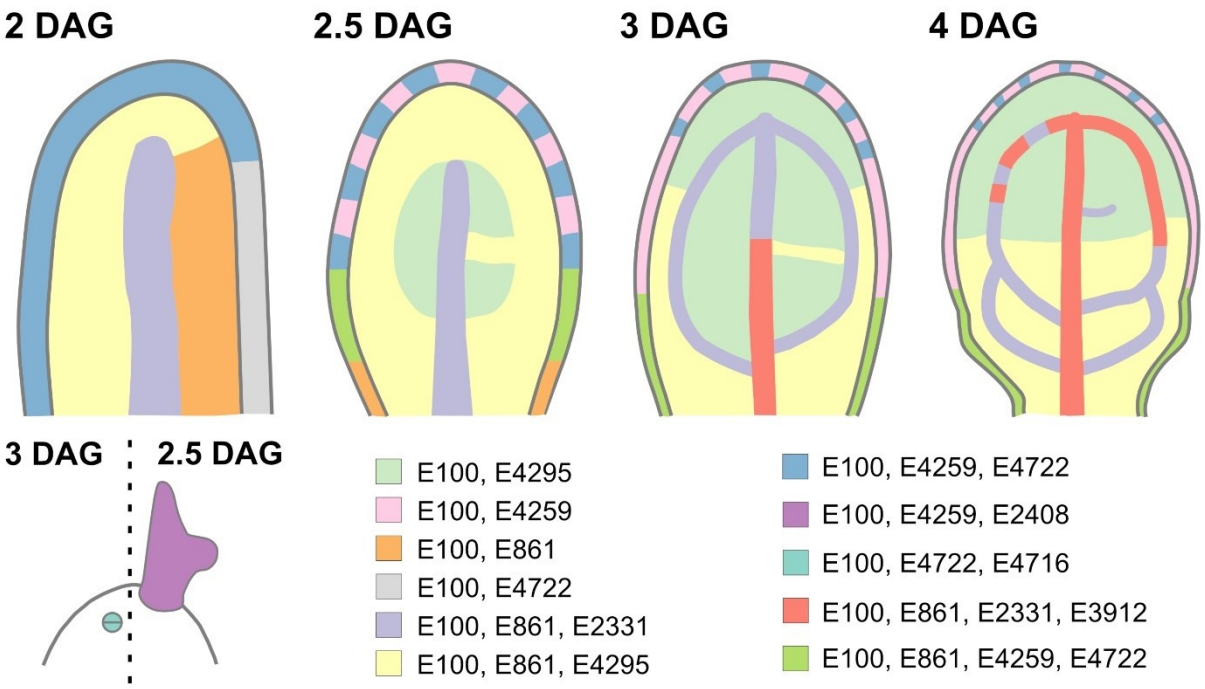

Figure 3.7. Expression Map of E100>>, E861>>, E4295>>, E4259>>, E4722>>, E2408>>, E4716>>, E2331>> and E3912>>erGFP in Leaf Development.

First leaves. Top: leaf age in days after germination (DAG); see Materials & Methods for definition. 2-DAG leaf primordium: side view, median plane; abaxial (ventral) side to the left, adaxial (dorsal) side to the right. Leaves 2.5–4 DAG: front view, median plane. 2.5-/3-DAG leaf composite: front ventral (left) or dorsal (right) view, epidermal plane. Map illustrates inferred overlap and exclusivity of expression. See text for details.

3.3. Materials & Methods

3.3.1. Plants

Origin and nature of GAL4 enhancer-trap lines are in Table 3.1. *gn-13* (SALK_045424; ABRC) (Alonso et al., 2003; Verna et al., 2019) contains a T-DNA insertion after nucleotide +2835 of *GN* and was genotyped with the "SALK_045424 gn LP" (5'-TGATCCAAATCACTGGGTTTC-3') and "SALK_045424 gn RP" (5'-AGCTGAAGATAGGGAATTCGC-3') oligonucleotides (*GN*) and with the "SALK_045424 gn RP" and "LBb1.3" (5'-ATTTTGCCGATTTCGGAAC-3') oligonucleotides (*gn*). To generate the UAS::MPΔIII/IV:GR construct, the UAS promoter was amplified with the "UAS Promoter SalI Forward" (5'-ATAGTCGACCCAAGCGCGCAATTAACCCTCAC-3') and the "UAS Promoter XhoI Reverse" (5'-AGCCTCGAGCCTCTCCAAATGAAATGAACTTCC-3') oligonucleotides; MPΔIII/IV was amplified with the "MP Delta XhoI Forward" (5'-AAACTCGAGATGATGGCTTCATTGTCTTGTGTT-3') and the "MP EcoRI Reverse" (5'-ATTGAATTCGGTTCGGACGCGGGGTGTCGCAATT-3') oligonucleotides; and a fragment of the rat glucocorticoid (GR) receptor gene was amplified with the "SpeI GR Forward" (5'-GGGACTAGTGGAGAAGCTCGAAAAACAAAG-3') and the "GR ApaI Reverse" (5'-GCGGGGCCCTCATTTTTGATGAAACAG-3') oligonucleotides. Seeds were sterilized and sown as in (Sawchuk et al., 2008). Germination was synchronized as in (Scarpella et al., 2004). We refer to DAG as days after exposure of stratified seeds to light. Stratified seeds were germinated and seedlings were grown at 22°C under continuous fluorescent light (~80 μmol m^{-2} s^{-1}). Plants were grown at 24°C under fluorescent light (~85 μmol m^{-2} s^{-1}) in a 16-h-light/8-h-dark cycle. Plants were transformed and representative lines were selected as in (Sawchuk et al., 2008).

3.3.2. Chemicals

Dexamethasone (Sigma-Aldrich, catalogue no. D4902) was dissolved in dimethyl sulfoxide and was added to growth medium just before sowing.

3.3.3. Imaging

Seedlings were imaged with a 1.0x Planapochromat (NA, 0.041; WD, 55 mm) objective of a Leica MZ 16FA stereomicroscope equipped with an HBO103 mercury vapor short-arc lamp and an Andor iXonEM+ camera. GFP was detected with a 480/40-nm excitation filter and a 510-nm emission filter, or with a 470/40-nm excitation filter and a 525/50-nm emission filter. Seedling organs were imaged with a 5x Fluar (NA, 0.25; WD, 12.5 mm) or a 20x Planapochromat (NA, 0.8; WD, 0.55 mm) objective of an Axio Imager.M1 microscope (Carl Zeiss) equipped with an HBO103 mercury vapor short-arc lamp and a Hamamatsu ORCA-AG camera. GFP was detected with a BP 470/40 excitation filter, an FT495 beam splitter, and a BP 525/50 emission filter. Developing leaves were mounted and imaged as in (Sawchuk et al., 2013), except that emission was collected from ~1.5–5-µm-thick optical slices. Fluorophores were excited with the 488-nm line of a 30-mW Ar laser; GFP emission was collected with a BP 505–530 filter, and autofluorescence was collected between 550 and 754 nm. Mature leaves were fixed in 3 : 1 or 6 : 1 ethanol : acetic acid, rehydrated in 70% ethanol and in water, cleared briefly (few seconds to few minutes) — when necessary — in 0.4 M sodium hydroxide, washed in water, mounted in 80% glycerol or in 1 : 2 : 8 or 1 : 3 : 8 water : glycerol : chloral hydrate, and imaged as in (Odat et al., 2014). In the Fiji distribution (Schindelin et al., 2012) of ImageJ (Schneider et al., 2012; Schindelin et al., 2015; Rueden et al., 2017), grayscaled RGB color images were turned into 8-bit images; when necessary, 8-bit images were combined into stacks, and maximum-intensity

projection was applied to stacks; look-up-tables (Sawchuk et al., 2007) were applied to images or stacks, and brightness and contrast were adjusted by linear stretching of the histogram.

Chapter 4: Control of Vein Formation by Tissue-Specific Auxin Signaling

4.1. Introduction

Multicellular organisms solve the problem of long-distance transport of signals and nutrients by means of tissue networks such as the vascular system of vertebrate embryos and the vein networks of plant leaves; therefore, how vascular networks form is a key question in biology. In vertebrates, the formation of the embryonic vascular system relies on direct cell-cell interaction and at least in part on cell migration (e.g., (Noden, 1988; Xue et al., 1999)). Both direct cell-cell interaction and cell migration are precluded in plants by a cell wall that keeps cells apart and in place; therefore, vascular networks form differently in plant leaves.

How vein networks form in plant leaves is unclear, but available evidence suggests that polar transport and signal transduction of the plant hormone auxin are nonredundantly required for vein network formation (Przemeck et al., 1996; Hardtke and Berleth, 1998; Mattsson et al., 1999; Sieburth, 1999; Alonso-Peral et al., 2006; Stamatiou, 2007; Strader et al., 2008; Esteve-Bruna et al., 2013; Sawchuk et al., 2013; Verna et al., 2015; Verna et al., 2019; Mazur et al., 2020). Nonredundant functions of auxin transport in vein network formation depend on nonredundant functions of the PIN1 auxin transporter (Galweiler et al., 1998; Petrasek et al., 2006; Sawchuk et al., 2013; Zourelidou et al., 2014; Verna et al., 2019). In developing leaves, PIN1 polar localization at the plasma membrane of epidermal cells is directed toward single cells along the marginal epidermis (Benkova et al., 2003; Reinhardt et al., 2003; Heisler et al., 2005; Hay et al., 2006; Scarpella et al., 2006; Wenzel et al., 2007; Bayer et al., 2009). These convergence points of epidermal PIN1 polarity are associated with broad domains of PIN1 expression in the inner tissue of the developing leaf; over time, these broad domains become restricted to the narrow

sites where the midvein and lateral veins will form (Benkova et al., 2003; Reinhardt et al., 2003; Heisler et al., 2005; Scarpella et al., 2006; Wenzel et al., 2007; Bayer et al., 2009; Marcos and Berleth, 2014; Verna et al., 2019; Govindaraju et al., 2020). Consistent with these observations, the prevailing hypotheses of vein network formation had long been those proposing that auxin is transported by PIN1 from the epidermal convergence points into the inner tissue of the leaf, where auxin would induce vein formation (reviewed in (Prusinkiewicz and Runions, 2012; Bennett et al., 2014; Runions et al., 2014; Linh et al., 2018)). Instead, it turns out that epidermal PIN1 expression is neither required nor sufficient for auxin-transport-dependent vein-network formation; instead, it is PIN1 expression in the inner tissues that is both required and sufficient for auxin-transport-dependent vein-network formation, and such function of PIN1 expression seems to depend mainly on PIN1 expression in the vascular tissue (Govindaraju et al., 2020).

Nonredundant functions of auxin signaling in vein network formation depend on nonredundant functions of the MP transcription factor (Przemeck et al., 1996; Ulmasov et al., 1997; Hardtke and Berleth, 1998; Ulmasov et al., 1999; Stamatiou, 2007). Like PIN1, MP is expressed in all the cells of the leaf at early stages of tissue development, and over time, epidermal expression becomes restricted to the basalmost cells, and inner-tissue expression becomes restricted to developing veins (Wenzel et al., 2007; Donner et al., 2009; Krogan et al., 2012; Bhatia et al., 2016) (Chapter 2). Moreover, convergent points of epidermal PIN1 polarity are associated with peaks of auxin signaling (Benkova et al., 2003; Mattsson et al., 2003; Heisler et al., 2005; Hay et al., 2006; Scarpella et al., 2006; Smith et al., 2006; Wenzel et al., 2007; Kierzkowski et al., 2013; Marcos and Berleth, 2014). However, unlike for PIN1 in auxin-transport-dependent vein-network formation (Govindaraju et al., 2020), it is currently unknown what the function is of *MP* expression in the leaf epidermis and vascular tissue in auxin-

signaling-dependent vein-network formation.

Here we address this question and find that like PIN1 in auxin-transport-dependent vein-network formation (Govindaraju et al., 2020), *MP* expression in the leaf epidermis is dispensable and *MP* expression in the vascular tissue is sufficient for auxin-signaling-dependent vein-network formation. Moreover, we show that constitutively active auxin signaling in the epidermis is insufficient for vascular differentiation anywhere in the leaf, whereas constitutively active auxin signaling in the vascular tissue is sufficient for supernumerary vein formation.

4.2. Results & Discussion

4.2.1. Necessity and Sufficiency of *MP* for Auxin-Signaling-Dependent Vein-Network Formation

To understand what the function of MP expression in the leaf epidermis and vascular tissue is in auxin-signaling-dependent vein-network formation, we expressed a transcriptional fusion of the *UAS* promoter (Sabatini et al., 2003) to the *MP* gene in the strong *mp-13* mutant background (Odat et al., 2014) (1) by the E4259 driver, which expresses GAL4:VP16 and GAL4-responsive endoplasmic-reticulum-localized GFP (erGFP) in the leaf epidermis, or (2) by the E2331 driver, which expresses GAL4:VP16 and GAL4-responsive erGFP in the vascular tissue (Amalraj et al., 2020) (Chapter 3). We then compared erGFP expression in developing leaves 4 DAG and vein networks in mature leaves of the resulting backgrounds.

As previously reported (Amalraj et al., 2020) (Chapter 3), in 4-DAG E4259 leaves, erGFP expression was restricted to the epidermis, and in 4-DAG E2331 leaves, erGFP expression was restricted to the midvein and to the first and second loops (Fig. 4.1A,F). Likewise, in 4-DAG E4259;*mp-13* leaves, erGFP expression was restricted to the epidermis (Fig. 4.1B). Also in 4-

DAG E2331;*mp-13* leaves, erGFP expression was restricted to the veins; however, erGFP-labeled lateral veins were incompletely differentiated and failed to join distal veins in 4-DAG E2331;*mp-13* leaves (Fig. 4.1G). The expression of erGFP in 4-DAG E4259>>MP;*mp-13* leaves was no different from that in 4-DAG *mp-13* or WT leaves (Fig. 4.1A–C). By contrast, the expression of erGFP in 4-DAG E2331>>MP;*mp-13* leaves was no different from that in 4-DAG WT leaves (Fig. 4.1F,H).

WT Arabidopsis forms leaves whose vein networks are defined by at least four reproducible features (Telfer and Poethig, 1994; Nelson and Dengler, 1997; Kinsman and Pyke, 1998; Candela et al., 1999; Mattsson et al., 1999; Sieburth, 1999; Steynen and Schultz, 2003; Sawchuk et al., 2013; Verna et al., 2015; Verna et al., 2019) (Fig. 1I): (1) a narrow I-shaped midvein that runs the length of the leaf; (2) lateral veins that branch from the midvein and join distal veins to form closed loops; (3) minor veins that branch from midvein and loops, and either end freely or join other veins; (4) minor veins and loops that curve near the leaf margin, lending a scalloped outline to the vein network.

Consistent with previous reports (Przemeck et al., 1996; Wenzel et al., 2007; Donner et al., 2009) (Chapter 2), the vein networks of *mp-13* mature leaves were limited to a midvein and very few, incompletely differentiated lateral veins that failed to join distal veins (Fig. 4.1D). The vein networks of E4259>>MP;*mp-13* mature leaves were no different from those of *mp-13* mature leaves (Fig. 4.1D,E). By contrast, the vein networks of E2331>>MP;*mp-13* mature leaves were no different from those of WT mature leaves (Fig. 4.1I,J) or of *mp* mutants expressing the *MP* gene or an MP:YFP fusion protein by the *MP* promoter (Chapter 2).

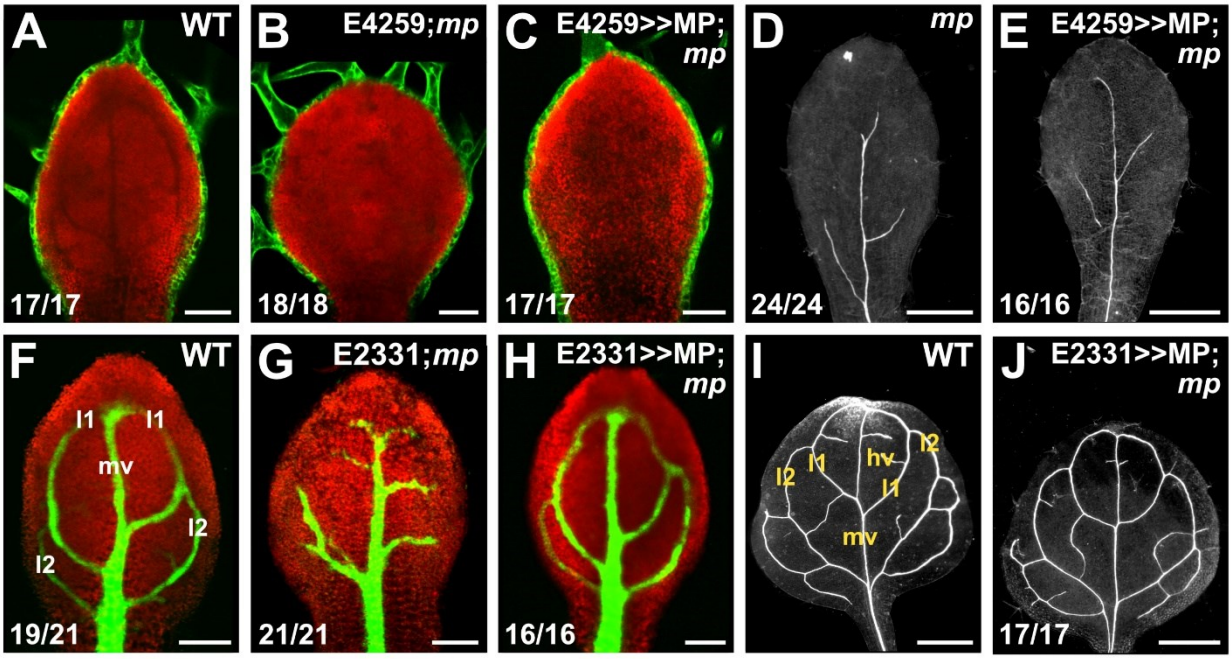

Figure 4.1. Necessity and Sufficiency of MP for Auxin-Signaling-Dependent Vein-Network Formation.

(A–H) Top right: genotype; bottom left: reproducibility index. (A–C,F–H) Confocal laser scanning microscopy of first leaves 4 days after germination (DAG). Green, GFP expression; red, autofluorescence. (D,E,I,J) Dark-field illumination of cleared first leaves 14 DAG. hv, minor vein; l1, first loop; l2, second loop; mv, midvein. Scale bars: (A–C,F–H) 50 μm; (D,E,I,J) 0.5 mm.

Consistent with interpretation of similar findings in other organisms (e.g., (Cherbas et al., 2003; Soloviev et al., 2011; Topalidou and Miller, 2017; Wisidagama et al., 2019)), and like PIN1 in auxin-transport-dependent vein-network formation (Govindaraju et al., 2020) and MP in patterning of other plant features (Bhatia et al., 2016), we conclude that MP expression in the leaf epidermis is neither required nor sufficient for auxin-signaling-dependent vein-network formation; by contrast, MP expression in the veins is sufficient for auxin-signaling-dependent vein-network formation.

We can rule out that compensatory functions provided by other *ARF* genes account for the observation that MP expression in the leaf epidermis is dispensable for auxin-signaling-dependent vein-network formation: no other gene encoding activating ARF proteins is expressed in the leaf epidermis (Schuetz et al., 2019). Our results do not rule out, however, an influence of the leaf epidermis on vein network formation — for example, through local auxin production (e.g., (Abley et al., 2016)) — but they do exclude that such influence is mediated by auxin signaling in the leaf epidermis. Available evidence also excludes that such influence is mediated by auxin transport in the leaf epidermis (Govindaraju et al., 2020). Therefore, peaks of auxin signaling and associated convergence of auxin transport in the leaf epidermis may only have local function, and an influence of the leaf epidermis on vein network formation would have to be mediated by an auxin-transport- and auxin-signaling-independent pathway.

Alternatively, patterning of local epidermal features — such as peaks of auxin production — and of the processes that depend on those features is mediated by auxin signaling in the vascular tissue; there is evidence for such possibility (e.g., (Hardtke et al., 2004; Bhatia et al., 2016; Schuetz et al., 2019)), and our results are consistent with that evidence. In the future, it will be interesting to test these possibilities and whether the leaf epidermis exerts an influence on vein

network formation, but already now, our results suggest that such an influence — if existing — is not mediated by auxin signaling in the leaf epidermis.

4.2.2. Sufficiency of Auxin Signaling for Vein Formation

MP expression in the leaf epidermis is neither required nor sufficient for auxin-signaling-dependent vein-network formation; by contrast, MP expression in the veins is sufficient for auxin-signaling-dependent vein-network formation (Figure 1). We next asked whether constitutively active auxin signaling in the leaf epidermis or in the veins were sufficient for vein formation.

To address this question, we created a constitutively active variant of MP by deleting its PHOX/BEM1 (PB1) domain, as done previously (Krogan et al., 2012; Smetana et al., 2019; Amalraj et al., 2020) (Chapters 2 and 3). We fused the resulting MPΔPB1 downstream of the *UAS* promoter (Sabatini et al., 2003), to confer GAL4-responsiveness, and upstream of a fragment of the rat glucocorticoid receptor (GR) (Picard et al., 1988), to confer dexamethsone (dex)-inducibility. We expressed the resulting UAS::MPΔPB1:GR (1) by the E4259 driver, which expresses GAL4:VP16 and GAL4-responsive endoplasmic-reticulum-localized GFP (erGFP) in the leaf epidermis, or (2) by the E2331 driver, which expresses GAL4:VP16 and GAL4-responsive erGFP in the vascular tissue (Amalraj et al., 2020) (Chapter 3) (Fig. 4.1A,F). We then compared erGFP expression in developing leaves and vein networks in mature leaves of the resulting backgrounds grown in the presence or absence of dex.

Consistent with previous observations (Amalraj et al., 2020) (Chapter 3), erGFP expression was restricted to the epidermis in E4259>>MPΔPB1:GR leaves developing in the absence of dex, and erGFP expression was restricted to the veins in E2331>>MPΔPB1:GR leaves developing in the absence of dex (Fig. 4.2A,C). Growth in the presence of dex failed to modify

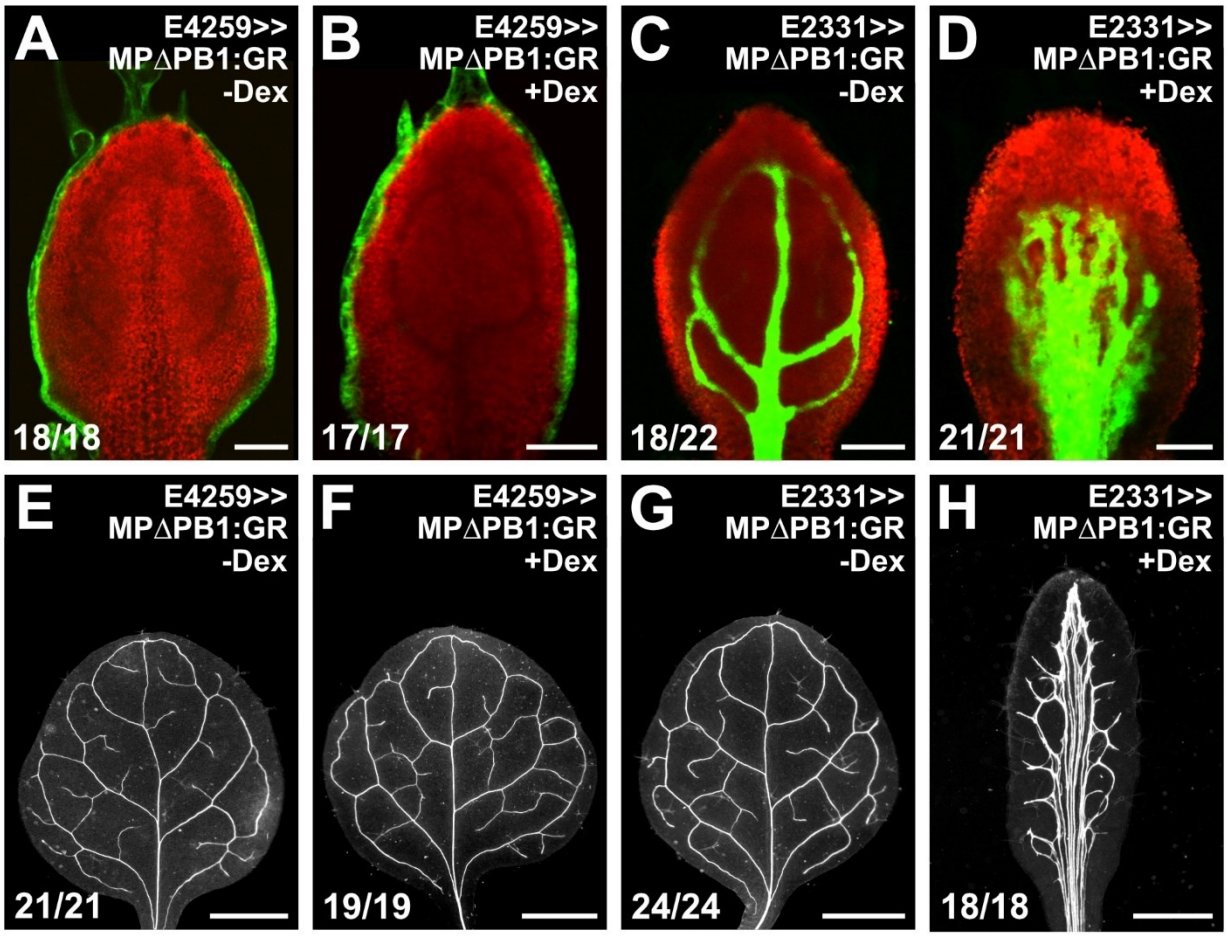

Figure 4.2. Sufficiency of Auxin Signaling for Vein Formation.

(A–H) Top right: genotype and treatment; bottom left: reproducibility index. (A–D) Confocal laser scanning microscopy of first leaves 4 DAG. Green, GFP expression; red, autofluorescence. (E–H) Dark-field illumination of cleared first leaves 14 DAG. Scale bars: (A–D) 50 μm; (E–H) 0.5 mm.

the domain of erGFP expression in E4259>>MPΔPB1:GR developing leaves (Fig. 4.2A,B). By contrast, in E2331>>MPΔPB1:GR leaves developing in the presence of dex, erGFP was expressed in broad domains that spanned almost the entire width of the developing leaves (Fig. 4.2D).

Consistent with previous observations (Amalraj et al., 2020) (Chapter 3) and erGFP expression data (Fig. 4.2A–D), growth in the presence of dex failed to modify the vein networks of E4259>>MPΔPB1:GR mature leaves (Fig. 4.2E,F). By contrast, in the middle of dex-grown E2331>>MPΔPB1:GR mature leaves, supernumerary veins ran parallel to one another for the entire length of the narrow laminae to give rise to wide midveins (Fig. 4.2G,H). Toward the margin of dex-grown E2331>>MPΔPB1:GR mature leaves, veins ran close to one another for varying stretches of the laminae; then diverged; and finally ran close to other veins, converged back to give rise to elongated meshes, or diverged further to end freely perpendicular to the leaf edge (Fig. 4.2G,H).

In conclusion, our results suggest that constitutively active auxin signaling in the epidermis is unable to induce ectopic vascular differentiation anywhere in the leaf, whereas constitutively active auxin signaling in the vascular tissue is sufficient for supernumerary vein formation. This conclusion is surprising because constitutively active auxin signaling in the vascular tissue of the embryonic axis is unable to induce formation of supernumerary vascular cells (Smit et al., 2020). Therefore our results point to an unexpected mechanistic difference between vascular strand formation in the embryonic axis and vein formation in lateral organs such as leaves.

4.3. Materials & Methods

4.3.1. Plants

Origin and nature of lines, and oligonucleotide sequences are in Tables 4.1 and 4.2, respectively. *mp-13* was genotyped with the "WiscDsLoxHs148_12G/148_11H LP" and "WiscDsLoxHs148_12G/149_11H RP" primers (WT allele), and with the "WiscDsLoxHs148_12G/149_11H RP" and "L4" primers (mutant allele). Seeds were sterilized and sowed as in (Sawchuk et al., 2008). Dexamethasone (Sigma-Aldrich, catalogue no. D4902) was dissolved in dimethyl sulfoxide and added to growth medium just before sowing. Stratified seeds were germinated and seedlings were grown at 22°C under continuous light (~90 μmol m^{-2} s^{-1}). Plants were grown at 25°C under fluorescent light (~100 μmol $m^{-2}s^{-1}$) in a 16-h-light/8-h-dark cycle and transformed as in (Sawchuk et al., 2008).

4.3.2. Imaging

Developing leaves were mounted and imaged as in (Amalraj et al., 2020) (Chapter 3). Mature leaves were fixed, cleared, and mounted as in (Chapter 3), and mounted leaves were imaged as in (Odat et al., 2014). Image brightness and contrast were adjusted by linear stretching of the histogram in the Fiji distribution of ImageJ (Schindelin et al., 2012; Schneider et al., 2012; Schindelin et al., 2015; Rueden et al., 2017).

Table 4.1. Origin and Nature of Lines.

Line	Origin/Nature
E4259	(Amalraj et al., 2020) (Chapter 3)
E2331	(Gillmor et al., 2010; Amalraj et al., 2020) (Chapter 3)
mp-13	(Odat et al., 2014)
UAS::MP	Transcriptional fusion of the *UAS* promoter (Sabatini et al., 2003) (primers: "UAS Sal I Forward – UAS::MP Cloning" and "UAS Apa I Reverse – UAS::MP Cloning" to *MP* (AT1G19850; +1 to +4297; primers: "MP Apa I Forward – UAS::MP Cloning" and "Kpn I Reverse – UAS::MP Cloning")
UAS::MP$^{\Delta PB1}$:GR	Transcriptional fusion of the *UAS* promoter (Sabatini et al., 2003) (primers: "UAS Promoter SalI Forward" and "UAS Promoter XhoI Reverse") to a translational fusion of the sequence encoding PB1-domain-deleted *MP* (AT1G19850; +1 to +2388; primers: "MP Delta XhoI Forward" and "MP EcoRI Reverse") to the sequence encoding a fragment of the rat glucocorticoid receptor (GR) (Aoyama and Chua, 1997) (primers: "SpeI GR Forward" and "GR ApaI Reverse")

Table 4.2. Oligonucleotide Sequences.

Name	Sequence (5' to 3')
WiscDsLoxHs148_12G/148_11H LP	TTTGTCCTTTGAAAATGTGCC
WiscDsLoxHs148_12G/149_11H RP	GTTAGCTTGTTTTGTGGCTGC
L4	TGATCCATGTAGATTTCCCGGACATGAAG
UAS Sal I Forward – UAS::MP Cloning	AGTGTCGACGGTGGCGGCCGCTCTAG
UAS Apa I Reverse – UAS::MP Cloning	AGCGGGCCCTCCTCTCCAAATGAAATGAACTT
MP Apa I Forward – UAS::MP Cloning	AAAGGGCCCATGATGGCTTCATTGTCTTG
Kpn I Reverse – UAS::MP Cloning	ACAGGTACCGCATACCACACATGCTCTCT
UAS Promoter SalI Forward	ATAGTCGACCCAAGCGCGCAATTAACCCTCAC
UAS Promoter XhoI Reverse	AGCCTCGAGCCTCTCCAAATGAAATGAACTTCC
MP Delta XhoI Forward	AAACTCGAGATGATGGCTTCATTGTCTTGTGTT
MP EcoRI Reverse	ATTGAATTCGGTTCGGACGCGGGGTGTCGCAATT
SpeI GR Forward	GGGACTAGTGGAGAAGCTCGAAAAACAAAG
GR ApaI Reverse	GCGGGGCCCTCATTTTTGATGAAACAG

Chapter 5: General Discussion

5.1. Conclusion Summary

The evidence discussed in Chapter 1 suggests that auxin signaling controls vascular strand formation, but details of such control were scarce when I started my M.Sc.. The scope of my M.Sc. thesis was therefore to address this limitation and advance our knowledge of how auxin signaling controls vein formation.

Expression of the *ATHB8* gene is activated in files of preprocambial cells (Kang and Dengler, 2004; Scarpella et al., 2004; Sawchuk et al., 2007; Marcos and Berleth, 2014). Activation of *ATHB8* expression in files of preprocambial cells depends on binding of the MP/ARF5 transcription factor to a low-affinity MP-binding site in the *ATHB8* promoter (Donner et al., 2009). However, the biological relevance of the activation of *ATHB8* expression by MP was unresolved when I started my M.Sc.: whereas *MP* was known to promote vein formation (Przemeck et al., 1996), *ATHB8* seemed to have only transient or conditional functions in vein formation (Baima et al., 2001; Donner et al., 2009). Furthermore, whereas both *ATHB8* and MP are expressed in files of preprocambial cells, MP is additionally expressed in surrounding nonvascular cells, which fail to activate *ATHB8* expression (Donner et al., 2009). Why *ATHB8* expression is only activated in a subset of MP-expressing cells was unclear when I started my M.Sc..

In Chapter 2, we showed that ATHB8 promotes vein formation and that both levels of *ATHB8* expression and width of *ATHB8* expression domains are relevant to vein formation. Furthermore, we showed that *ATHB8* expression is restricted to files of preprocambial cells by a combination of (1) activation of *ATHB8* expression through binding of peak levels of MP to the low-affinity

MP-binding site in the *ATHB8* promoter and (2) repression of *ATHB8* expression by MP target genes of the *AUX*/*IAA* family.

Testing ATHB8 functions in vein formation (Chapter 2) required expression of *ATHB8* by different promoters. This imposed the burden of generating different constructs for different promoter–*ATHB8* combinations. This approach could have been simplified if GAL4/GFP enhancer-trap lines had existed in Col-0, the genotype of reference in Arabidopsis (Koornneef and Meinke, 2010), with which to drive expression of genes of interest in desired cells and tissues of developing leaves. Unfortunately, such lines were not available when I started my M.Sc.. In Chapter 3 (Amalraj et al., 2020), we addressed this limitation and provided GAL4/GFP enhancer-trap lines in the Co-0 background of Arabidopsis for the identification and manipulation of cells and tissues in developing leaves.

Nonredundant functions of auxin signaling in vein formation depend on nonredundant MP functions (Przemeck et al., 1996; Ulmasov et al., 1997; Hardtke and Berleth, 1998; Ulmasov et al., 1999; Stamatiou, 2007). Like PIN1, MP is expressed in all the cells of the leaf at early stages of tissue development, but over time, epidermal expression becomes restricted to the basalmost cells, and inner-tissue expression becomes restricted to developing veins (Wenzel et al., 2007; Donner et al., 2009; Krogan et al., 2012; Bhatia et al., 2016) (Chapter 2). Moreover, convergent points of epidermal PIN1 polarity are associated with peaks of auxin signaling (Benkova et al., 2003; Mattsson et al., 2003; Heisler et al., 2005; Hay et al., 2006; Scarpella et al., 2006; Smith et al., 2006; Wenzel et al., 2007; Kierzkowski et al., 2013; Marcos and Berleth, 2014). However, when I started my M.Sc., it was unknown what the function of MP expression in the leaf epidermis and vascular tissue is in auxin-signaling-dependent vein formation.

In Chapter 4, we addressed this question by leveraging the resources we had generated in Chapter 3 (Amalraj et al., 2020), and found that like PIN1 in auxin-transport-dependent vein patterning (Govindaraju et al., 2020), MP expression in the leaf epidermis is dispensable and MP expression in the vascular tissue is sufficient for auxin-signaling-dependent vein formation. Moreover, we showed that constitutively active auxin signaling in the epidermis is insufficient for vascular differentiation anywhere in the leaf, whereas constitutively active auxin signaling in the vascular tissue is sufficient for supernumerary vein formation.

In the discussion section of the respective chapters, we provided an account of how we reached these conclusions from the experimental data and how these conclusions could be integrated with one another and with those in studies of others to advance our understanding of vein formation. Here I instead wish to propose and discuss a hypotheses that seeks to account for the observation that constitutively active auxin signaling leads to supernumerary vein formation (Garrett et al., 2012; Krogan et al., 2012; Amalraj et al., 2020) (Chapters 2–4). This hypothesis should be understood as an attempt to develop a conceptual framework to guide future experimentation and not as an exhaustive mechanistic account.

5.2. The Observations

Expression of an AUX/IAA-irrepressible, constitutively active version of MP — MPΔPB1 — by the *MP* promoter (Krogan et al., 2012) (Chapter 2) or by a vascular driver (Chapters 3 and 4), or an *mp* mutation — *autobahn* (*abn*) — that abolishes binding of the mutant mp protein to AUX/IAA proteins (Garrett et al., 2012) all lead to supernumerary veins running parallel to one another along the entire length of the leaf.

5.3. First Account of the Observations (Krogan et al., 2012)

Available evidence suggests that PIN1 is nonredundantly required for auxin-transport-dependent vein patterning: (1) PIN1 is the only plasma-membrane-localized PIN protein to be expressed where and when veins are being formed (Scarpella 2006; Wenzel 2007; Bayer et al., 2009; Marcos & Berleth 2014; Verna et al., 2019; Govindaraju et al., 2020); and (2) *pin1* mutants are the only *pin* single mutants with vein pattern defects (Mattsson 1999; Sawchuk 2013; Verna 2015 and 2019; Govindaraju 2020). Furthermore, loss-of-function alleles have identified *MP* as a direct or indirect regulator of *PIN1* (Krogan et al., 2016; Wenzel et al., 2007).

In MPΔPB1 leaves, PIN1 was expressed more strongly, and domains of PIN1 expression were broader (Krogan et al., 2012). For example, in WT, a broad PIN1 expression domain in the center of the emerging leaf primordium becomes over time restricted to the site of midvein formation (Scarpella 2006; Wenzel 2007; Bayer et al., 2009). By contrast, in MPΔPB1, the broader PIN1 expression domain in the center of the emerging leaf primordium fails to become restricted altogether (Krogan et al., 2012).

In spite of the defects in PIN1 expression in MPΔPB1, polarity of PIN1 localization remains normal during MPΔPB1 leaf development, suggesting that the vein pattern defects of MPΔPB1 are not the result of reduced auxin transport (Krogan et al., 2012). In fact, that polarity of PIN1 localization remains normal during MPΔPB1 leaf development suggests quite the opposite: because in MPΔPB1 leaves many more cells seem to be transporting auxin in the correct direction, the vein pattern defects of MPΔPB1 could be the results of increased auxin transport. Besides, the vein pattern defects induced by auxin transport inhibition are qualitatively different from those in MPΔPB1 leaves (Mattsson 1999; Sieburth 1999; Sawchuk 2013; Verna 2015 and 2019).

Based on all these observations, Berleth and co-authors proposed that the vein pattern defects of MPΔPB1 are caused by the inability to switch off PIN1 expression (Krogan et al., 2012).

5.4. Second Account of the Observations (Garett et al., 2012)

Like in MPΔPB1, in *mp-abn*, PIN1 expression remains nearly ubiquitous and fails to become restricted to narrow domains even at very late stages of leaf development (Garett et al., 2012). However, unlike in in MPΔPB1, in *mp-abn* leaf development, PIN1 localization at the plasma membrane fails to polarize and remains mainly isotropic. Because of the abnormal expression and localization of PIN1 in *mp-abn* leaves, Schultz and co-authors proposed that the vein pattern defects of *mp-abn* are the results of either increased auxin transport — because of the broader domains of PIN1 expression — or decreased auxin transport — because of the reduced polarization of PIN1 localization (Garrett et al., 2012).

Should the vein pattern defects of *mp-abn* be the result of increased auxin transport, auxin transport inhibition would suppress the mutant defects. By contrast, should the vein pattern defects of *mp-abn* be the result of decreased auxin transport, auxin transport inhibition would enhance the mutant defects. The vein pattern defects of *mp-abn* were enhanced by the *pin1* mutation or by growth in the presence of auxin transport inhibitors (Garrett et al., 2012).

Based on these observations, Schultz and co-authors proposed that the vein pattern defects of *mp-abn* are the result of reduced auxin transport (Garrett et al., 2012).

5.5. Comparing the Two Accounts: Mutual Inconsistencies

Upon critical analysis of the hypotheses presented in (Krogan et al., 2012) and (Garett et al., 2012), it becomes apparent that the hypotheses contradict each other.

Berleth and co-authors proposed that irrepressible PIN1 expression combined with normal PIN1 polarity leads to increased auxin transport and to the MPΔPB1 phenotype (Krogan et al., 2012). Should this interpretation be correct, one would expect auxin transport inhibition to suppress the MPΔPB1 phenotype; instead, the *mp-abn* phenotype is enhanced by auxin transport inhibition (Garett et al, 2012).

On the other hand, Schultz and co-authors proposed that delayed or altogether absent PIN1 polarization leads to reduced auxin transport and to the *mp-abn* phenotype (Garrett et al., 2012). Should this interpretation be correct, however, one would expect auxin-transport-inhibited WT to phenocopy the *mp-abn* phenotype, which is not the case (Mattsson et al., 1999; Sieburth, 1999; Sawchuk et al., 2013; Verna et al., 2015; Verna et al., 2019; Garrett et al., 2012).

5.6. Reconciling the Two Accounts: A Blended Hypothesis

To reconcile the two, seemingly contradicting hypotheses (Garrett et al., 2012; Krogan et al., 2012), I propose that the phenotype of MPΔPB1 and *mp-abn* leaves can be accounted for by combining aspects of both hypotheses: increased auxin transport in some areas of the leaf — as Berleth and co-authors suggested (Krogan et al., 2012) — and reduced auxin transport in other areas of the leaf — as Schultz and co-authors suggested (Garett et al., 2012).

5.7. Testing the Blended Hypothesis

In MPΔPB1, PIN1 expression is no longer restricted to the median domain of the leaf, as it is in WT; instead, PIN1 is additionally expressed in the adaxial (i.e. dorsal) domain of the leaf in MPΔPB1 (Krogan et al., 2012). According to the blended hypothesis, the phenotype of MPΔPB1 — and by extension that of *mp-abn* — would result from increased auxin transport in the leaf adaxial domain and reduced auxin transport in the leaf median domain. Should this prediction of

the blended hypothesis be correct, simultaneously increasing auxin transport in the median domain of MPΔPB1 leaves and decreasing auxin transport in the median domain of MPΔPB1 mutant leaves would suppress the MPΔPB1 phenotype.

To test this prediction, I would first introduce the *pin1* mutation in the MP::MPΔPB1:GR background (Chapter 2). I would then generate a UAS::PIN1 transgene — as I generated a UAS::MP transgene (Chapters 3 and 4) — and introduce it in the MP::MPΔPB1:GR;*pin1* background. I would drive PIN1 expression in the median domain of UAS::PIN1;MP::MPΔPB1:GR;*pin1* leaves by crossing this background with the E861 driver (Chapter 3). Finally, I would activate MPΔPB1:GR by growing E861>>PIN1;MP::MPΔPB1:GR;*pin1* on dex-containing medium — as I did in Chapters 2–4.

Should the prediction of the blended hypothesis be correct, I would expect the mature leaves of dex-grown E861>>PIN1;MP::MPΔPB1:GR;*pin1* to be no different from those of WT. Should instead the prediction of the blended hypothesis be incorrect, I would expect the mature leaves of dex-grown E861>>PIN1;MP::MPΔPB1:GR;*pin1* to be no different from those of dex-grown MP::MPΔPB1:GR.

Literature Cited

Abley, K., Sauret-Gueto, S., Maree, A. F. and Coen, E. (2016). Formation of polarity convergences underlying shoot outgrowths. *Elife* 5, e18165.

Alonso-Peral, M. M., Candela, H., del Pozo, J. C., Martinez-Laborda, A., Ponce, M. R. and Micol, J. L. (2006). The HVE/CAND1 gene is required for the early patterning of leaf venation in Arabidopsis. *Development* 133, 3755-3766.

Alonso JM, Stepanova AN, Leisse TJ et al. Genome-wide insertional mutagenesis of Arabidopsis thaliana. *Science*. 2003; 301: 653-657.

Amalraj, B., Govindaraju, P., Krishna, A., Lavania, D., Linh, N. M., Ravichandran, S. J. and Scarpella, E. (2020). GAL4/GFP enhancer-trap lines for identification and manipulation of cells and tissues in developing Arabidopsis leaves. *Developmental Dynamics*. 2020 Apr 21. doi: 10.1002/dvdy.181. Online ahead of print.

Aoyama, T., & Chua, N. (1997). The Plant journal for cell and molecular biology_A glucocorticoid-mediated transcriptional induction system in transgenic plants. *11*, 605–612.

Ashe, H. L. and Briscoe, J. (2006). The interpretation of morphogen gradients. *Development* 133, 385-394.

Baima, S., Forte, V., Possenti, M., Penalosa, A., Leoni, G., Salvi, S., … Morelli, G. (2014). Negative feedback regulation of auxin signaling by ATHB8/ACL5-BUD2 transcription module. *Mol Plant*, *7*(6), 1006–1025.

Baima, S., Nobili, F., Sessa, G., Lucchetti, S., Ruberti, I., & Morelli, G. (1995). The expression of the Athb-8 homeobox gene is restricted to provascular cells in Arabidopsis thaliana. *Development*, *121*(12), 4171–4182.

Baima, S., Possenti, M., Matteucci, A., Wisman, E., Altamura, M. M., Ruberti, I., & Morelli, G. (2001). The arabidopsis ATHB-8 HD-zip protein acts as a differentiation-promoting transcription factor of the vascular meristems. *Plant Physiol*, *126*(2), 643–655.

Bayer, E. M., Smith, R. S., Mandel, T., Nakayama, N., Sauer, M., Prusinkiewicz, P. and Kuhlemeier, C. (2009). Integration of transport-based models for phyllotaxis and midvein formation. *Genes Dev* 23, 373-384.

Beeckman, T., Przemeck, G. K., Stamatiou, G., Lau, R., Terryn, N., De Rycke, R., … Berleth, T. (2002). Genetic complexity of cellulose synthase a gene function in Arabidopsis embryogenesis. *Plant Physiol*, *130*(4), 1883–1893.

Bellusci, S., Grindley, J., Emoto, H., Itoh, N. and Hogan, B. L. (1997). Fibroblast growth factor 10 (FGF10) and branching morphogenesis in the embryonic mouse lung. *Development* 124, 4867-4878.

Benkova, E., Michniewicz, M., Sauer, M., Teichmann, T., Seifertova, D., Jurgens, G., & Friml, J. (2003). Local, efflux-dependent auxin gradients as a common module for plant organ formation. *Cell*, *115*(5), 591–602.

Bennett, T., Hines, G. and Leyser, O. (2014). Canalization: what the flux. *Trends Genet* 30, 41-48.

Berger F, Linstead P, Dolan L, Haseloff J (1998). Stomata patterning on the hypocotyl of Arabidopsis thaliana is controlled by genes involved in the control of root epidermis patterning. *Dev Biol*, 194, 226-234.

Berleth, T., & Jurgens, G. (1993). The Role of the Monopteros Gene in Organizing the Basal Body Region of the Arabidopsis Embryo. *Development*, *118*(2), 575–587.

Berleth, T., Mattsson, J., & Hardtke, C. S. (2000). Vascular continuity and auxin signals. *Trends Plant Sci*, *5*(9), 387–393.

Berleth, T., & Sachs, T. (2001). Plant morphogenesis: long-distance coordination and local patterning. *Curr Opin Plant Biol*, *4*(1), 57–62.

Bhatia, N., Bozorg, B., Larsson, A., Ohno, C., Jönsson, H., & Heisler, M. G. (2016). Auxin Acts through MONOPTEROS to Regulate Plant Cell Polarity and Pattern Phyllotaxis. *Curr Biol*, *26*(23), 3202–3208.

Bilsborough GD, Runions A, Barkoulas M et al (2011). Model for the regulation of Arabidopsis

thaliana leaf margin development. *Proc Natl Acad Sci U S A*, 108, 3424-3429.

Brady, S. M., Zhang, L., Megraw, M., Martinez, N. J., Jiang, E., Yi, C. S., … Benfey, P. N. (2011). A stele-enriched gene regulatory network in the Arabidopsis root. *Mol Syst Biol*, *7*, 459.

Brand AH, Perrimon N (1993). Targeted gene expression as a means of altering cell fates and generating dominant phenotypes. *Development*, 118, 401-415.

Burke R, Basler K (1996). Dpp receptors are autonomously required for cell proliferation in the entire developing Drosophila wing. *Development*, 122, 2261-2269.

Calleja M, Moreno E, Pelaz S, Morata G (1996). Visualization of gene expression in living adult Drosophila. *Science*, 274, 252-255.

Candela, H., Martinez-Laborda, A., & Micol, J. L. (1999). Venation pattern formation in Arabidopsis thaliana vegetative leaves. *Dev Biol*, *205*(1), 205–216.

Causier, B., Ashworth, M., Guo, W., & Davies, B. (2012). The TOPLESS interactome: A framework for gene repression in Arabidopsis. *Plant Physiology*, *158*(1), 423–438.

Chandler, J. W. (2016). Auxin response factors. *Plant Cell and Environment*, *39*(5), 1014–1028.

Cherbas, L., Hu, X., Zhimulev, I., Belyaeva, E. and Cherbas, P. (2003). EcR isoforms in Drosophila: testing tissue-specific requirements by targeted blockade and rescue. *Development* 130, 271-284.

Ckurshumova W, Koizumi K, Chatfield SP et al (2009). Tissue-specific GAL4 expression patterns as a resource enabling targeted gene expression, cell type-specific transcript profiling and gene function characterization in the Arabidopsis vascular system. *Plant Cell Physiol*, 50, 141-150.

Cotterell, J. and Sharpe, J. (2010). An atlas of gene regulatory networks reveals multiple three-gene mechanisms for interpreting morphogen gradients. *Mol Syst Biol* 6, 425.

Dharmasiri, N., Dharmasiri, S., Weijers, D., Lechner, E., Yamada, M., Hobbie, L., … Estelle, M. (2005). Plant Development Is Regulated by a Family of Auxin Receptor F Box Proteins. *Developmental Cell*, *9*(1), 109–119.

Donnelly PM, Bonetta D, Tsukaya H, Dengler RE, Dengler NG (1999). Cell cycling and cell enlargement in developing leaves of Arabidopsis. *Dev Biol*, 215, 407-419.

Donner, T. J., & Scarpella, E. (2013). Transcriptional control of early vein expression of CYCA2; 1 and CYCA2;4 in Arabidopsis leaves. *Mech Dev*, *130*(1), 14–24.

Donner, T. J., Sherr, I., & Scarpella, E. (2009). Regulation of preprocambial cell state acquisition by auxin signaling in Arabidopsis leaves. *Development*, *136*(19), 3235–3246.

Elefant F, Palter KB (1999). Tissue-specific expression of dominant negative mutant Drosophila HSC70 causes developmental defects and lethality. *Mol Biol Cell*, 10, 2101-2117.

Esau, K. (1965). *Plant anatomy* (2nd ed.). New York ; London: John Wiley.

Esteve-Bruna, D., Perez-Perez, J. M., Ponce, M. R., & Micol, J. L. (2013). incurvata13, a novel allele of AUXIN RESISTANT6, reveals a specific role for auxin and the SCF complex in Arabidopsis embryogenesis, vascular specification, and leaf flatness. *Plant Physiol*, *161*(3), 1303–1320.

Foster, A. S. (1952). Foliar Venation in Angiosperms from an Ontogenetic Standpoint. *American Journal of Botany*, *39*(10), 752–766.

Fukaki H, Nakao Y, Okushima Y, Theologis A, Tasaka M (2005). Tissue-specific expression of stabilized SOLITARY-ROOT/IAA14 alters lateral root development in Arabidopsis. *Plant J*, 44, 382-395.

Gallei M, Luschnig C, Friml J. Auxin signalling in growth (2020): Schrödinger's cat out of the bag. *Curr Opin Plant Biol*, 53, 43-49.

Galweiler, L., Guan, C., Muller, A., Wisman, E., Mendgen, K., Yephremov, A. and Palme, K. (1998). Regulation of polar auxin transport by AtPIN1 in Arabidopsis vascular tissue. *Science* 282, 2226-2230.

Gardiner, J., Donner, T. J., & Scarpella, E. (2011). Simultaneous activation of SHR and ATHB8 expression defines switch to preprocambial cell state in Arabidopsis leaf development. *Dev Dyn*, *240*(1), 261–270.

Gardner MJ, Baker AJ, Assie JM, Poethig RS, Haseloff JP, Webb AA (2009). GAL4 GFP

enhancer trap lines for analysis of stomatal guard cell development and gene expression. *J Exp Bot*, 60, 213-226.

Garrett, J. J., Meents, M. J., Blackshaw, M. T., Blackshaw, L. C., Hou, H., Styranko, D. M., … Schultz, E. A. (2012). A novel, semi-dominant allele of MONOPTEROS provides insight into leaf initiation and vein pattern formation. *Planta*, *236*(1), 297–312.

Gillmor CS, Park MY, Smith MR, Pepitone R, Kerstetter RA, Poethig RS (2010). The MED12-MED13 module of Mediator regulates the timing of embryo patterning in Arabidopsis. *Development*, 137, 113-122.

Gordon, S. P., Heisler, M. G., Reddy, G. V, Ohno, C., Das, P., & Meyerowitz, E. M. (2007). Pattern formation during de novo assembly of the Arabidopsis shoot meristem. *Development*, *134*(19), 3539–3548.

Govindaraju, P., Verna, C., Zhu, T., & Scarpella, E. (2020). Vein patterning by tissue-specific auxin transport. *Development*, dev.187666.

Gray, W. M., Kepinski, S., Rouse, D., Leyser, O., & Estelle, M. (2001). Auxin regulates SCF(TIR1)-dependent degradation of AUX/IAA proteins. *Nature*, *414*(6861), 271–276.

Groszmann M, Gonzalez-Bayon R, Greaves IK et al (2014). Intraspecific Arabidopsis hybrids show different patterns of heterosis despite the close relatedness of the parental genomes. *Plant Physiol*. 2014, 166, 265-280.

Guitton AE, Page DR, Chambrier P et al (2004). Identification of new members of Fertilisation Independent Seed Polycomb Group pathway involved in the control of seed development in Arabidopsis thaliana. *Development*. 2004, 131, 2971-2981.

Gunthorpe D, Beatty KE, Taylor MV (1999). Different levels, but not different isoforms, of the Drosophila transcription factor DMEF2 affect distinct aspects of muscle differentiation. *Dev Biol*, 215, 130-145.

Hamann, T, Mayer, U., & Jurgens, G. (1999). The auxin-insensitive bodenlos mutation affects primary root formation and apical-basal patterning in the Arabidopsis embryo. *Development*, *126*(7), 1387–1395.

Hamann, Thorsten, Benkova, E., Baurle, I., Kientz, M., & Jurgens, G. (2002). The Arabidopsis BODENLOS gene encodes an auxin response protein inhibiting MONOPTEROS-mediated embryo patterning. *Genes & Development*, *16*(13), 1610–1615.

Hardtke, C. S., & Berleth, T. (1998). The Arabidopsis gene MONOPTEROS encodes a transcription factor mediating embryo axis formation and vascular development. *Embo J*, *17*(5), 1405–1411.

Hardtke, C. S., Ckurshumova, W., Vidaurre, D. P., Singh, S. A., Stamatiou, G., Tiwari, S. B., … Berleth, T. (2004). Overlapping and non-redundant functions of the Arabidopsis auxin response factors MONOPTEROS and NONPHOTOTROPIC HYPOCOTYL 4. *Development*, *131*(5), 1089–1100.

Haseloff J. GFP variants for multispectral imaging of living cells (1999). *Methods Cell Biol*, 58, 139-151.

Haseloff J, Siemering KR, Prasher DC, Hodge S (1997). Removal of a cryptic intron and subcellular localization of green fluorescent protein are required to mark transgenic Arabidopsis plants brightly. *Proc Natl Acad Sci U S A*, 94, 2122-2127.

Hay, A., Barkoulas, M., & Tsiantis, M. (2006). ASYMMETRIC LEAVES1 and auxin activities converge to repress BREVIPEDICELLUS expression and promote leaf development in Arabidopsis. *Development*, *133*(20), 3955–3961.

Hay A, Jackson D, Ori N, Hake S (2003). Analysis of the Competence to Respond to KNOTTED1 Activity in Arabidopsis Leaves Using a Steroid Induction System. *Plant Physiology*, 131, 1671-1680.

Heisler, M. G., Ohno, C., Das, P., Sieber, P., Reddy, G. V, Long, J. A., & Meyerowitz, E. M. (2005). Patterns of Auxin Transport and Gene Expression during Primordium Development Revealed by Live Imaging of the Arabidopsis Inflorescence Meristem. *Curr Biol*, *15*(21), 1899–1911.

Hiratsu, K., Matsui, K., Koyama, T., & Ohme-Takagi, M. (2003). Dominant repression of target genes by chimeric repressors that include the EAR motif, a repression domain, in Arabidopsis. *Plant J*, *34*(5), 733–739.

Hironaka, K. and Morishita, Y. (2012). Encoding and decoding of positional information in morphogen-dependent patterning. *Curr Opin Genet Dev* 22, 553-561.

Hobbie, L., McGovern, M., Hurwitz, L. R., Pierro, A., Liu, N. Y., Bandyopadhyay, A., & Estelle, M. (2000). The axr6 mutants of Arabidopsis thaliana define a gene involved in auxin response and early development. *Development*, *127*(1), 23–32.

Huang T, Harrar Y, Lin C et al (2014). Arabidopsis KANADI1 acts as a transcriptional repressor by interacting with a specific cis-element and regulates auxin biosynthesis, transport, and signaling in opposition to HD-ZIPIII factors. *Plant Cell*, 26 246-262.

Irion, U., Singh, A. P. and Nüsslein-Volhard, C. (2016). The Developmental Genetics of Vertebrate Color Pattern Formation: Lessons from Zebrafish. *Curr Top Dev Biol* 117, 141-169.

Kang J, Dengler N (2002). Cell cycling frequency and expression of the homeobox gene ATHB-8 during leaf vein development in Arabidopsis. *Planta*, 216, 212-219.

Kang, J., & Dengler, N. (2004). Vein pattern development in adult leaves of Arabidopsis thaliana. *International Journal of Plant Sciences*, *165*(2), 231–242.

Kawanabe T, Ishikura S, Miyaji N et al (2016). Role of DNA methylation in hybrid vigor in Arabidopsis thaliana. *Proceedings of the National Academy of Sciences*, 113, E6704-E6711.

Kierzkowski, D., Lenhard, M., Smith, R., & Kuhlemeier, C. (2013). Interaction between meristem tissue layers controls phyllotaxis. *Dev Cell*, *26*(6), 616–628.

Kinsman, E. A., & Pyke, K. A. (1998). Bundle sheath cells and cell-specific plastid development in Arabidopsis leaves. *Development*, *125*(10), 1815–1822.

Koornneef, M., & Meinke, D. (2010). The development of Arabidopsis as a model plant. *The Plant Journal*, *61*(6), 909–921.

Korasick, D. A., Westfall, C. S., Lee, S. G., Nanao, M. H., Dumas, R., Hagen, G., … Strader, L. C. (2014). Molecular basis for AUXIN RESPONSE FACTOR protein interaction and the control of auxin response repression. *Proceedings of the National Academy of Sciences of the United States of America*, *111*(14), 5427–5432.

Krogan, N. T., Ckurshumova, W., Marcos, D., Caragea, A. E., & Berleth, T. (2012). Deletion of MP/ARF5 domains III and IV reveals a requirement for Aux/IAA regulation in Arabidopsis leaf vascular patterning. *New Phytol*.

Krogan, N. T., Yin, X., Ckurshumova, W., & Berleth, T. (2014). Distinct subclades of Aux/IAA genes are direct targets of ARF5/MP transcriptional regulation. *New Phytol*, *204*(3), 474–483.

Kubo M, Udagawa M, Nishikubo N et al (2005). Transcription switches for protoxylem and metaxylem vessel formation. *Genes Dev*, 19, 1855-1860.

Laplaze L, Parizot B, Baker A et al (2005). GAL4-GFP enhancer trap lines for genetic manipulation of lateral root development in Arabidopsis thaliana. *J Exp Bot*, 56, 2433-2442.

Larkin JC, Young N, Prigge M, Marks MD (1996). The control of trichome spacing and number in Arabidopsis. *Development*, 122, 997-1005.

Latinkić, B. V., Umbhauer, M., Neal, K. A., Lerchner, W., Smith, J. C. and Cunliffe, V. (1997). The Xenopus Brachyury promoter is activated by FGF and low concentrations of activin and suppressed by high concentrations of activin and by paired-type homeodomain proteins. *Genes Dev* 11, 3265-3276.

Lau, S., De Smet, I., Kolb, M., Meinhardt, H., & Jurgens, G. (2011). Auxin triggers a genetic switch. *Nat Cell Biol*, *13*(5), 611–615.

Leyser O (2018). Auxin Signaling. *Plant Physiol*, 176, 465-479.

Li, H., Cheng, Y., Murphy, A., Hagen, G., & Guilfoyle, T. J. (2009). Constitutive repression and activation of auxin signaling in Arabidopsis. *Plant Physiol*, *149*(3), 1277–1288.

Li, H., Tiwari, S. B., Hagen, G., & Guilfoyle, T. J. (2011). Identical amino acid substitutions in the repression domain of auxin/indole-3-acetic acid proteins have contrasting effects on auxin signaling. *Plant Physiol*, *155*(3), 1252–1263.

Liao, C. Y., Smet, W., Brunoud, G., Yoshida, S., Vernoux, T., & Weijers, D. (2015). Reporters for sensitive and quantitative measurement of auxin response. *Nature Methods*, *12*(3), 207–210.

Linh, N. M., Verna, C. and Scarpella, E. (2018). Coordination of cell polarity and the patterning of leaf vein networks. *Curr Opin Plant Biol* 41, 116-124.

Livak, K. J. and Schmittgen, T. D. (2001). Analysis of relative gene expression data using real-time quantitative PCR and the 2(-Delta Delta C(T)) Method. *Methods* 25, 402-408.

Long, J. A., Woody, S., Poethig, S., Meyerowitz, E. M., & Barton, M. K. (2002). Transformation of shoots into roots in Arabidopsis embryos mutant at the TOPLESS locus. *Development*, *129*(12), 2797–2806.

Lu P, Porat R, Nadeau JA, O'Neill SD (1996). Identification of a meristem L1 layer-specific gene in Arabidopsis that is expressed during embryonic pattern formation and defines a new class of homeobox genes. *The Plant Cell*, 8, 2155-2168.

Mangan, S. and Alon, U. (2003). Structure and function of the feed-forward loop network motif. *Proc Natl Acad Sci U S A* 100, 11980-11985.

Marcos, D., & Berleth, T. (2014). Dynamic auxin transport patterns preceding vein formation revealed by live-imaging of Arabidopsis leaf primordia. *Front Plant Sci*, *5*, 235.

Mattsson, J., Ckurshumova, W., & Berleth, T. (2003). Auxin signaling in Arabidopsis leaf vascular development. *Plant Physiol*, *131*(3), 1327–1339.

Mattsson, J., Sung, Z. R., & Berleth, T. (1999). Responses of plant vascular systems to auxin transport inhibition. *Development*, *126*(13), 2979–2991.

Mayer, U., Buttner, G., & Jurgens, G. (1993). Apical-basal pattern formation in the Arabidopsis embryo: studies on the role of the gnom gene. *Development*, *117*(1), 149–162.

Mazur, E., Benková, E., & Friml, J. (2016). Vascular cambium regeneration and vessel formation in wounded inflorescence stems of Arabidopsis. *Scientific Reports*, *6*, 1–15.

Mazur, E., Kulik, I., Hajný, J. and Friml, J. (2020). Auxin Canalization and Vascular Tissue Formation by TIR1/AFB-Mediated Auxin Signaling in Arabidopsis. *New Phytol*

McGuire S, Roman G, Davies RL (2004). Gene expression systems in Drosophila: a synthesis of time and space. *Trends Genet*, 20, 384-391.

Merelo, P., Ram, H., Caggiano, M. P., Ohno, C., Ott, F., Straub, D., … Heisler, M. G. (2016).

Regulation of MIR165/166 by class II and class III homeodomain leucine zipper proteins establishes leaf polarity. *Proceedings of the National Academy of Sciences of the United States of America*, *113*(42), 11973–11978.

Michniewicz, M., Zago, M. K., Abas, L., Weijers, D., Schweighofer, A., Meskiene, I., … Friml, J. (2007). Antagonistic regulation of PIN phosphorylation by PP2A and PINOID directs auxin flux. *Cell*, *130*(6), 1044–1056.

Morgan TH, Bridges CB. The Origin of Gynandromorphs (1919). *Contributions to the Genetics of Drosophila melanogaster*. Washington, D.C.: Carnegie Institution of Washington. Press of Gibson Bross, Inc, 1-122.

Mutte, S. K., Kato, H., Rothfels, C., Melkonian, M., Wong, G. K. S., & Weijers, D. (2018). Origin and evolution of the nuclear auxin response system. *ELife*, *7*, 1–25.

Nagel AC, Maier D, Preiss A (2002). Green fluorescent protein as a convenient and versatile marker for studies on functional genomics in Drosophila. *Development Genes and Evolution*, 212, 93-98.

Nakata MT, Tameshige T, Takahara M, Mitsuda N, Okada K (2018). The functional balance between the WUSCHEL-RELATED HOMEOBOX1 gene and the phytohormone auxin is a key factor for cell proliferation in Arabidopsis seedlings. *Plant Biotechnology*, 35, 141-154.

Nelson, T., & Dengler, N. (1997). Leaf Vascular Pattern Formation. *Plant Cell*, *9*(7), 1121–1135.

Noden, D. M. (1988). Interactions and fates of avian craniofacial mesenchyme. *Development* 103 Supplement, 121-140.

Normanly, J. (2010). Approaching cellular and molecular resolution of auxin biosynthesis and metabolism. *Cold Spring Harb Perspect Biol*, *2*(1), a001594. doi:10.1101/cshperspect.a001594.

Odat, O., Gardiner, J., Sawchuk, M. G., Verna, C., Donner, T. J., & Scarpella, E. (2014). Characterization of an allelic series in the MONOPTEROS gene of Arabidopsis. *Genesis*, *52*(2), 127–133.

Ohashi-Ito, K., Oguchi, M., Kojima, M., Sakakibara, H., & Fukuda, H. (2013). Auxin-associated

initiation of vascular cell differentiation by LONESOME HIGHWAY. *Development*, *140*(4), 765–769.

Overvoorde, P. J., Okushima, Y., Alonso, J. M., Chan, A., Chang, C., Ecker, J. R., … Theologis, A. (2005). Functional genomic analysis of the AUXIN/INDOLE-3-ACETIC ACID gene family members in Arabidopsis thaliana. *Plant Cell*, *17*(12), 3282–3300.

Papatsenko, D. (2009). Stripe formation in the early fly embryo: principles, models, and networks. *BioEssays* 31, 1172-1180.

Pautot V, Dockx J, Hamant O et al (2001). KNAT2: evidence for a link between knotted-like genes and carpel development. *Plant Cell*, 13, 1719-1734.

Petrasek, J., Mravec, J., Bouchard, R., Blakeslee, J. J., Abas, M., Seifertova, D., … Friml, J. (2006). PIN proteins perform a rate-limiting function in cellular auxin efflux. *Science*, *312*(5775), 914–918.

Picard D, Salser SJ, Yamamoto KR (1988). A movable and regulable inactivation function within the steroid binding domain of the glucocorticoid receptor. *Cell*, 54, 1073-1080.

Ploense, S. E., Wu, M. F., Nagpal, P., & Reed, J. W. (2009). A gain-of-function mutation in IAA18 alters Arabidopsis embryonic apical patterning. *Development*, *136*(9), 1509–1517.

Posakony LG, Raftery LA, Gelbart WM (1991). Wing formation in Drosophilamelanogasterequires decapentaplegigcenefunction along the anterior-posterior compartment boundary. *Mech Dev*, 33, 69-82.

Powers, S. K., & Strader, L. C. (2020). Regulation of auxin transcriptional responses. *Developmental Dynamics*, *249*(4), 483–495.

Pray, T. R. (1955). Foliar venation in Angiosperms. II. Histogenesis of the venation of Liriodendron. *American Journal of Botany*, *42*(1), 18–27.

Prigge, M. J., Otsuga, D., Alonso, J. M., Ecker, J. R., Drews, G. N., & Clark, S. E. (2005). Class III homeodomain-leucine zipper gene family members have overlapping, antagonistic, and distinct roles in Arabidopsis development. *Plant Cell*, *17*(1), 61–76.

Prusinkiewicz, P. and Runions, A. (2012). Computational models of plant development and form. *New Phytol* 193, 549-569.

Przemeck, G. K., Mattsson, J., Hardtke, C. S., Sung, Z. R., & Berleth, T. (1996). Studies on the role of the Arabidopsis gene MONOPTEROS in vascular development and plant cell axialization. *Planta*, *200*(2), 229–237.

Pyke KA, Marrison JL, Leech RM (1991). Temporal and Spatial Development of the Cells of the Expanding 1st Leaf of Arabidopsis-Thaliana (L) Heynh. *Journal of Experimental Botany*, 42, 1407-1416.

Radoeva T, Ten Hove CA, Saiga S, Weijers D (2016). Molecular Characterization of Arabidopsis GAL4/UAS Enhancer Trap Lines Identifies Novel Cell-Type-Specific Promoters. *Plant Physiol*. 2016, 171, 1169-1181.

Raven, J. A. (1975). Transport of indole acetic acid in plant cells in relation to pH and electrical potential gradients, and its significance for polar IAA transport. *New Phytologist*, *74*, 163–172.

Reddy S, Jin P, Trimarchi J, Caruccio P, Phillis R, Murphey RK (1997). Mutant molecular motors disrupt neural circuits in Drosophila. *J Neurobiol*. 1997, 33, 711-723.

Reeves, G. T. and Stathopoulos, A. (2009). Graded dorsal and differential gene regulation in the Drosophila embryo. *Cold Spring Harb Perspect Biol* 1, a000836.

Reinhardt, D., Pesce, E. R., Stieger, P., Mandel, T., Baltensperger, K., Bennett, M., … Kuhlemeier, C. (2003). Regulation of phyllotaxis by polar auxin transport. *Nature*, *426*(6964), 255–260.

Rogers, K. W. and Schier, A. F. (2011). Morphogen gradients: from generation to interpretation. *Annu Rev Cell Dev Biol* 27, 377-407.

Rubery, P. H., & Sheldrake, A. R. (1974). Carrier-Mediated Auxin Transport. *Planta*, *118*(2), 101–121.

Rueden, C. T., Schindelin, J., Hiner, M. C., DeZonia, B. E., Walter, A. E., Arena, E. T., & Eliceiri, K. W. (2017). ImageJ2: ImageJ for the next generation of scientific image data.

BMC Bioinformatics, *18*(1), 529.

Runions, A., Smith, R. S. and Prusinkiewicz, P. (2014). Computational Models of Auxin-Driven Development. In *Auxin and Its Role in Plant Development* (ed. E. Zažímalová, J. Petrasek and E. Benková), pp. 315-357. Vienna: Springer.

Sabatini S, Beis D, Wolkenfelt H et al (1999). An auxin-dependent distal organizer of pattern and polarity in the Arabidopsis root. *Cell*, 99, 463-472.

Sabatini, S., Heidstra, R., Wildwater, M. and Scheres, B. (2003). SCARECROW is involved in positioning the stem cell niche in the Arabidopsis root meristem. *Genes Dev* 17, 354-358.

Sachs, T. (1981). The control of the patterned differentiation of vascular tissues. *Advances in Botanical Research* , *9*, 151–262.

Sachs, T. (1991). Pattern Formation in Plant Tissues. In B. P. W., B. P. B., G. J. M., & S. W. (Eds.), *Development and cell biology series*.

Sachs, Tsvi. (2000). Integrating Cellular and Organismic Aspects of Vascular Differentiation. *Plant and Cell Physiology*, *41*(6), 649–656.

Sadowski, I., Ma, J., Triezenberg, S. and Ptashne, M. (1988). GAL4-VP16 is an unusually potent transcriptional activator. *Nature* 335, 563-564.

Sagner, A. and Briscoe, J. (2017). Morphogen interpretation: concentration, time, competence, and signaling dynamics. *Wiley Interdiscip Rev Dev Biol* 6,

Sato, M. and Saigo, K. (2000). Involvement of pannier and u-shaped in regulation of decapentaplegic-dependent wingless expression in developing Drosophila notum. *Mech Dev* 93, 127-138.

Sauer, M., Balla, J., Luschnig, C., Wisniewska, J., Reinohl, V., Friml, J., & Benkova, E. (2006). Canalization of auxin flow by Aux/IAA-ARF-dependent feedback regulation of PIN polarity. *Genes Dev*, *20*(20), 2902–2911.

Sawchuk, M. G., Donner, T. J., Head, P., & Scarpella, E. (2008). Unique and overlapping expression patterns among members of photosynthesis-associated nuclear gene families in Arabidopsis. *Plant Physiol*, *148*(4), 1908–1924.

Sawchuk, M. G., Edgar, A., & Scarpella, E. (2013). Patterning of leaf vein networks by convergent auxin transport pathways. *PLoS Genet*, *9*(2), e1003294.

Sawchuk, M. G., Head, P., Donner, T. J., & Scarpella, E. (2007). Time-lapse imaging of Arabidopsis leaf development shows dynamic patterns of procambium formation. *New Phytol*, *176*(3), 560–571.

Scarpella, E., Francis, P., & Berleth, T. (2004). Stage-specific markers define early steps of procambium development in Arabidopsis leaves and correlate termination of vein formation with mesophyll differentiation. *Development*, *131*(14), 3445–3455.

Scarpella, E., Marcos, D., Friml, J., & Berleth, T. (2006). Control of leaf vascular patterning by polar auxin transport. *Genes Dev*, *20*(8), 1015–1027.

Schena M, Lloyd AM, Davis RW (1991). A steroid-inducible gene expression system for plant cells. *Proc Natl Acad Sci U S A*, 88, 10421-10425.

Scheres, B., Wolkenfelt, H., Willemsen, V., Terlouw, M., Lawson, E., Dean, C., & Weisbeek, P. (1994). Embryonic Origin of the Arabidopsis Primary Root and Root-Meristem Initials. *Development*, *120*(9), 2475–2487.

Schindelin, J., Arganda-Carreras, I., Frise, E., Kaynig, V., Longair, M., Pietzsch, T., … Cardona, A. (2012). Fiji: an open-source platform for biological-image analysis. *Nat Methods*, *9*(7), 676–682.

Schindelin, J., Rueden, C. T., Hiner, M. C., & Eliceiri, K. W. (2015). The ImageJ ecosystem: An open platform for biomedical image analysis. *Mol Reprod Dev*, *82*(7–8), 518–529.

Schlereth, A., Moller, B., Liu, W., Kientz, M., Flipse, J., Rademacher, E. H., … Weijers, D. (2010). MONOPTEROS controls embryonic root initiation by regulating a mobile transcription factor. *Nature*, *464*(7290), 913–916.

Schneider, C. A., Rasband, W. S., & Eliceiri, K. W. (2012). NIH Image to ImageJ: 25 years of image analysis. *Nat Methods*, *9*(7), 671–675.

Schuetz, M., Fidanza, M. and Mattsson, J. (2019). Identification of Auxin Response Factor-Encoding Genes Expressed in Distinct Phases of Leaf Vein Development and with Overlapping Functions in Leaf Formation. *Plants (Basel)* 8,

Sessa, G., Steindler, C., Morelli, G., & Ruberti, I. (1998). The Arabidopsis Athb-8, -9 and -14 genes are members of a small gene family coding for highly related HD-ZIP proteins. *Plant Mol Biol*, *38*(4), 609–622.

Sessions A, Weigel D, Yanofsky MF (1999). The Arabidopsis thaliana MERISTEM LAYER 1 promoter specifies epidermal expression in meristems and young primordia. *Plant J*, 20, 259-263.

Shevell DE, Kunkel T, Chua NH (2000). Cell wall alterations in the arabidopsis emb30 mutant. *Plant Cell*, 12, 2047-2060.

Sieburth, L. E. (1999). Auxin is required for leaf vein pattern in Arabidopsis. *Plant Physiol*, *121*(4), 1179–1190.

Siemering KR, Golbik R, Sever R, Haseloff J (1996). Mutations that suppress the thermosensitivity of green fluorescent protein. *Curr Biol*, 6, 1653-1663.

Simon R, Igeño MI, Coupland G (1996). Activation of floral meristem identity genes in Arabidopsis. *Nature*, 384, 59-62.

Smetana, O., Mäkilä, R., Lyu, M., Amiryousefi, A., Sánchez Rodríguez, F., Wu, M. F., … Mähönen, A. P. (2019). High levels of auxin signalling define the stem-cell organizer of the vascular cambium. *Nature*, *565*(7740), 485–489.

Smit, M. E., Llavata-Peris, C. I., Roosjen, M., van Beijnum, H., Novikova, D., Levitsky, V., … Weijers, D. (2020). Specification and regulation of vascular tissue identity in the Arabidopsis embryo. *Development (Cambridge)*, *147*(8).

Smith, R. S., & Bayer, E. M. (2009). Auxin transport-feedback models of patterning in plants. *Plant Cell Environ*, *32*(9), 1258–1271.

Smith, R. S., Guyomarc'h, S., Mandel, T., Reinhardt, D., Kuhlemeier, C., & Prusinkiewicz, P. (2006). A plausible model of phyllotaxis. *Proc Natl Acad Sci U S A*, *103*(5), 1301–1306.

Solereder H (1908). *Systematic Anatomy of the Dicotyledons*. Oxford: Clarendon Press.

Soloviev, A., Gallagher, J., Marnef, A. and Kuwabara, P. E. (2011). C. elegans patched-3 is an essential gene implicated in osmoregulation and requiring an intact permease transporter domain. *Dev Biol* 351, 242-253.

Stamatiou G (2007). The roles of auxin response factors in patterning processes during Arabidopsis development. *Department of Cell and Systems Biology*, Ph.D., i-xiv,1.

Stewart RN (1978). Ontogeny of the primary body in chimeral forms of higher plants. In: Subtelny S, Sussex IM, eds. *The Clonal Basis of Development*. New York: Academic Press, 131-160.

Steynen, Q. J., & Schultz, E. A. (2003). The FORKED genes are essential for distal vein meeting in Arabidopsis. *Development*, *130*(19), 4695–4708.

Strader, L. C., Monroe-Augustus, M., & Bartel, B. (2008). The IBR5 phosphatase promotes Arabidopsis auxin responses through a novel mechanism distinct from TIR1-mediated repressor degradation. *Bmc Plant Biology*, *8*.

Sturtevant AH (1920). The Vermilion Gene and Gynandromorphism. *Proc Soc Exp Biol Med*, 17, 70-71.

Sturtevant AH (1932). The use of mosaics in the study of the developmental effects of genes. *Proceedings of the 6th International Congress of Genetics*, 1, 304-307.

Szemenyei, H., Hannon, M., & Long, J. A. (2008). TOPLESS mediates auxin-dependent transcriptional repression during Arabidopsis embryogenesis. *Science*, *319*(5868), 1384–1386.

Taiz, L., & Zeiger, E. (2010). *Plant Physiology* (5th ed.). Sunderland (MA): Sinauer Associates Inc.

Takada S, Jürgens G (2007). Transcriptional regulation of epidermal cell fate in the Arabidopsis embryo. *Development*, 134, 1141-1150.

Telfer, A., & Poethig, R. S. (1994). Leaf development in Arabidopsis. In E. M. Meyerowitz & C. R. Somerville (Eds.), *Arabidopsis* (pp. 379–401). New York: Cold Spring Harbor Press.

Tilney-Bassett RAE (1986). *Plant Chimeras*. London: Edward Arnold.

Tiwari, S B, Hagen, G., & Guilfoyle, T. (2003). The roles of auxin response factor domains in auxin-responsive transcription. *Plant Cell*, *15*(2), 533–543.

Tiwari, Shiv B, Wang, X., & Guilfoyle, T. J. (2001). AUX / IAA Proteins Are Active Repressors , and Their Stability and Activity Are Modulated by Auxin Author (s): Shiv B . Tiwari , Xiao-Jun Wang , Gretchen Hagen and Tom J . Guilfoyle Published by : American Society of Plant Biologists (ASPB) Stable URL. *The Plant Cell*, *13*(12), 2809–2822.

Topalidou, I. and Miller, D. L. (2017). Caenorhabditis elegans HIF-1 Is Broadly Required for Survival in Hydrogen Sulfide. *G3 (Bethesda)* 7, 3699-3704.

Ulmasov, T., Hagen, G., & Guilfoyle, T. J. (1997). ARF1, a transcription factor that binds to auxin response elements. *Science*, *276*(5320), 1865–1868.

Ulmasov, T., Hagen, G., & Guilfoyle, T. J. (1999). Activation and repression of transcription by auxin-response factors. *Proc Natl Acad Sci U S A*, *96*(10), 5844–5849.

Ulmasov, T., Hagen, G. and Guilfoyle, T. J. (1999). Dimerization and DNA binding of auxin response factors. *Plant Journal* 19, 309-319.

Verna, C, Sawchuk, M. G., Linh, N. M., & Scarpella, E. (2015). Control of vein network topology by auxin transport. *BMC Biol*, *13*, 94.

Verna, Carla, Ravichandran, S. J., Sawchuk, M. G., Linh, N. M., & Scarpella, E. (2019). Coordination of tissue cell polarity by auxin transport and signaling. *ELife*, *8*, 1–30.

Wang, S., Tiwari, S. B., Hagen, G., & Guilfoyle, T. J. (2005). AUXIN RESPONSE FACTOR7 restores the expression of auxin-responsive genes in mutant Arabidopsis leaf mesophyll protoplasts. *Plant Cell*, *17*(7), 1979–1993.

Weijers, D., Benkova, E., Jager, K. E., Schlereth, A., Hamann, T., Kientz, M., … Jurgens, G. (2005). Developmental specificity of auxin response by pairs of ARF and Aux/IAA transcriptional regulators. *Embo J*, *24*(10), 1874–1885.

Weijers, D., Franke-van Dijk, M., Vencken, R. J., Quint, A., Hooykaas, P., & Offringa, R. (2001). An Arabidopsis Minute-like phenotype caused by a semi-dominant mutation in a

RIBOSOMAL PROTEIN S5 gene. *Development*, *128*(21), 4289–4299.

Weijers, D., Schlereth, A., Ehrismann, J. S., Schwank, G., Kientz, M., & Jurgens, G. (2006). Auxin triggers transient local signaling for cell specification in Arabidopsis embryogenesis. *Developmental Cell*, *10*(2), 265–270.

Weijers D, Van Hamburg JP, Van Rijn E, Hooykaas PJ, Offringa R (2003). Diphtheria toxin-mediated cell ablation reveals interregional communication during Arabidopsis seed development. *Plant Physiol*, 133, 1882-1892.

Wenzel CL, Marrison J, Mattsson J, Haseloff J, Bougourd SM (2012). Ectopic divisions in vascular and ground tissues of Arabidopsis thaliana result in distinct leaf venation defects. *J Exp Bot*, 63, 5351-5364.

Wenzel, C. L., Schuetz, M., Yu, Q., & Mattsson, J. (2007). Dynamics of MONOPTEROS and PIN-FORMED1 expression during leaf vein pattern formation in Arabidopsis thaliana. *Plant J*, *49*(3), 387–398.

Wisidagama, D. R., Thomas, S. M., Lam, G. and Thummel, C. S. (2019). Functional analysis of Aarf domain-containing kinase 1 in Drosophila melanogaster. *Dev Dyn* 248, 762-770.

Wisniewska, J., Xu, J., Seifertova, D., Brewer, P. B., Ruzicka, K., Blilou, I., … Friml, J. (2006). Polar PIN localization directs auxin flow in plants. *Science*, *312*(5775), 883.

Wu, W., Liu, Y., Wang, Y., Li, H., Liu, J., Tan, J., … Ma, H. (2017). Evolution analysis of the Aux/IAA gene family in plants shows dual origins and variable nuclear localization signals. *International Journal of Molecular Sciences*, *18*(10).

Wu, M.-F., Yamaguchi, N., Xiao, J., Bargmann, B., Estelle, M., Sang, Y. and Wagner, D. (2015). Auxin-regulated chromatin switch directs acquisition of flower primordium founder fate. *eLife* 4, e09269.

Xue, Y., Gao, X., Lindsell, C. E., Norton, C. R., Chang, B., Hicks, C., Gendron-Maguire, M., Rand, E. B., Weinmaster, G. and Gridley, T. (1999). Embryonic lethality and vascular defects in mice lacking the Notch ligand Jagged1. *Hum Mol Genet* 8, 723-730.

Yamaguchi M, Goué N, Igarashi H et al (2010). VASCULAR-RELATED NAC-DOMAIN6 and VASCULAR-RELATED NAC-DOMAIN7 effectively induce transdifferentiation into xylem vessel elements under control of an induction system. *Plant Physiol*, 153, 906-914.

Yang MY, Armstrong JD, Vilinsky I, Strausfeld NJ, Kaiser K (1995). Subdivision of the Drosophila mushroom bodies by enhancer-trap expression patterns. *Neuron*, 15, 45-54.

Yoshida, S., Barbier de Reuille, P., Lane, B., Bassel, G. W., Prusinkiewicz, P., Smith, R. S., & Weijers, D. (2014). Genetic control of plant development by overriding a geometric division rule. *Dev Cell*, *29*(1), 75–87.

Zenser, N., Ellsmore, A., Leasure, C., & Callis, J. (2001). Auxin modulates the degradation rate of Aux/IAA proteins. *Proc Natl Acad Sci U S A*, *98*(20), 11795–11800.

Zhang, C., Gong, F.C., Lambert, G.M., and Galbraith, D.W. (2005). Cell type-specific characterization of nuclear DNA contents within complex tissues and organs. Plant Methods 1, 7

Zhang Q, Wang D, Lang Z et al (2016). Methylation interactions in Arabidopsis hybrids require RNA-directed DNA methylation and are influenced by genetic variation. *Proc Natl Acad Sci U S A*, 113, E4248-56.

Zhao, Y. (2010). Auxin biosynthesis and its role in plant development. *Annu Rev Plant Biol*, *61*, 49–64.

Zhou, G. K., Kubo, M., Zhong, R., Demura, T., & Ye, Z. H. (2007). Overexpression of miR165 affects apical meristem formation, organ polarity establishment and vascular development in Arabidopsis. *Plant Cell Physiol*, *48*(3), 391–404.

Zourelidou, M., Absmanner, B., Weller, B., Barbosa, I. C., Willige, B. C., Fastner, A., Streit, V., Port, S. A., Colcombet, J., de la Fuente van Bentem, S. et al. (2014). Auxin efflux by PIN-FORMED proteins is activated by two different protein kinases, D6 PROTEIN KINASE and PINOID. *Elife* 3, e02860.